

DYNAMIC CAPACITY OF
ISOLATED SLAB COLUMN SPECIMENS

A Thesis

presented to

the Faculty of the Graduate School

at the University of Missouri-Columbia

In Partial Fulfillment

of the Requirements for the Degree

Master of Science

by

SPENCER CURTIS BEARDEN

Dr. Sarah L. Orton, Thesis Supervisor

MAY 2015

The undersigned, appointed by the dean of the Graduate School, have examined the thesis entitled

DYNAMIC CAPACITY OF ISOLATED SLAB COLUMN SPECIMENS

presented by Spencer Curtis Bearden,

a candidate for the degree of Master of Science,

and hereby certify that, in their opinion, it is worthy of acceptance.

Professor Sarah Orton

Professor Hani Salim

Professor Sanjeev Khanna

DEDICATION

I would like to dedicate this work to my friends and family, I am fortunate to be surrounded by such great people in my life. I would like to thank my parents for the encouragement they have given me throughout life, nothing is more fulfilling than making them proud and I appreciate everything they have done for me.

Acknowledgements

I would like to thank the faculty and staff of the Civil and Environmental Engineering Department at the University of Missouri – Columbia. With special thanks to my advisor Dr. Sarah Orton for her guidance throughout my undergraduate and graduate career. I would also like to thank Zhonghua Peng as I have thoroughly enjoyed working alongside him during my time as a graduate student.

I would like to thank Rex Gish, Richard Oberto and Mike Harlow of Engineering Technical Services for taking the time to share their knowledge and experience throughout the project. I would like to thank previous students Zach Treece and Austin Stake for their previous work on the project, as well as Aaron Saucier for his help and expertise at the research testing facility. I would certainly like to thank our group of undergraduate research assistants; Ginny Trauth, Carmen Aboytes, Katy Beyer, Andrew Pelikan, Andrew Briedwell, and Matt Fliessner for their time and contributions to the project.

This work was supported by The National Science Foundation under Grant No. 1100146. This support is gratefully acknowledged.

Table of Contents

Acknowledgements.....	ii
List of Figures.....	v
List of Tables.....	x
Abstract.....	xi
1. Introduction.....	1
1.1 Problem.....	2
1.2 Objective and Research Plan.....	3
1.3 Scope.....	4
2. Literature Review.....	6
2.1 Introduction to Progressive Collapse.....	6
2.2 Introduction to Punching Shear.....	8
2.2.1 Current Design Codes.....	13
2.3 Material Strength Under Dynamic Loading.....	15
2.4 Previous Dynamic Testing.....	18
2.4.1 Ghali, Elmasri, and Dilger (1976).....	18
2.4.2 Criswell.....	20
2.4.3 Zinneddin and Krauthammer (2007).....	23
2.4.4 Jacobs and De Roeck.....	25
2.4.5 Habibi et al. (2012).....	26

2.4.6	Shah and Kulkarni (1998).....	28
3.	Experimental Setup.....	31
3.1	Prototype Structure Design	31
3.2	Design of Test Specimens	34
3.3	Test Specimen Construction.....	38
3.4	Test Setup Design.....	43
3.5	Instrumentation.....	51
3.6	Material Properties	59
4.	Results.....	61
4.1	Dynamic 1 Test - 0.64% Reinforced.....	62
4.2	Dynamic 2 Test – 0.64% Reinforced	72
4.3	Dynamic 3 Test – 1.0% Reinforced	79
4.4	Comparison of Static and Dynamic Test Results.....	86
4.4.1	Comparison of 0.64% Reinforced Tests	86
4.4.2	Comparison of 1.0% Reinforced Tests	92
5.	Summary and Conclusions	99
	References.....	102
	Appendix.....	103

List of Figures

Figure 2.1.1 - Complete progressive collapse of North wing of Sampoong Department Store	8
Figure 2.2.1 – Diagonal cracking resulting from shear forces (Harris 2004)	9
Figure 2.2.2 – Illustration of the moment couple resisting shear forces (Broms 1990) ...	10
Figure 2.2.3 – Resulting net tensile stress at slab midpoint (Vecchio and Tang 1989)....	11
Figure 2.2.4 – Illustration of compressive membrane forces and relation to flexural capacity (Vecchio and Tang 1989)	12
Figure 2.3.1 – DIF for Ultimate Compressive Concrete Strength (2500psi - 5000psi) (UFC)	17
Figure 2.3.2 – DIF for Yield and Ultimate Stresses of Reinforcing Steel (UFC).....	17
Figure 2.4.1.1 – Slab Specimen and Applied Loading of Ghali, Elmasri, Dilger (1976).	19
Figure 2.4.2.1 – Criswell Slab-Column Specimen (Criswell)	21
Figure 2.4.2.2 – Load and Deflection Response Results of Criswell Testing (Criswell).	22
Figure 2.4.3.1 – Crack pattern and punching shear on top slab face (Zinneddin 2007) ...	24
Figure 2.4.3.2 – Direct shearing of mesh reinforcement (Zinneddin 2007)	24
Figure 2.4.4.1 – Dynamic beam test setup (Jacobs)	25
Figure 2.4.5.1 – Slab-column connection test specimen (Habibi 2012).....	27
Figure 2.4.6.1 – Beam test setup (Shah 1998)	29
Figure 2.4.6.2 – Load – Deflection results and crack patterns for tested beam specimens (Shah 1998).....	30
Figure 3.1.1 – Plan view of prototype structure.....	32
Figure 3.1.2 – Initial sketch of top reinforcement in the prototype structure	33

Figure 3.1.3 – Initial sketch of bottom reinforcement in the prototype structure	34
Figure 3.2.1 – Isolated slab removed from the overall prototype structure	35
Figure 3.2.2 – Tension reinforcement for 1.0% reinforcement ratio	35
Figure 3.2.3 – Compression reinforcement for 1.0% reinforcement ratio	36
Figure 3.2.4 – Tension reinforcement for 0.64% reinforcement ratio	36
Figure 3.2.5 – Compression reinforcement for 0.64% reinforcement ratio	37
Figure 3.2.6 – Elevation view of slab column specimen	37
Figure 3.2.7 – Cross section view of column section	38
Figure 3.3.1 – Completed isolated slab formwork without top column form in place	40
Figure 3.3.2 – Picture of formwork with rebar placed and top column form in place	41
Figure 3.3.3 – Completed slab formwork prior to concrete pour	42
Figure 3.3.4 – Slab after pouring and surface finishing was complete	43
Figure 3.4.1 – 2D view of test setup with slab installed	44
Figure 3.4.2 – 3D view of final test setup	44
Figure 3.4.3 – Schematic of restrained connection	46
Figure 3.4.4 – Complete assembly of support connection to steel frame	46
Figure 3.4.5 – Details of anchorage and connections to support angle	47
Figure 3.4.6 – Anchorage assembly and vertical PVC to be cast into slab	48
Figure 3.4.7 – Angle stops welded at the base of each vertical column	48
Figure 3.4.8 – Compression brace welded to support columns	49
Figure 3.4.9 – Test setup with dynamic actuator, full ram displacement	50
Figure 3.4.10 – Hydraulic tank used to power ram	51

Figure 3.5.1 – Compression reinforcement strain gage layout for 0.64% reinforcement ratio	52
Figure 3.5.2 – Tension reinforcement strain gage layout for 0.64% reinforcement ratio.	53
Figure 3.5.3 - Compression reinforcement strain gage layout for 1.0% reinforcement ratio	54
Figure 3.5.4 - Tension reinforcement strain gage layout for 1.0% reinforcement ratio ...	54
Figure 3.5.5 – Picture from above slab showing LVDT against outer face of slab.....	55
Figure 3.5.6 – lateral LVDTs placed against threaded rod and beneath pin connection ..	56
Figure 3.5.7 – String pot located directly beneath bottom column to measure deflection	57
Figure 3.5.8 – Dynamically loaded test specimen after failure has occurred	58
Figure 3.5.9 – Location of tension (blue) and compression (silver) load cells to measure lateral forces.....	59
Figure 4.1 – Overall view of test setup and slab specimen.....	61
Figure 4.1.1 – Punching capacity vs. time for Dynamic 1 test	62
Figure 4.1.2 – Vertical load vs. center column displacement for Dynamic 1 test	63
Figure 4.1.3 – Tension gage strain vs. center deflection for Dynamic 1 test.....	65
Figure 4.1.4 – Compression gage strain vs. center deflection for Dynamic 1 test	65
Figure 4.1.5 – 0.64% Dynamic 1 tension gages vs. column displacement pre-punching	66
Figure 4.1.6 – 0.64% Dynamic 1 compression gages vs. column displacement pre-punching.....	67
Figure 4.1.7 – Dynamic test 1 after failure of the connection	69
Figure 4.1.8 - Concrete strain parallel and perpendicular vs. time	70
Figure 4.1.9 – Lateral load measured from threaded rod restraints	71

Figure 4.2.1 – Vertical load vs center column displacement for Dynamic 2 test	73
Figure 4.2.2 - Tension gage strain vs. center deflection for Dynamic 2 test	73
Figure 4.2.3 - 0.64% Dynamic 2 tension gages vs. column displacement pre-punching .	74
Figure 4.2.4 - Compression gage strain vs center deflection for Dynamic 2 test	75
Figure 4.2.5 - 0.64% Dynamic 2 compression gages vs. column displacement pre-punching.....	76
Figure 4.2.6 – Failed Dynamic 2 specimen	77
Figure 4.2.7 – Concrete parallel and perpendicular vs. time for Dynamic 2 test	78
Figure 4.2.8 – Lateral load measured from threaded rod restraints	78
Figure 4.3.1 – Vertical load vs. center column displacement for Dynamic 3 test	80
Figure 4.3.2 – Tension gage response for Dynamic 3 test.....	80
Figure 4.3.3 – 1.0% Dynamic 3 tension gages vs center column deflection pre-punching	81
Figure 4.3.4 – Compression gages throughout Dynamic 3 test	82
Figure 4.3.5 – 1.0% Dynamic 3 compression gages vs. column displacement pre-punching.....	83
Figure 4.3.6 – Concrete parallel and perpendicular vs. time	84
Figure 4.3.7 – Lateral loads calculated from threaded rods in support connection	85
Figure 4.3.8 – Lateral displacements recorded from exterior LVDTs.....	85
Figure 4.4.1.1 – Underside of 0.64% static test at punching failure of testing.....	87
Figure 4.4.1.2 – Underside of the Dynamic 1 test at punching failure	87
Figure 4.4.1.3 – Underside of the static 0.64% test at conclusion of testing.....	88
Figure 4.4.1.4 – Underside of the Dynamic 1 test at the conclusion of testing	88

Figure 4.4.1.5 – Comparison of Static and Dynamic 0.64% Load-Displacement Curves	89
Figure 4.4.1.6 – Center and mid-span deflections prior to punching failure	90
Figure 4.4.1.7 – Average Gage Strain vs. Center Deflection for 0.64% Tests	91
Figure 4.4.2.1 – Dynamic 3 test just after punching failure	93
Figure 4.4.2.2 – Static 1.0% test just after punching failure.....	93
Figure 4.4.2.3 – Underside of 1.0% static test at the conclusion of testing	94
Figure 4.4.2.4 – Underside of the Dynamic 3 test at the conclusion of testing	94
Figure 4.4.2.5 – Normalized capacity vs. Deflection for 1.0% test specimens	95
Figure 4.4.2.6 – Center and mid-span deflections prior to punching failure	96
Figure 4.4.2.7 – Average tension strains for 1.0% reinforced specimens	97

List of Tables

Table 1.2.1 - Test matrix of isolated slab specimen tests	4
Table 2.3.1 – Dynamic Increase Factor (DIF) for design of Reinforced Concrete Elements	16
Table 2.4.1.1 – Summary of Test Data and Results by Ghali, Elmasri, and Dilger (1976)	20
Table 3.6.1 – Concrete compressive strengths for each dynamic test	60
Table 5.1 – Punching capacity data for dynamically tested slabs.....	99

Abstract

Localized damage, particularly in flat plate structures, can cause a chain reaction of subsequent failures resulting in failure of a large portion or even the entire structure. This type of failure is known as a progressive or disproportionate collapse. While there are well documented cases of progressive collapses, there is still a lack of knowledge in regard to a structure's capacity to resist this potentially catastrophic failure mode.

The goal of the overall research project is to determine the potential for progressive punching shear failures in flat plate buildings. After initial failure of a supporting member in a structural system, the loads initially carried by that member will be redistributed to surrounding connections at a dynamic rate. There has been little research to date on the dynamic loading effects on flat plate structures. By understanding the behavior of these slab-column connections and their response to dynamically applied loads, better predictions and more refined modeling can be done to investigate a structures ability to resist progressive collapse. Dynamic loading of the specimen will affect the material strength, failure mode response, and load distribution throughout the slab. Therefore, the goal of this test is to assess the capacity of slab-column connections under dynamically applied load.

This project consisted of three dynamically loaded slab-column specimens designed to replicate a typical flat-plate support connection element. Two dynamic specimens had a reinforcement ratio of 0.64%, while the third specimen had a 1.0% reinforcement ratio. The tests were conducted using a high speed hydraulic ram to load the specimens, which were subject to laterally restrained conditions. A high speed data acquisition system was

used to record readings of several instruments used to measure load, deflections, and strains at various locations of the slab.

There were several conclusions made from the individual dynamic tests, as well as conclusions drawn from comparing the dynamic response to similar slabs previously tested under statically applied loading. Neither the 0.64% specimens (Dynamic 1 and Dynamic 2) nor the 1.0% specimen (Dynamic 3) displayed an increase in punching capacity in comparison to corresponding static tests.

The capacity of Dynamic 1 and 2 were 98% and 90% of the corresponding static test, respectively. The Dynamic 3 test was significantly lower with a punching capacity 75% of that observed in the static test. The dynamically tested specimens did, however, display more ductility at the punching shear failure in comparison to static testing. The vertical column deflection of the 0.64% static test was 78% of the Dynamic 1 deflection and 56% of the Dynamic 2 deflection at punching shear failure. A similar correlation was seen in the 1.0% reinforcement ratio tests, where the static deflection at punching failure was 70% of the deflection in the Dynamic 3 test.

The loading and strain rates obtained in these dynamic tests did not correlate to any significant material strength increase factors. Dynamic increase factors for concrete and steel are much larger for blast and seismic testing, both of which display much larger strain rates than observed in this research. The strain response of the dynamic specimens displayed a concentration of higher strains near the column at punching failure. Strain measurements were measured at various locations of the reinforcement mesh, up to 12 inches from the column face. At distances larger than 5 inches, the static tests displayed

larger strain values throughout the test, until punching failure occurred. At locations closer to the column face, the strain of the slab reinforcement at punching failure reached values ranging between 20% to 50% larger for the dynamic test in comparison to corresponding static tests.

1. Introduction

A progressive collapse initiates from the loss of one primary structural member, most commonly a supporting column or girder. The initial loss of a structural member can then lead to a chain of subsequent failures in the surrounding members creating a domino effect that eventually leads to collapse of some or all of the structure. Failures of this nature are potentially life threatening and form the motivation behind this research project. The particular concern of this project focuses on the progressive collapse potential of older flat plate building structures which are known to be vulnerable to this failure type due to brittle punching shear failures around the columns.

Flat plate structures are a commonly used design option due to relatively low cost and ease of construction. The main components of a flat plate structure are the reinforced concrete slab and vertical column supports. There are no beams, girders, or column capitals in a flat-plate structure. Due to this design, the flat-plate structure is vulnerable to punching shear failures at the slab column connections. When one of these connections fails, for any number of reasons, the load previously carried by that connection must be redistributed to the surrounding connections. This load redistribution can cause subsequent failures in nearby slab column connections, causing a failure pattern that leads to an eventual progressive collapse.

Punching shear failures are the result of high localized stresses at the connection between the slab and column. If the capacity of the connection is not large enough to resist the applied forces, a punching shear failure will occur. Resistance to punching shear failure is considered in the design procedures found in codes published by the American

Concrete Institute (ACI) and the American Society of Civil Engineers (ASCE). The formulation of these codes is heavily reliant on testing results of slab column connection specimens that have been isolated from the surrounding structure without the presence of any lateral restraints. In addition the majority of these tests have been conducted statically, whereas the progressive punching shear is a dynamic load redistribution. Little research has been done involving dynamic loading of isolated slab column connections and its effect on overall capacity before and after punching failure has occurred.

1.1 Problem

After initial punching shear failure of a slab-column connection, loads will be rapidly redistributed to surrounding columns. There exists little knowledge of the behavior of a flat slab structure subject to dynamic loading conditions. It is well understood that materials like steel and concrete experience increased strength capacity under dynamic loading. However, it is not clear what the strain rate for the materials in a punching shear type loading will be or what the increase in material strength under those rates would be. In addition, previous dynamic tests on beams and slabs have shown a change in failure behavior and deformed shape at failure. It is not clear if the punching shear cone shape will be affected by the dynamic loading, and if it is what would be the effect on the punching shear capacity. Understanding the dynamic loading effects on slab-column connections is critical to determine the potential of progressive collapse in a flat-plate structure.

1.2 Objective and Research Plan

The objective of this research is to replicate the behavior of a slab column connection within the surrounding structure by providing lateral restraint and dynamic loading of the isolated test specimens. This research will better predict the capacity of these slab column connections by replicating the conditions present in a complete structure as closely as possible. By improving the capacity predictions based on the known parameters of a structure, the overall analysis of a structure's potential for progressive collapse can be improved as well.

This research in particular, investigated the resulting connection capacities for different lateral restraint, loading rate, and reinforcement conditions. Earlier stages of this project investigated isolated slab-column behavior analysis under statically applied loading conditions and has been completed and published. The focus of this research will be in comparing the dynamic tests to the static tests. The comparison will not only look at the punching shear capacity but also the post-punching behavior as post-punching capacity can potentially provide adequate resistance to prevent progressive collapse after the initial failure.

This project included constructing and testing three isolated slab column specimens. These specimens were the final three of nine total isolated slab tests done throughout the course of a larger research project simultaneously being completed. The final three isolated tests were unique from the previous six due to the load being applied at a dynamic rate, rather than static. The slab column specimens were constructed at a 0.73 scale to accommodate for the space available in the testing location. The test setup was identical for each of the nine specimens; the slab was connected to vertical supports on

each of the four sides, the supports were connected to a reaction frame to provide lateral restraint when desired. The only major modification to the test setup for dynamic slabs was the installation of a different hydraulic ram capable of the desired loading rate. The first two dynamically tested slabs were constructed with a 0.64% reinforcement ratio, while the final dynamic test had a reinforcement ratio of 1%. All three of these final test specimens were tested under laterally restrained conditions. The full test matrix of isolated slab specimens can be seen in Table 1.2.1.

Table 1.2.1 - Test matrix of isolated slab specimen tests

Test #	Loading Rate	Slab Reinforcement Ratio	In-Plane Restraint	Slab Bending
Test # 1	Static	1.0%	Unrestrained	Negative
Test # 2	Static	0.64%	Unrestrained	Negative
Test # 3	Static	1.0%	Restrained	Negative
Test # 4	Static	0.64%	Restrained	Negative
Test # 5	Static	0.64%	Restrained	Positive
Test # 6	Static	0.64%	Restrained	Negative
Test # 7	Dynamic	0.64%	Restrained	Negative
Test # 8	Dynamic	0.64%	Restrained	Negative
Test # 9	Dynamic	1.0%	Restrained	Negative

1.3 Scope

This thesis is organized into five different chapters. A literature review is provided in Chapter 2 which focuses on previous research in punching shear of concrete in relation to reinforcement ratio, lateral restraint and dynamic loading effects. The literature review will also include case studies on previous structural failures occurring from progressive collapse. Chapter 3 provides details on the design and construction of the isolated slab

column specimens, as well as the configuration of the test setup used to test each of the specimens. Chapter 4 presents the data obtained from the three dynamic tests. Results from the dynamically loaded specimens are also compared with corresponding static tests to further understand loading rate effects. Chapter 5 provides a summary of the results and states the conclusions that have been reached at this stage in the project. The final section includes an appendix and list of references in conclusion of this thesis.

2. Literature Review

The purpose of this chapter is to provide detail on the topic of progressive collapse, punching shear, and their relation to the research presented in this thesis paper. The first portion of this review will focus on the topics of progressive collapse and punching shear failure. This will be followed by past research on the topic of material and load increase factors in relation to dynamic loading conditions. The final section of the literature review will discuss previous research that has been completed on dynamic loading of reinforced concrete specimens.

2.1 Introduction to Progressive Collapse

The progressive collapse potential following sudden loss of a supporting column will depend on the strength and deformation capacity of neighboring support connections. The applied forces and deformation demands resulting from this load distribution will be subject to dynamic loading effects. To date, there is a scarce amount of knowledge on the dynamic response of the behavior of typical slab-column connections, and even less on the response of entire flat plate structural systems. Current guidelines existing for evaluating a structure's progressive collapse potential are primarily based on seismic testing data and unverified numerical analysis.

Previous studies (Multi-hazard Mitigation Council 2003, Ellingwood et al. 2009) have stated the need of further research on the topic of disproportionate collapse. Particular areas of interest include the following; development of criteria to identify structures at high risk, investigation of behavior through testing, and compiling experimental data essential for developing substantial constitutive and capacity models for structural elements. Although full-scale progressive collapse testing is not common, further

research is warranted to prevent such hazardous failures causing considerable damage and potentially harming human life.

There have been a handful of significant structural failures over the past 50 years that can be directly related to progressive collapse. Flat-plate building structures are of particular concern as they are prone to punching shear failure which is of brittle nature and can lead to a chain reaction of subsequent failures with little to no warning. There are documented cases of progressive collapse in flat-plate structures occurring before construction has fully completed. Such a case took place in Boston Massachusetts on January 25, 1971. An initial punching shear failure on the top floor of a 16 story building lead to collapse of the roof and eventual progressive collapse of the east side of the building, leaving 4 workers dead and 20 more injured. While poor quality control and weather conditions leading to low concrete strength played a role in the initial failure, this example illustrates the domino effect that results in large scale failures. One of the most prominent progressive collapses to date was the failure of the 5-story Sampoong Department Store in Seoul, South Korea. The building had been fully operational for six years before the failure in 1995. Initial failure occurred due to increased loadings on the fifth floor and the movement of a heavy cooling tower from the east to west side of the building, causing damage to the roof slab and surrounding connections. A complete progressive collapse of the North wing of the building occurred as a result of a single column failure on the fifth structure. The tragic failure resulted in the loss of 502 lives and a total of 937 injured; the fully collapsed building can be seen in Figure 2.1.1 (Park).

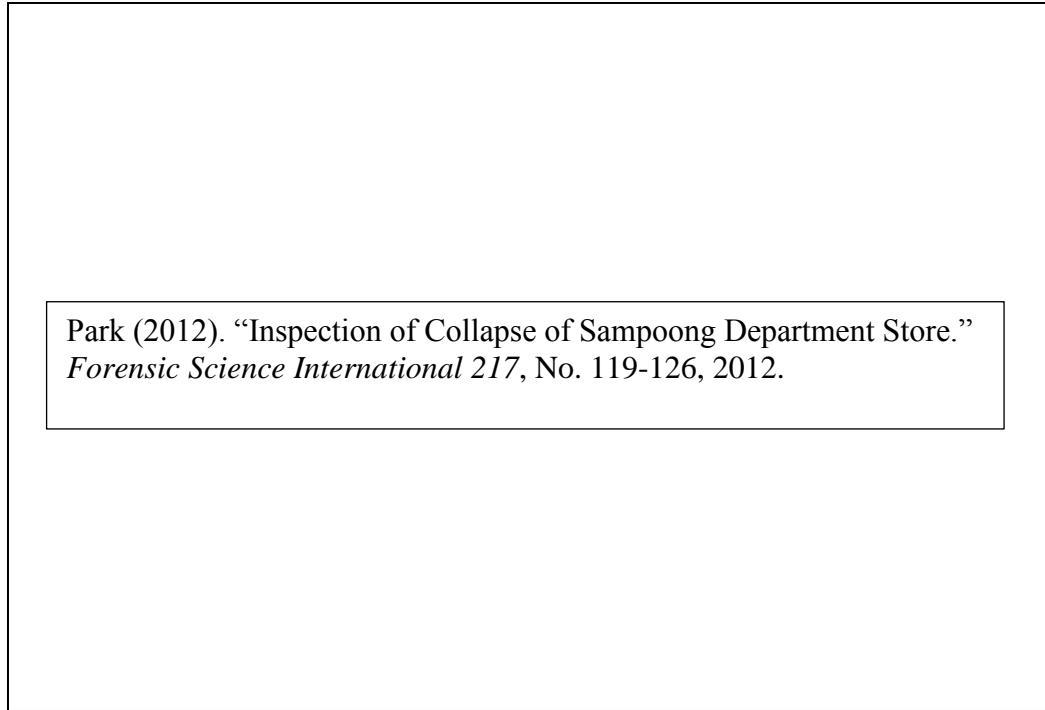


Figure 2.1.1 - Complete progressive collapse of North wing of Sampoong Department Store

2.2 Introduction to Punching Shear

Punching shear failure, also known as two way shear failure, is a structural failure occurring at the slab column connection in a reinforced concrete structure. Punching shear failures are the primary cause of structural failure in a flat-plate structure,.

Punching shear failures occur as a result of high stresses building around the perimeter of the slab column connection. The stresses applied in this region are due to the gravity loading over the tributary area of the slab around that particular connection. Failure of the connection will occur when the capacity of the slab column connection is exceeded by the applied stresses, these stresses are typically dominated by shear forces.

In a continuous framing system, such as a typical flat plate building structure, large negative moments occur near the slab column connections while the maximum positive

moments are present at the midspan of the slab between column connections. In a flat plate structure, the moment forces are transferred from the slab into the column. Flexural cracks will begin to form when the applied moment at the slab column interface increases to a certain level. The flexural cracks will form a circular pattern on the slab, centered around the column. If the shear forces near the column become large enough, shear cracks will begin to form around the column, this behavior can be seen in Figure 2.2.1.

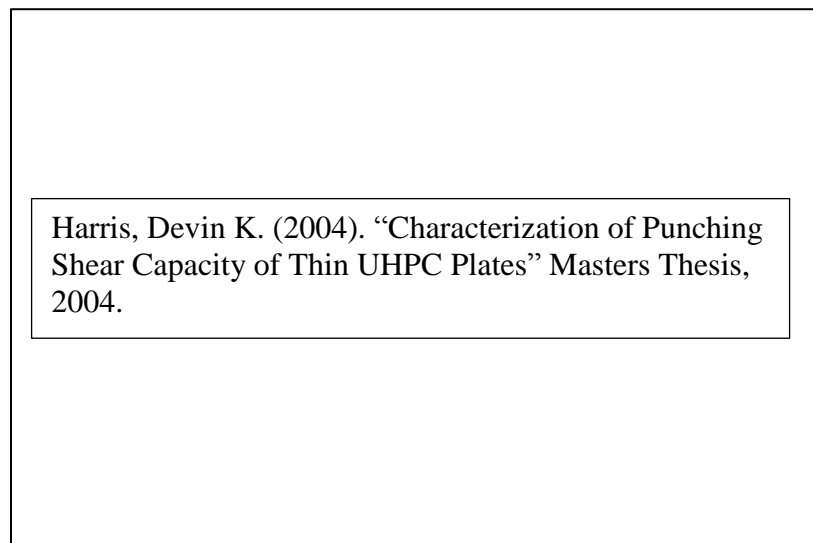


Figure 2.2.1 – Diagonal cracking resulting from shear forces (Harris 2004)

Shear forces are resisted by a moment couple that is formed by a conical shell at the bottom of the slab which is in compression, and a tension tie provided by the top reinforcement in the slab. Broms (1990) created an illustration of this moment couple resisting the shear forces, seen in Figure 2.2.2. Punching failure of the connection occurs when the concrete inside of the conical shell is crushed, preventing the moment couple from resisting the shear forces.

Broms, Carl E. (1990). "Punching of Flat Plates – A Question of Concrete Properties in Biaxial Compression and Size Effect." *ACI Structural Journal*, No. 87-S30, June 1990.

Figure 2.2.2 – Illustration of the moment couple resisting shear forces (Broms 1990)

Increased punching capacity of slabs can be developed through in-plane lateral compressive forces. Compressive membrane action will occur when the applied loading causes the tensile face of the concrete slab to begin cracking. As loading continues, the stress distribution along the depth of the slab shifts and the max tensile stress on the bottom face becomes larger than the max compressive force on the top of the slab, resulting in a net tensile stress at the slab midpoint (Vecchio and Tang 1989). This shift in the strain distribution is illustrated in Figure 2.2.3.

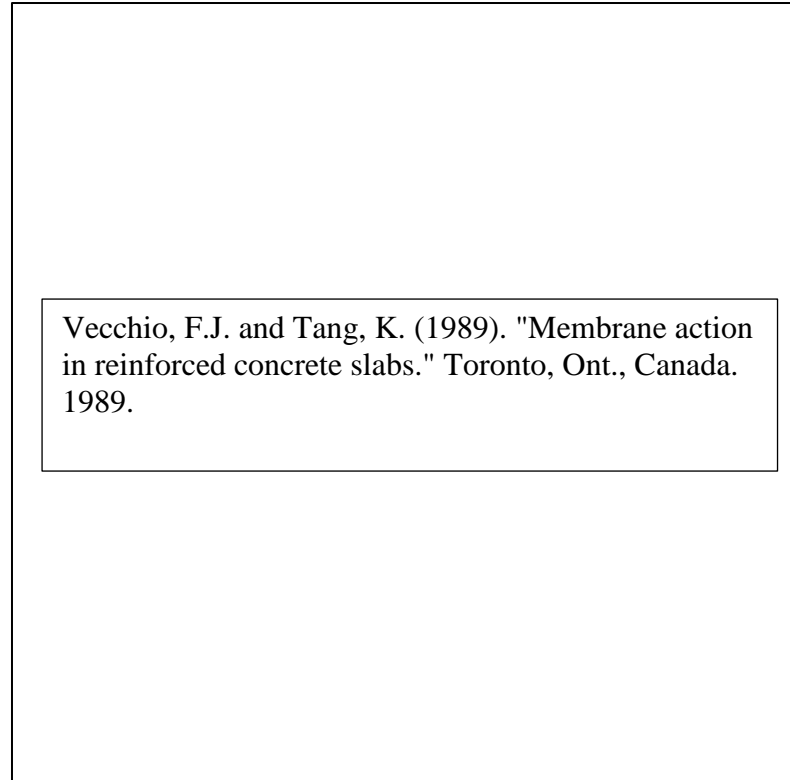
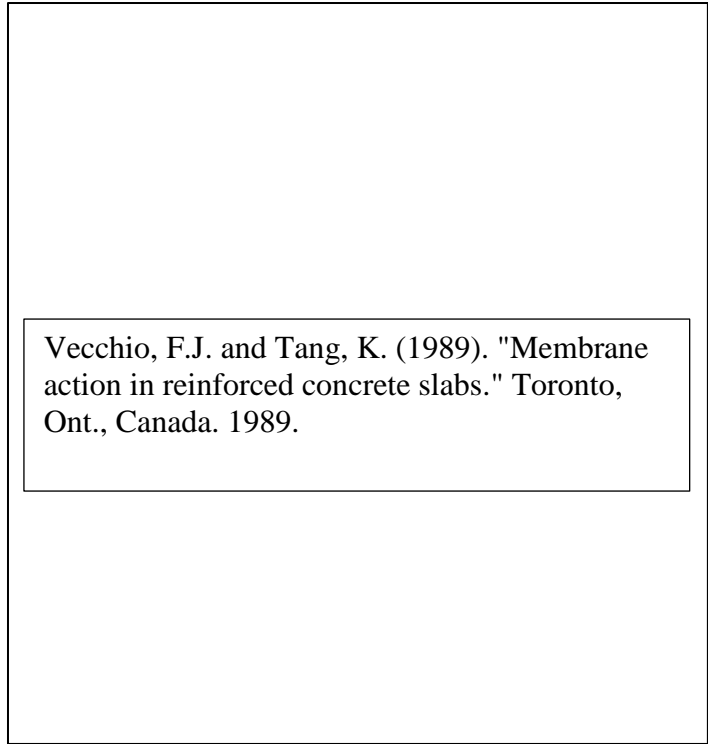


Figure 2.2.3 – Resulting net tensile stress at slab midpoint (Vecchio and Tang 1989)

The net tensile stress of the slab results in the slab attempting to expand outward between column connection points. This expansion is restricted by the connection between the slab and column, resulting in applied compressive forces in the lateral direction. These induced compressive forces in the slab will increase the punching and flexural capacity, and as a result increase capacity of the slab itself. Figure 2.2.4 displays this compressive force and shows the relationship between applied lateral compression and resulting flexural capacity.



**Figure 2.2.4 – Illustration of compressive membrane forces and relation to flexural capacity
(Vecchio and Tang 1989)**

Punching shear failures are of brittle nature and as a result can occur rapidly without any apparent warning. In comparison, flexural failures are ductile and have well defined warning signs that can be identified before complete failure occurs. After initial punching failure has occurred, the load initially carried by that particular support must be transferred to the surrounding connections. The amount of load being redistributed will depend on whether or not the failed connection develops any residual post-punching capacity. If the redistributed loads are too large, overloading of surrounding connections can occur causing subsequent failures, potentially leading to progressive collapse. The redistribution of loads and equilibrium of the structural system will occur at a dynamic rate. The concept for the research presented in this project is to more accurately simulate

this scenario by dynamically loading isolated slab column connections and observing the response.

2.2.1 Current Design Codes

There are current design standards that can be used to calculate the expected punching shear capacity of a typical structural connection. In most cases, the codes will not account for all of the strength present in the connection and results may vary depending on the design code chosen. The following section will highlight some of the more common design standards used to predict punching shear capacity of slab-column connections.

The equations discussed are based on established codes published by the ACI, Eurocode 2, and Model Code 90. The results obtained from each source will be dependent on the variables deemed critical to the connection capacity. One of the most common differences among them is the definition of the critical section area. The critical section for punching shear capacity is defined as the area surrounding the column in which the failure crack is expected to occur.

The ACI code defines this critical section as a distance $d/2$ from the face of the column (ACI 2008). In contrast, the Eurocode 2 defines the critical section at a distance of $1.5d$ from the face of the column (Eurocode 1998). The largest assumed critical section of the three methods is given in the Model code 90, in which the critical section is defined to be $2d$ from the column face (Model Code 90). By comparing the definition of critical section area alone, it can be seen that these three common codes can vary by a wide margin when predicting capacity.

The ACI provides three separate equations to calculate shear capacity. The smallest value calculated among the three equations is determined to be the controlling value. These equations are seen as Equations 1-3 below. The values used in the calculations are as follows; V_c is the shear strength of the slab, d is the effective depth, b_o is the perimeter of the critical section, α_s is an empirical factor based on column location in the structure, β is the ratio of the long side of the column to the short side, and f'_c is the compressive strength of the concrete. Equation 1 will control for rectangular columns, Equation 2 for exterior/corner columns, and Equation 3 controls for interior square columns.

$$V_c = (2 + \frac{4}{\beta})\lambda\sqrt{f'_c}b_o d \quad \text{Equation 1 (ACI 1999)}$$

$$V_c = (\frac{\alpha_s d}{b_o} + 2)\lambda\sqrt{f'_c}b_o d \quad \text{Equation 2 (ACI 1999)}$$

$$V_c = 4\lambda\sqrt{f'_c}b_o d \quad \text{Equation 3 (ACI 1999)}$$

The Model Code (1990) equation uses slightly different input parameters for the calculation of shear capacity. The following parameters include; concrete strength f'_c , reinforcement ratio ρ , effective slab depth d , and the critical section perimeter b_w (at a distance $2d$ from the column face). The calculation can be seen in Equation 4.

$$V_c = \left[0.12 \left(1 + \left(\frac{200}{d} \right)^{\frac{1}{2}} \right) (100 * \rho * f'_c)^{\frac{1}{3}} \right] b_w * d \quad \text{Equation 4 (Model Code 1990)}$$

As with Model Code 90, the Eurocode 2 has a slight variation in the input parameters due to the different critical area assumption. They are as follows; compressive concrete strength f'_c , reinforcement ratio ρ , effective slab depth d , and the critical section

perimeter b_w (at a distance $1.5d$ from the column face). The calculation can be seen in Equation 5

$$V_c = [0.167(1.6 - d)f_c(1.2 + 40 * \rho)]b_w * d \quad \text{Equation 5(Eurocode 2, 1998)}$$

2.3 Material Strength Under Dynamic Loading

Structural elements subject to a dynamic loading exhibit a higher strength than a similar element under static loading rates. After initial failure of a slab column connection in a flat plate structure, load redistribution to surrounding connections will occur at a dynamic rate. As a result, the rapid rates of strain occurring in both the concrete and steel reinforcement will lead to increase in material strength. Increased strengths of steel and concrete are used to evaluate the resistance of slab column connections to applied dynamic loading.

A dynamic increase factor, DIF, is used to quantify the material strength increase under dynamic loading. The DIF is the ratio of dynamic stress to static stress and is dependent on the strain rate of the element. Higher strain rates will correlate to a higher DIF for steel and concrete materials. A document by the Unified Facilities Criteria (UFC) of the US Department of Defense, discusses the behavior of reinforced concrete structures subject to dynamic blast loading. The final design of structural members subject to dynamic loads may be significantly affected when the proper DIF values are applied. Table 2.3.1 presents typical design DIF factors that can generally be used.

Table 2.3.1 – Dynamic Increase Factor (DIF) for design of Reinforced Concrete Elements (UFC)

<p>Unified Facilities Criteria. (2009). “Design of Buildings to Resist Progressive Collapse (UFC 4-023-03).”</p>
--

Due to the large influence DIF may have on the design of structural members, the DIF factors can be calculated and compared to the typical values given in Table 2.3.1. Figure 2.3.1 (UFC) is a plot of DIF values for compressive concrete strength in relation to the average strain rate of the concrete. Figure 2.3.2 (UFC) is of the same format and presents DIF values for both the yield and ultimate steel strengths in relation to the average steel strain rate. Calculation of the DIF values based on the strain rate will result in a more realistic estimate of the ultimate flexural resistance, shear, and bonding stresses resisted by the structural member.

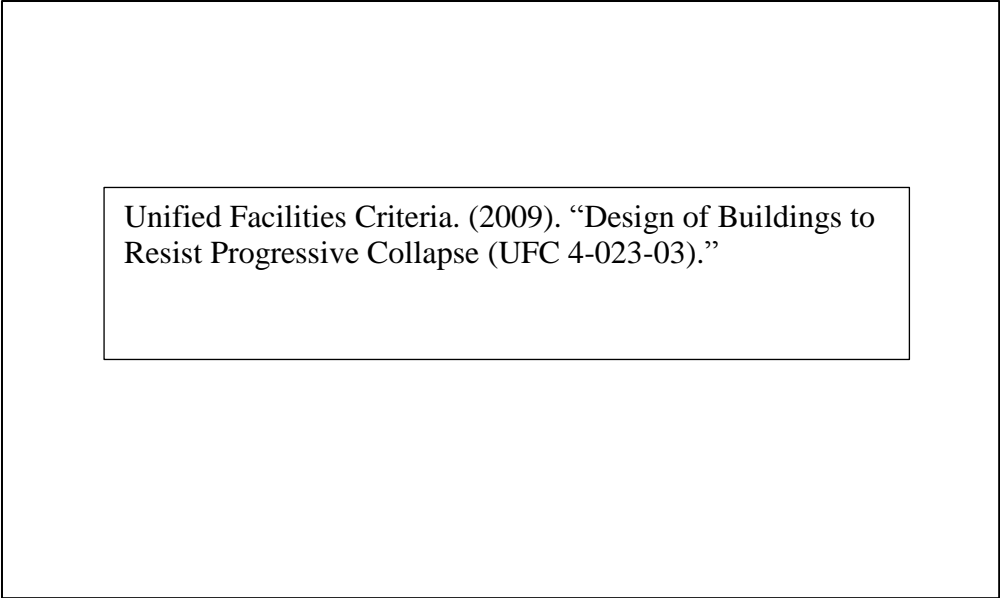


Figure 2.3.1 – DIF for Ultimate Compressive Concrete Strength (2500psi - 5000psi) (UFC)

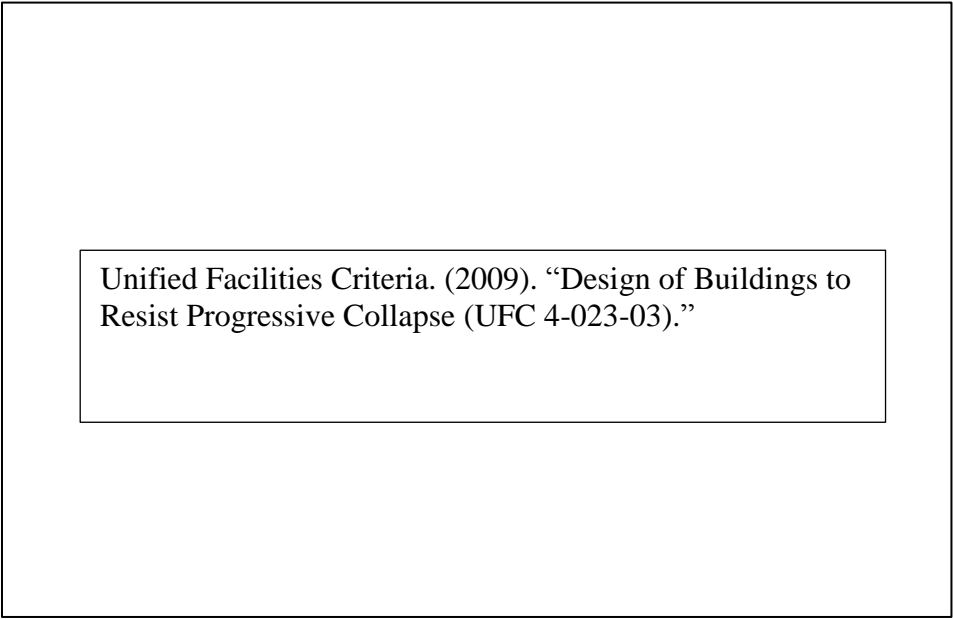


Figure 2.3.2 – DIF for Yield and Ultimate Stresses of Reinforcing Steel (UFC)

2.4 Previous Dynamic Testing

For older flat-plate building structures, when a supporting column member is removed, the likelihood of progressive collapse will depend on the strength and deformation capacity of the surrounding support connections. These surrounding connections will be subject to increased shear and unbalanced moment loads applied at a dynamic rate. Available capacity of these connections to resist further collapse will depend heavily on in-plane lateral restraint, loading rate, and the ability to develop any post-punching capacity. To date, there is limited knowledge on flat plate structures subject to fast loading. This chapter will discuss previous research involving dynamic loading and other relevant topics for reinforced concrete structural members.

2.4.1 Ghali, Elmasri, and Dilger (1976)

The tests completed by Ghali, Elmasri, and Dilger observed the strength and deformation of flat slab floors at the slab-column connection subjected to static or dynamic horizontal forces. The research consisted of six full scale slab-column connections subject to a constant axial force representing the gravity load, and a varying static and dynamic moment transferred between the column and the slab. The specimens tested had variable amounts of flexure reinforcement and no shear reinforcement. A general illustration of the slab-column specimens tested can be seen in Figure 2.4.1.1.

Ghali, Elsmari and Dilger (1976). "Punching of Flat Plates Under Static and Dynamic Horizontal Forces."
ACI Structural Journal, No. 73-47, October 1976.

Figure 2.4.1.1 – Slab Specimen and Applied Loading of Ghali, Elmasri, Dilger (1976)

The results of their testing indicated higher strength, rotational ductility, and energy absorption capacity in the dynamically loaded specimens. When comparing the specimens based on amount of flexural reinforcement; the slabs displayed higher strengths, lower ductility, and lower energy absorption capacity as the amount of bending reinforcement increased. This relationship was seen for both the static and dynamically loaded specimens. The results of the six tests completed by Ghali, Elmasri, and Dilger can be seen in Table 2.4.1.1.

**Table 2.4.1.1 – Summary of Test Data and Results by Ghali, Elmasri, and Dilger
(1976)**

Ghali, Elsmari and Dilger (1976). “Punching of Flat Plates Under Static and Dynamic Horizontal Forces.” *ACI Structural Journal*, No. 73-47, October 1976.

The tests under dynamic loading assumed a strain rate of 0.04 to 0.05 per second. The calculated dynamic strength increase under the dynamic loading was determined to be 25 percent for concrete and 15 percent for steel reinforcement. This increase factor was determined using the Air Force Design Manual developed in 1962. Experimental strengths obtained from testing exhibited actual DIFs of 15, 18, and 28 percent for corresponding reinforcement ratios of 0.5, 1.0, and 1.5 percent, respectively.

2.4.2 Criswell

The overall analysis reported by Criswell considered results from two testing programs, the first of which consisted of testing of full scale isolated slab-column connections, and the second being one-quarter scale nine panel slab models. The isolated slab tests included a total of nineteen tests, 8 statically loaded and 11 dynamically loaded. Isolated specimens were constructed to represent the design model; 6.5 inch slab, with 17 foot. 6 inch column spacing and supported on rollers at the assumed contra-flexure line on the slab. Typical values for concrete strength (4000psi – 5600psi), reinforcement ratio (.75% - 1.5%), and nominal column size to depth ratio (2 or 4) were used in the isolated slab

specimens. Dynamic loads were applied at a rise time of approximately 9 to 32 milliseconds, simulating a blast-loaded structure. The load was applied to the column stub using a pull bar extending through the column. The pull bar was then connected to a hydraulic testing device capable of the desired loading rates. A typical slab-column connection specimen tested by Criswell can be seen in Figure 2.4.2.1.

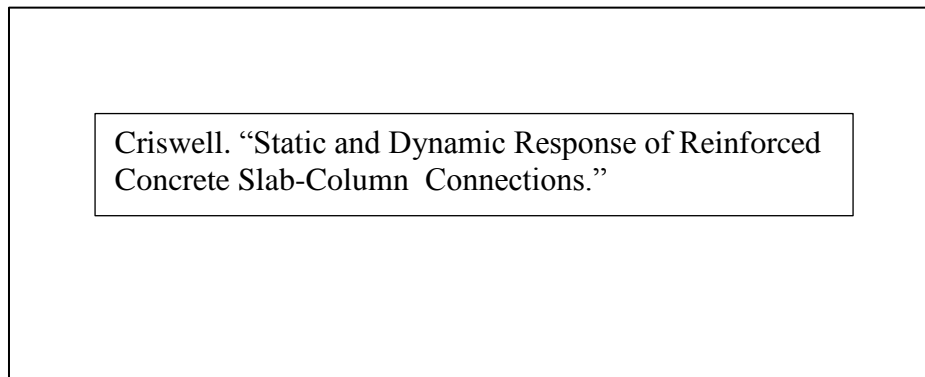


Figure 2.4.2.1 – Criswell Slab-Column Specimen (Criswell)

The study by Criswell noted several important points to consider when using isolated slab-column specimens to study the response of a much more complex slab system. These points apply to the wide usage of isolated slab-column tests, both static and dynamic. Criswell notes two particular limitations that the slab-column connections do not replicate in relation to the actual slab system. The first is inaccurate modeling of in-plane forces resulting from the more heavily stressed regions around the column jamming against other portions of the slab system. The second significant limitation is the lack of continuity in the model that is needed to allow the contra-flexure line to move and redistribute moments as different portions of the slab reach yielding. As a result of these limitations, isolated specimens have a tendency to underestimate shear capacity and overestimate the ductility, particularly in lightly reinforced connections.

Results of the dynamic tests simulating blast loading can be found in Figure 2.4.2.2. Deflections of the dynamically loaded slabs increased 25 to 50 percent in comparison to the static load tests. The specimens also experienced a strength increase factor under the dynamic loading; an average of 18 percent increase on lightly reinforced slabs and 26 percent dynamic increase for more heavily reinforced slabs. These values corresponded to the expected strength increase for the observed strain rates during testing. Criswell notes that the dynamic specimens displayed the same general behavior around connection areas for both static and dynamic loading tests.

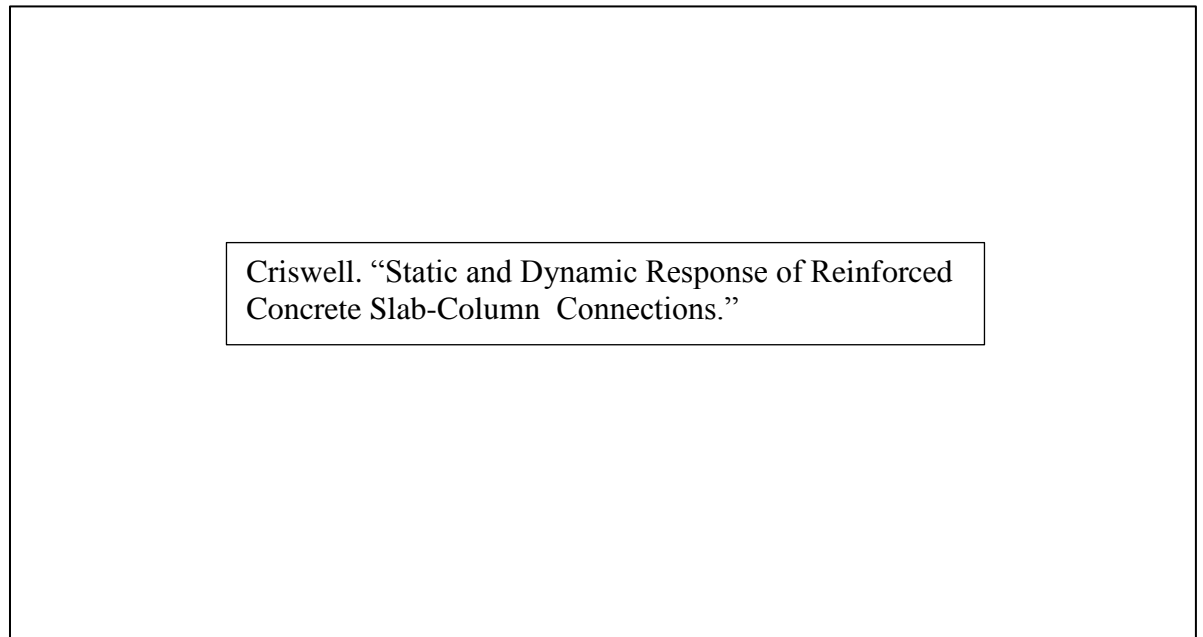


Figure 2.4.2.2 – Load and Deflection Response Results of Criswell Testing (Criswell)

Criswell states that very large dynamic loads can be resisted by a slab if the loads are very rapidly applied and have duration considerably shorter than the time required for flexural yielding to develop around the loaded area. As a result, certain loading rates will correspond to different failure modes in a slab-column connection. Another conclusion

of the tests was that compressive in-plane forces increase compressive strength, but may increase flexural strength of lightly reinforced slabs at a higher rate, causing shear to become more critical.

2.4.3 Zinneddin and Krauthammer (2007)

This study was completed at the Department of Civil and Environmental Engineering HQ of the United States Air Force. The objective was to determine the dynamic response and behavior of reinforced concrete slabs under impact loading. Three different slab types were tested, each slab was 3.5 inches thick with length of 11 feet and width of 5 feet. The first slab type was reinforced with two (6"x6") welded steel wire meshes, the meshes were placed at the top and bottom of the slab with 1 inch cover at both locations. The second slab type consisted of one (6"x6") No. 3 reinforcing bar mesh placed at the mid-point of the slab thickness. The third and final slab type consisted of two (6"x6") spaced No. 3 reinforcing bar meshes, one mesh placed at the top of the slab and the other at the bottom with both having 1 inch of concrete cover. The slabs were tested with a drop hammer device, the impact mass had an approximate weight of 5750 pounds. Each of the three slabs was tested at drop heights of 6 inches, 12 inches, and 24 inches for a total of nine tests.

In general, the test results were typical for that of a drop test on a reinforced concrete specimen. The maximum load was relatively the same for each of the reinforcement types and the presence of additional reinforcement induced a localized punching failure, this failure type seen in each test can be seen in Figure 2.4.3.1.

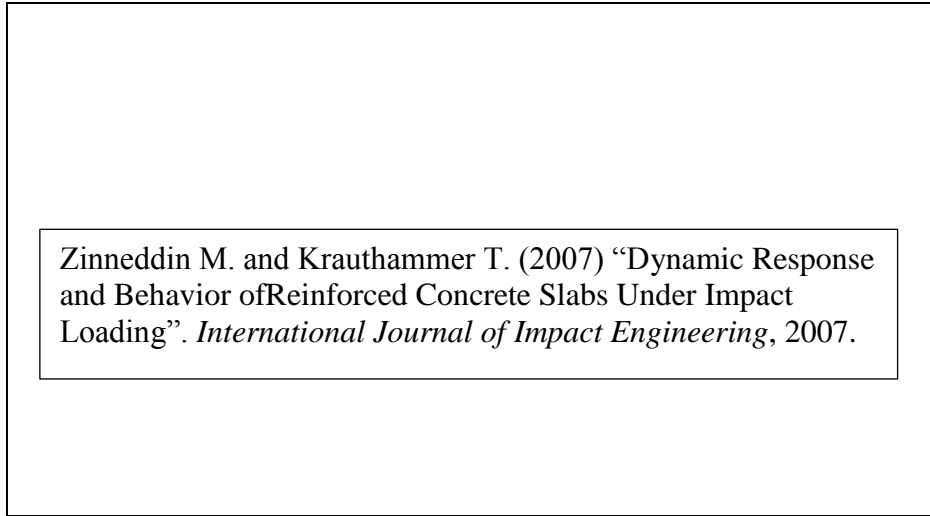


Figure 2.4.3.1 – Crack pattern and punching shear on top slab face (Zinneddin 2007)

In contrast, the less reinforced specimens still resulted in a brittle failure due to the response of the drop weight with the concrete member. In the case of mesh wire reinforcement, the weight directly cut the wire in a shear manner, rather than developing any sort of flexural behavior. The direct shearing of the wire mesh can be seen in Figure 2.4.3.2.



Figure 2.4.3.2 – Direct shearing of mesh reinforcement (Zinneddin 2007)

2.4.4 Jacobs and De Roeck

Testing done by Jacobs and De Roeck consider static and dynamic loading of pre-stressed concrete beams. A 253 pound weight is dropped from an approximate height of 3.3 feet at one end of the beam which is subject to free-free conditions. The boundary conditions are achieved by lifting the beam on air cushions and fixing steel cables to prevent movement in the lateral and transverse direction while still allowing bending and torsional rotation. Static loads are initially applied to the specimen to induce cracking and controlled damage. After the desired static load is reached, it is completely removed and a series of dynamic tests. The dynamic tests are performed to determine eigenfrequencies, mode shapes, damping values, and modal strains. The dynamic strains in the specimen were measured using Fiber Optic Sensors (FOS) placed both internally and externally at two different cross sectional locations. The dynamic test setup is seen in Figure 2.4.4.1.

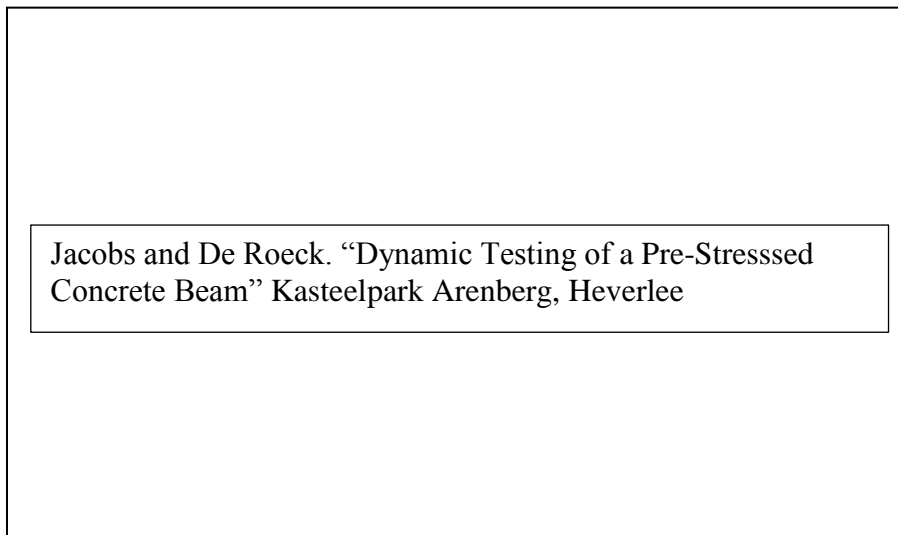


Figure 2.4.4.1 – Dynamic beam test setup (Jacobs)

Conclusions from the testing showed that the eigenfrequencies drop with increasing damage to the beam, with significant drops noticed once the reinforcement begins to yield. Changes in the mode shape of the beam are also noticed as the reinforcement begins to yield. Bending stiffness decreases around areas that the largest cracks have occurred. Although these tests were performed on beams that behave in a different manner than an isolated slab-column connection, these general behaviors seen in dynamic testing of concrete members could possibly still apply to our results.

2.4.5 Habibi et al. (2012)

An important aspect to consider when evaluating the potential progressive collapse of a flat-plate structure is the post-punching capacity of the slab-column connections. A study conducted by Habibi et. al (2012) was done to further research post-punching capacity, specifically in relation to integrity reinforcement. Slabs tested for this research were constructed in accordance with the Canadian CSA A23.3 Standards. Slab-column specimens tested without integrity reinforcement failed in a brittle manner immediately after initial punching failure, showing little to no post-punching capacity. It was determined that the presence of structural integrity reinforcement could greatly improve the post-punching load carrying capacity of the slab-column connections. Tests performed on specimens constructed with integrity reinforcement present displayed the ability to provide significant post-punching capacity. Complete failure of these specimens occurred in one of two ways; pulling out of the reinforcement from the

concrete cover, or fracture of the reinforcing bars. A photo of a typical test specimen can be seen in Figure 2.5.5.1.

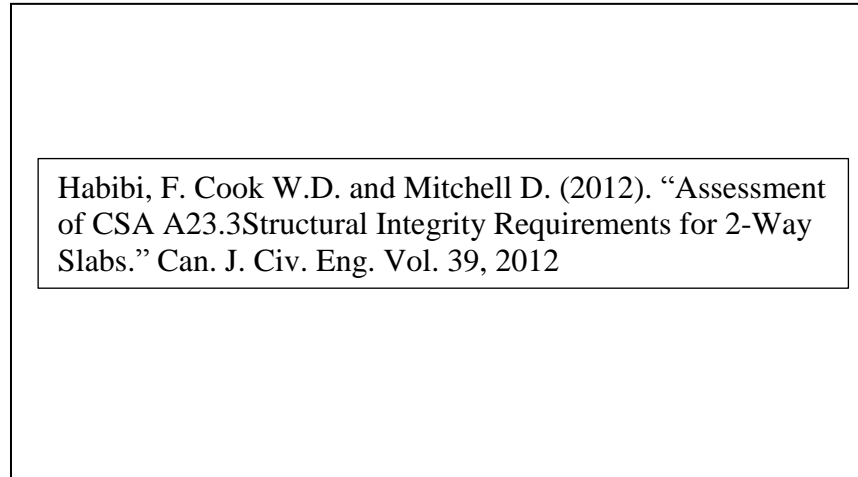


Figure 2.4.5.1 – Slab-column connection test specimen (Habibi 2012)

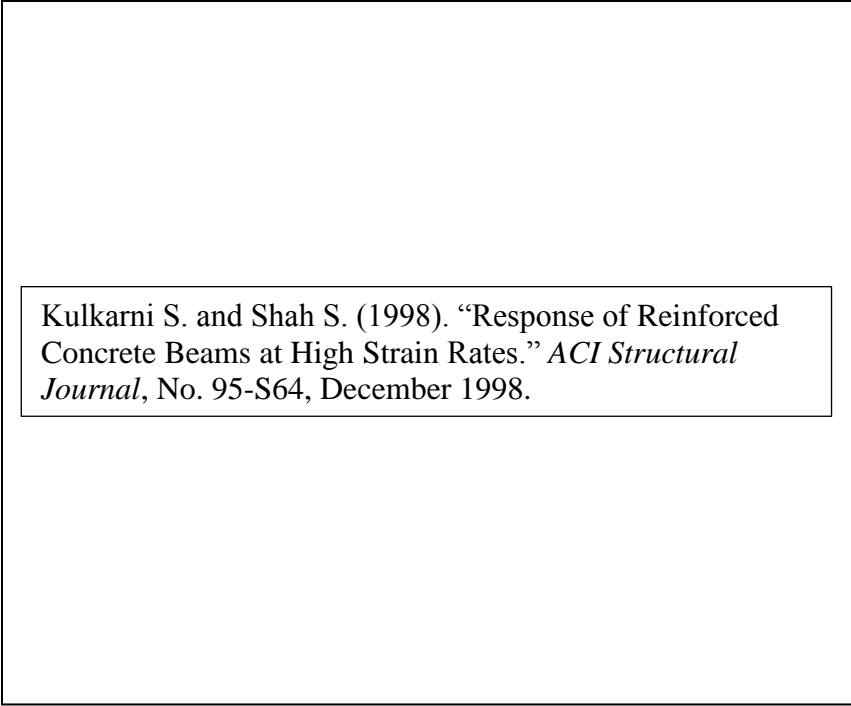
It was shown that increasing the slab thickness and providing the reinforcement with additional concrete cover increased the post-punching capacity, this is due to the additional force required to rip reinforcement from the slab. In general, the thicker slabs failed due to fracture of the reinforcement while reinforcement pull-out occurred more frequently in thinner slab designs. An equation to predict post punching capacity of the slab-column specimens was generated by Habibi. This equation is presented as Equation 1, where V_{se} is the post punching resistance, A_{sb} is the total area of integrity reinforcement and f_y is the yield strength of the reinforcement.

$$V_{se} = 0.5 * \sum(A_{sb} * f_y)$$

Equation 6 (Habibi 2012)

2.4.6 Shah and Kulkarni (1998)

The tests performed by Shah and Kulkarni utilized a hydraulic loading apparatus to conduct high rate tests on reinforced concrete beams. A total of seven pairs of beams without shear reinforcement were tested under displacement controlled conditions. Each “pair” of beams consisted of one statically loaded beam (piston velocity = 0.00071 cm/sec) and one dynamically loaded beam (piston velocity = 38 cm/sec). The dynamic loads in this test are designed to replicate that of a seismic loading. Behavior of the specimens indicated that peak load and energy absorption increased at higher rates of strain. The total number of cracks observed in the beams also reduced significantly in the higher strain rate tests. One interesting result of the beam tests performed is the shifting of final failure mode from shear at static rates to flexural failure at the dynamic rate. This phenomenon is opposite to the brittle mode of failure reported by other researchers conducting similar tests. This behavior is believed to be related to the rate sensitivity of the different steels used throughout these studies. The setup used to test the reinforced beams can be seen in Figure 2.4.6.1.



Kulkarni S. and Shah S. (1998). "Response of Reinforced Concrete Beams at High Strain Rates." *ACI Structural Journal*, No. 95-S64, December 1998.

Figure 2.4.6.1 – Beam test setup (Shah 1998)

In the report, Shah and Kulkarni propose that inertia plays a significant role in the failure mode of reinforced concrete members subject to high loading rates. While the rate sensitivity of certain materials and nature of the loading factor into the failure mode, it is proposed that significant inertial forces force the beams to take on a different deflected shape in comparison to the shape under static loading. The results of the test show that spacing of the cracks is observed to increase with higher loading rates. As a result this study concludes that after yielding, the strain on the bar becomes localized at these crack locations. The localized strain on the reinforcement can have an influence on the post-yielding shape of the beam, and possibly cause premature fracture of the reinforcing bars.

Kulkarni S. and Shah S. (1998). "Response of Reinforced Concrete Beams at High Strain Rates." *ACI Structural Journal*, No. 95-S64, December 1998.

Figure 2.4.6.2 – Load – Deflection results and crack patterns for tested beam specimens

(Shah 1998)

The results in Figure 2.4.6.2 display what was seen for most of the “pairs” of beams tested. The statically loaded specimens reached a peak load before a sudden shear failure occurred. The interesting result of the tests performed is the transition from brittle failure to the flexural response seen in the load displacement plots. Figure 2.4.6.2 also includes the crack profiles from the four beams represented on the load displacement plots. It can be seen that the dynamic tests had less overall cracking and were concentrated around the point of load application.

3. Experimental Setup

A total of nine isolated slabs were tested throughout this research project, six of which were statically loaded and the final three under dynamic loading. This paper focuses specifically on the dynamic isolated tests.

The previous research consisted of statically loaded slabs with reinforcement ratios of either 1.0% or 0.64%. The static tests also consisted of two different configurations, one with lateral restraint applied and one without lateral restraint applied. The three dynamically tested slabs were either 0.64% or 1.0% reinforced and under full restraint conditions for each of the three tests.

This chapter will discuss the design and construction process of the isolated slab specimens. The design and construction parameters of the overall prototype structure, the isolated slab specimens, and the test setup will be detailed in this chapter. The prototype structure was designed to replicate a desirable flat plate structure prone to a progressive collapse. The slab column connections of this prototype were then scaled down and a test setup was designed accordingly to perform the punching shear tests on the specimens.

3.1 Prototype Structure Design

The design of the prototype structure was one of the initial tasks early in the overall research project. The structure was designed using the 1971 ACI concrete provisions to replicate an older style flat plate reinforced structure with discontinuous bottom reinforcement, due to their susceptibility to progressive collapse. The structure is five stories tall and has a square layout that consists of four bays in each direction. The supporting columns were spaced 20 feet apart in each direction. Concrete and steel

material properties were chosen for the design structure as well. Concrete unit weight was assumed to be 150 pcf and the 28 day compressive strength was 4000psi. The steel reinforcement was assumed to have a yield strength of 60 ksi. The assumed loading on the structure consisted of a 20 psf dead load, 50 psf live load, as well as the self weight of the slab. The reinforcement was designed to have a minimum cover of 0.75 inches and the minimum slab thickness was calculated to be 6.875 inches. The design thickness was chosen to be 7.5 inches to satisfy the minimum requirement; each column was designed to have a 15 inch by 15 inch cross section. Bending moment in the slab was calculated from the design loads to determine the tensile and compressive reinforcement using the direct design procedure. The main focus of this research is the punching capacity of these slab column connections, which is directly influenced by the reinforcement ratio. As a result, a high reinforcement ratio of 1.0% and a lower ratio of 0.64% were utilized in different test specimens. A plan view of the prototype structure can be seen in Figure 3.1.1.

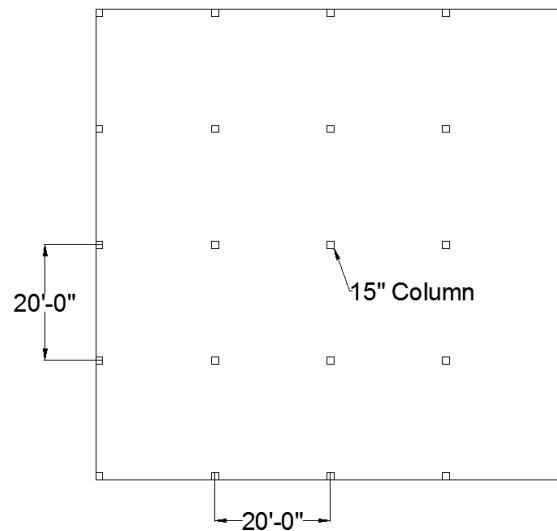


Figure 3.1.1 – Plan view of prototype structure

In a continuous framing system, large negative moments develop near the column and large positive moments are seen at the mid-span locations. Due to this moment distribution, the bottom slab reinforcing bars are not needed to resist the negative moments and are discontinuous through the column. Figures 3.1.2 and 3.1.3 provide sketched of the top and bottom reinforcing bar layouts, respectively. The bottom bar discontinuity seen in the prototype design is acceptable according to procedures in the ACI 1971 design code. If this structure were to be designed with a post 1971 ACI code, the slab bottom bars would need to be continuous through the column to provide structural integrity reinforcement.

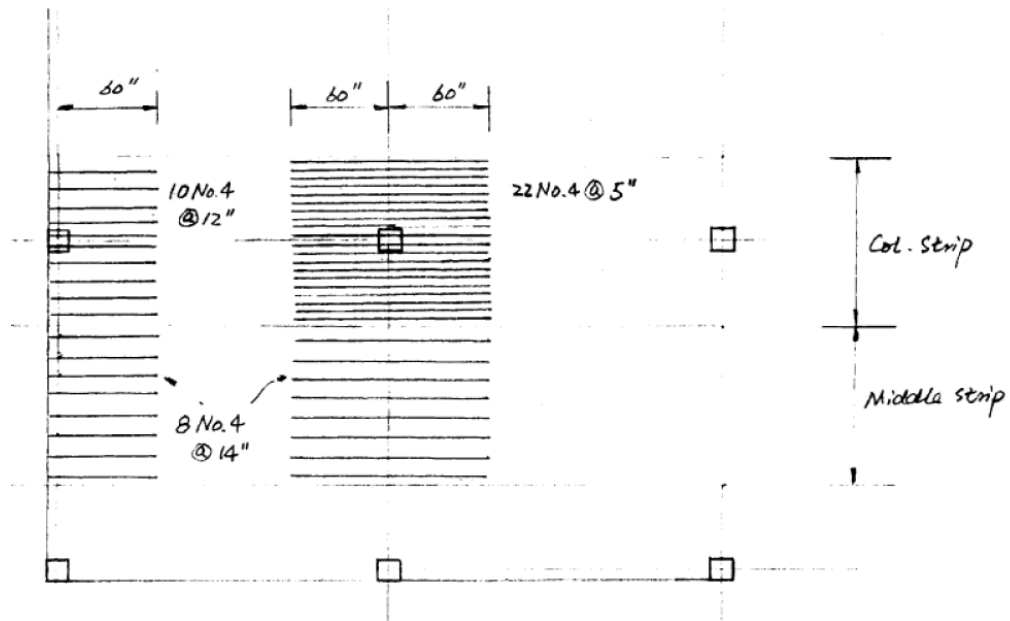


Figure 3.1.2 – Initial sketch of top reinforcement in the prototype structure

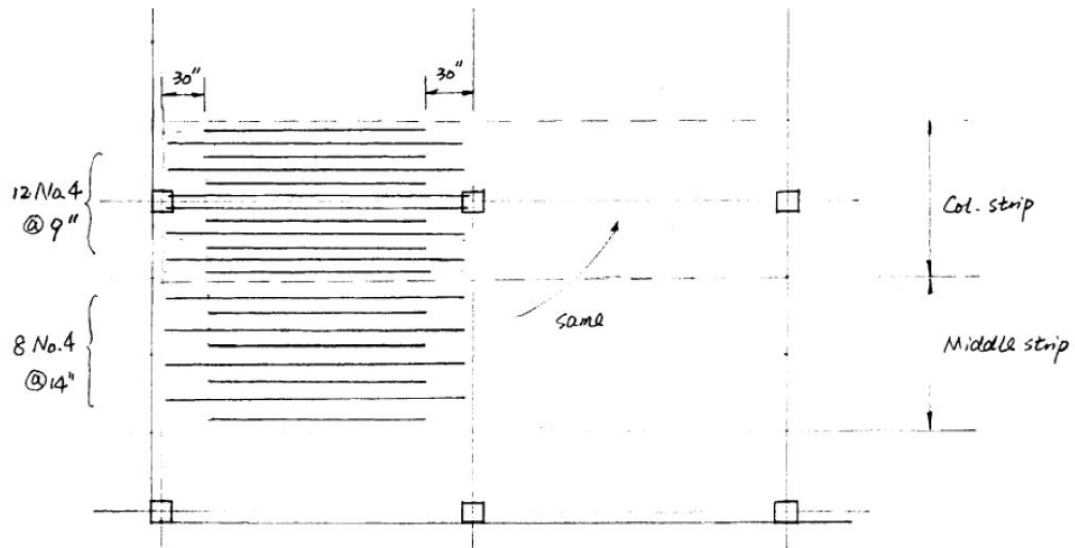


Figure 3.1.3 – Initial sketch of bottom reinforcement in the prototype structure

3.2 Design of Test Specimens

Isolated slab-column specimens are tested to simulate an interior slab column connection, the relation between these isolated specimens to the overall prototype structure can be seen in Figure 3.2.1. The isolated specimens were also designed to replicate older flat-plate structures that are the basis of this research due to their susceptibility to progressive collapse. This phase of research focused on the dynamically loaded isolated specimens, these test specimens still followed the same design parameters as previous isolated tests. Specimens were constructed at a 0.73 scale due to the overall constraints of the testing facility. The overall dimensions of the slab were 70 inch by 70 inch with a thickness of 5.5 inches. The column stub extended above and beneath the slab 9 inches, and had a cross sectional area of 11 square inches. These overall dimensions were the same for each of the nine isolated slab tests.

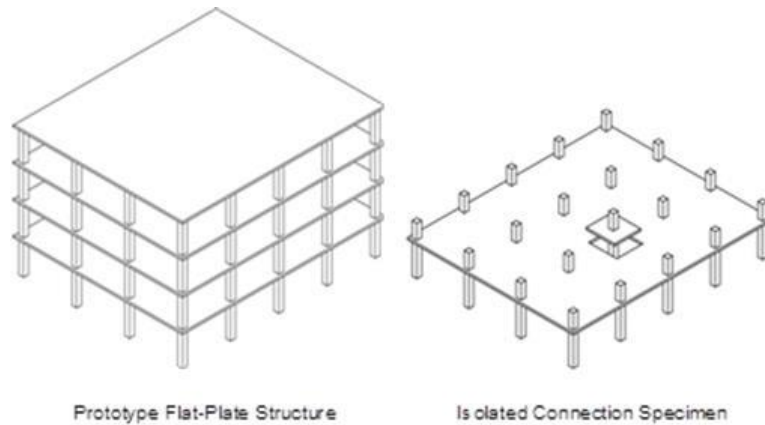


Figure 3.2.1 – Isolated slab removed from the overall prototype structure

While the overall dimensions were consistent for each isolated slab, each individual slab was designed with either a 1.0% or 0.64% reinforcement ratio. Slabs with a 1.0% reinforcement ratio used #4 reinforcing bars spaced 4.5 inches center to center for tensile reinforcement and #3 bars spaced 4.5 inches center to center for the compression reinforcement. The 1.0% reinforcement layouts can be seen in Figures 3.2.2 and 3.2.3.

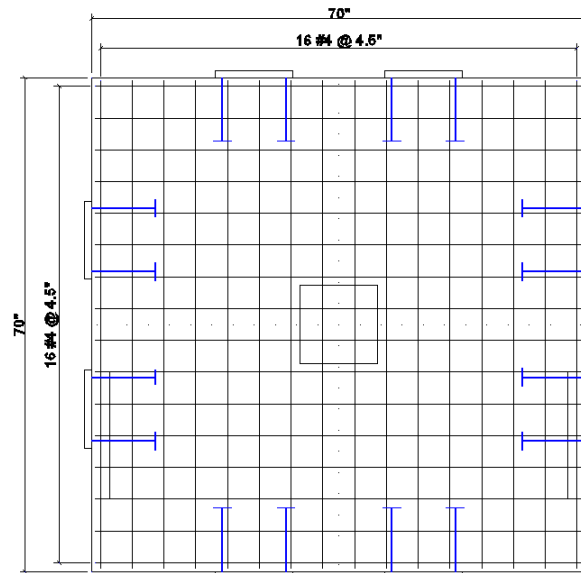


Figure 3.2.2 – Tension reinforcement for 1.0% reinforcement ratio

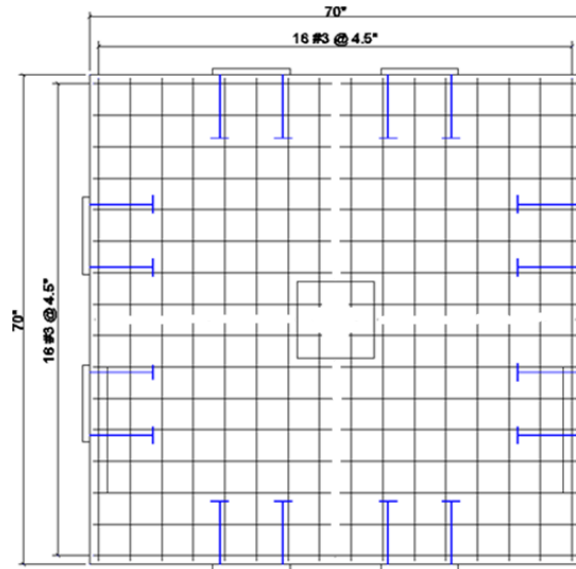


Figure 3.2.3 – Compression reinforcement for 1.0% reinforcement ratio

The slab specimens designed with 0.64% reinforcement ratio used #4 bars spaced 7 inches center to center for tensile reinforcement and #3 reinforcing bars spaced 7 inches center to center for compressive reinforcement. The compression and tension reinforcement layouts for 0.64% ratio can be seen in Figures 3.2.4 and 3.2.5.

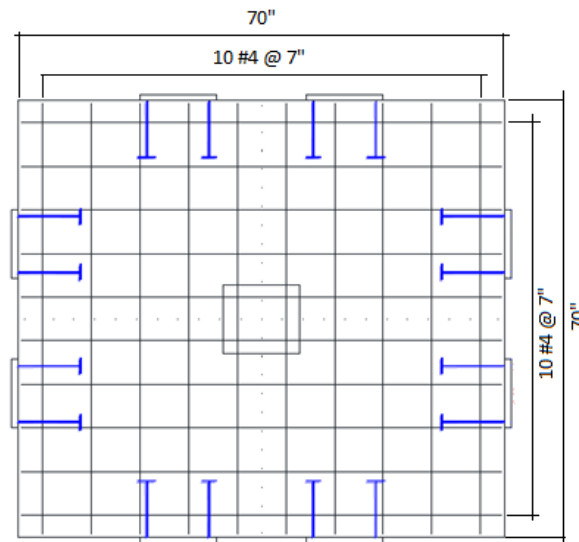


Figure 3.2.4 – Tension reinforcement for 0.64% reinforcement ratio

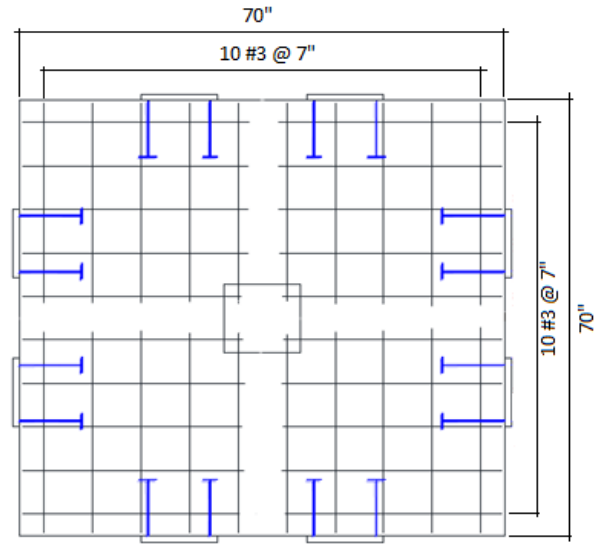


Figure 3.2.5 – Compression reinforcement for 0.64% reinforcement ratio

The column stub extending above and beneath the slab was reinforced with four #6 longitudinal reinforcing bars. The vertical column reinforcement was tied with #3 stirrups every 3 inches through the column. An overall elevation view of the slab specimen and a cross section view of the column can be seen in Figures 3.2.6 and 3.2.7.

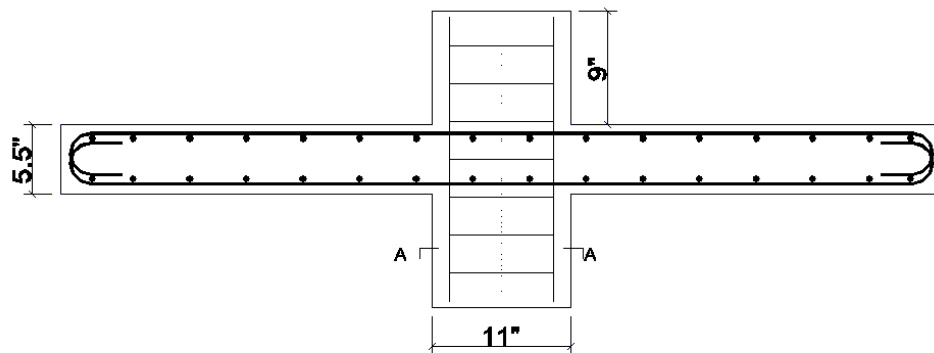


Figure 3.2.6 – Elevation view of slab column specimen

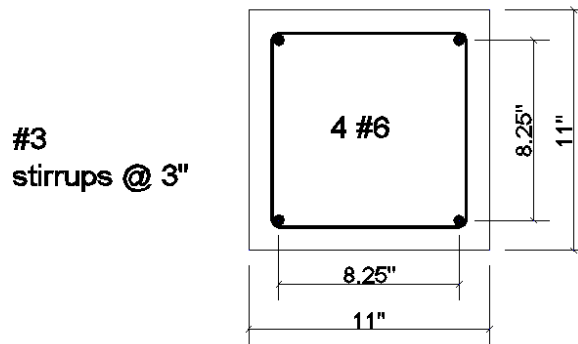


Figure 3.2.7 – Cross section view of column section

In following the ACI design codes from 1971 the compressive reinforcement was not continuous through the column; this causes the lack of “integrity reinforcement” seen in older flat plate buildings prone to progressive collapse. The tensile reinforcement was designed to be continuous through the column, as seen in Figures 3.2.2 and 3.2.4. Initial isolated slab tests used reinforcing bars with hooks on the end as seen in Figure 3.2.6. These hooks allowed for the reinforcing bars to develop their full stresses due to inadequate development length within the slab. These hooks, however, were only used in the first four test specimens. The final two static test slabs and all three dynamically tested slabs utilized straight reinforcing bar.

3.3 Test Specimen Construction

The construction process for the isolated slab column specimens followed the same general procedure for each of the nine specimens. The first step in the construction process was to construct wooden formwork for the concrete specimen. The formwork was raised nine inches above ground level to provide spacing for the column stub protruding from both sides of the slab. Once a solid base was created at the correct

height and properly leveled, $\frac{3}{4}$ inch plywood was screwed into the base to form the base for the slab itself. A hole was cut into the plywood to allow the bottom portion of the column to cast properly. The slab itself was designed to be 5.5 inches thick which allowed standard 2x6 wooden boards to be used around the perimeter of the formwork. The 2x6 edge boards required no modification as they are actually 5.5 inches in height. Four 2 x 6 boards were used to create the 70x70 inch cross sectional area above the plywood base. The 2x6 boards were braced along their length to avoid any bending or movement while casting the concrete. Two additional plywood boxes were constructed to the dimensions of the upper and lower column stub dimensions. Each stub was 11 inches squared and extended nine inches from the face of the slab. Since the formwork was raised, one column box was placed beneath the plywood base, properly aligned with the pre-cut hole. The top column form was suspended in place using two 2x4 boards spanning across the formwork. It was important to ensure the 5.5 inch spacing between the plywood base and top column form, as the slab thickness at the column-slab interface is critical. After removing the hardened concrete from the form, minor repairs were made to reuse the formwork or a completely new form was constructed. An example of the completed formwork can be seen in Figure 3.3.1.



Figure 3.3.1 – Completed isolated slab formwork without top column form in place

The initial formwork created for the isolated slabs required additional modification to cast certain elements into the slab. These elements were required to connect the slab to the test setup. A total of 16 threaded rods were cast into the slab, four on each side. The location of each was determined and holes were drilled in the 2x6 perimeter boards. The threaded rods were 12 inches long, with roughly 9 inches embedded in the concrete. PVC pipes were also used to cast holes running vertically through the slab near each connection. The PVC was cut to the proper length and holes were drilled in the plywood base at the proper locations. The PVC pipes would later be placed into the pre-drilled locations and secured in place. The embedded threaded rods and vertical holes through the slab allowed the slab to be properly secured to the test setup.

The next step in preparing the slab to be poured was placing the slab and column reinforcement. Measurements were constantly taken throughout this process to ensure the correct spacing between reinforcing bars and to ensure adequate concrete cover. A

photo of the slab and column reinforcement, along with a final measurement ensuring proper slab depth can be seen in Figure 3.3.2.

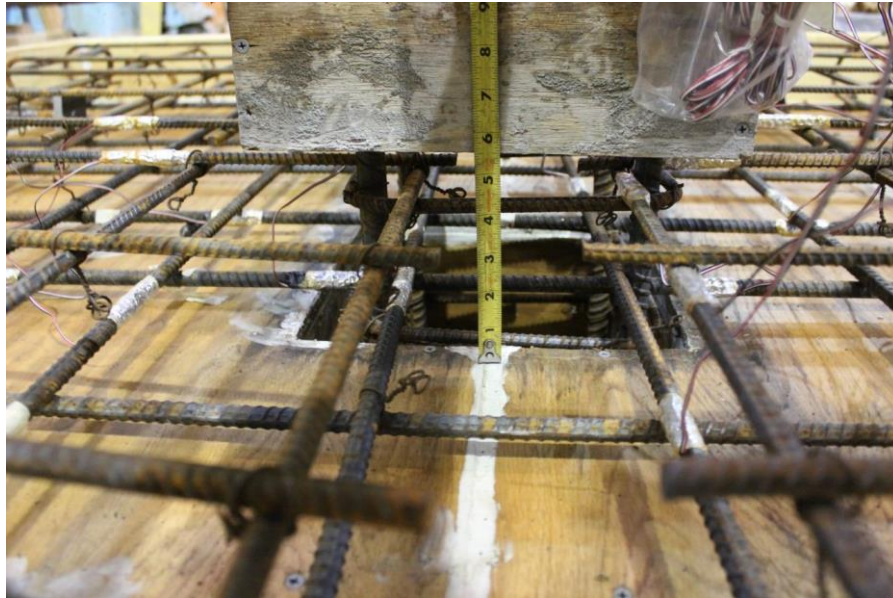


Figure 3.3.2 – Picture of formwork with rebar placed and top column form in place

Once the slab reinforcement was in place and properly tied, the remaining vertical stirrups were installed and tied to the vertical reinforcement. The top column formwork could then be slid over the column reinforcement and final measurements were taken to ensure column alignment, slab thickness, and reinforcement spacing. The next step was to install the PVC pipes that had been previously cut to length. The PVC pipes were inserted vertically into the proper locations in the base of the formwork. Steel wire was used to secure the PVC pipes and free ends of the anchor rods to help keep them in place during the concrete pour. An example of completed formwork ready for concrete pour can be seen in Figure 3.3.3.

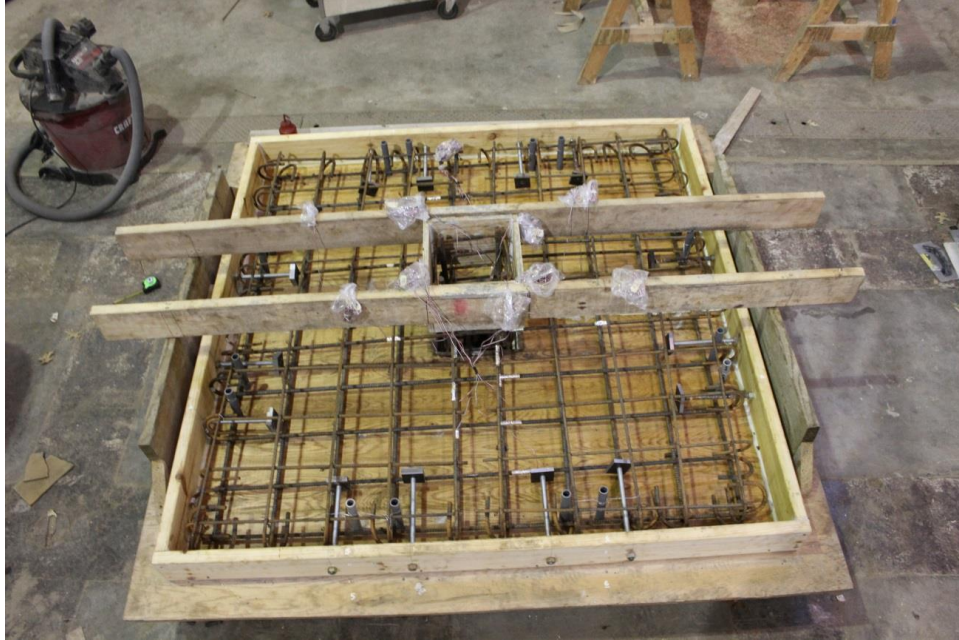


Figure 3.3.3 – Completed slab formwork prior to concrete pour

Once the formwork was properly assembled and all of the reinforcement was in place, the slab was ready to be poured. Concrete was placed into the form using shovels rather than directly dumping from the truck. This allowed careful placement of the concrete to avoid damaging instrumentation or any disturbance to components such as the vertical PVC pipes. The concrete was vibrated as the form was filled to aid consolidation along edges and into the column. Vibration was monitored to ensure the concrete was not over consolidated such that unwanted segregation would occur. Once the form began to fill with concrete, 2x4 boards were used to screen the surface and ensure a uniform slab thickness of 5.5 inches. Screening was made simple by the fact that the outside 2x6 boards were 5.5 inches in height as well. It was important to ensure a level surface beneath the top column form as the concrete had a tendency to flow out when vibrated. An increase in slab thickness around the slab-column interface would have direct effects on the punching strength of the slab. Once the slab was poured and the surface was

smoothed, dampened canvas or plastic sheets were placed over the top. These sheets helped prevent shrinkage of the slab by reducing evaporation; the slabs were monitored closely and kept hydrated for the first week of curing. A picture of a finished slab just after pouring can be seen in Figure 3.3.4.



Figure 3.3.4 – Slab after pouring and surface finishing was complete

3.4 Test Setup Design

This section will discuss the details of the test setup used to test the isolated slab specimens. The overall test setup was identical for each of the nine isolated tests specimens except for the loading actuator and presence of lateral restraint. There were two major conditions specified for each of the nine isolated tests. These conditions were the presence of lateral restraint and whether static or dynamic loading was used. The

restrained test setup created in-plane forces, these forces resemble what would be seen in an actual flat plate structure. The use of dynamic loading also allowed us to take another step in replicating a progressive collapse scenario to replicate the accurate load rate. Figures 3.4.1 and 3.4.2 show 2D and 3D renderings of the test setup, respectively.

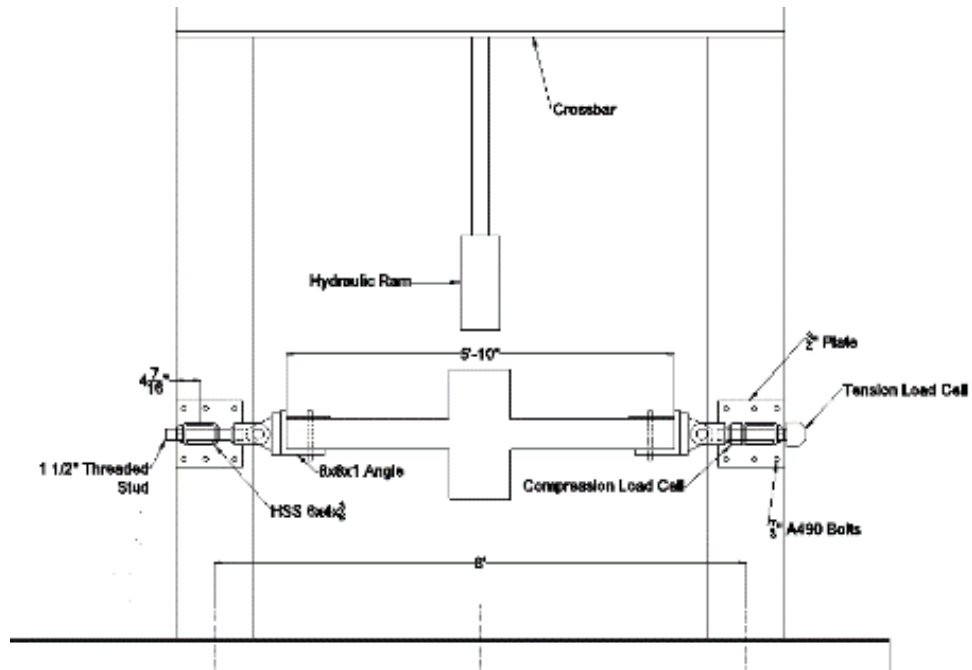


Figure 3.4.1 – 2D view of test setup with slab installed

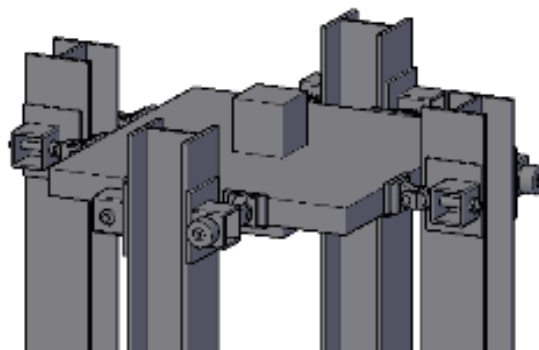


Figure 3.4.2 – 3D view of final test setup

It can be seen that four large W14x132 wide flange sections were used to support the slab and provide stiffness in the horizontal direction. These large flange sections were bolted to the lab floor using large threaded rods and plates at the bottom. Large steel cross braces were bolted in each direction roughly 5 feet above the slab. These braces provided extra stiffness and stability to the vertical W14x132 flanges and also served as the location to attach the static or dynamic loading ram. Careful consideration was used in determining how to effectively connect the slab to four vertical flanges. Eight identical connections were fabricated, two on each side of the slab. An 8x8x1 angle section was cut to 12 inch length; one leg of the section would support the slab while the other leg would connect to a horizontal bracket-female clevis assembly. The bracket was bolted to the angle and the female clevis was then pin connected to the bracket. This pin connection allowed rotational translation of the slab to take place during testing. A threaded stud was then connected to the female clevis. Sliding this threaded rod through a HSS 6x4x3/8 section provided the support for the slab. The HSS section was welded to a plate that was bolted to the large vertical flanges. After sliding the threaded rod through the HSS section, a nut was threaded on the outside to be tightened and provide the desired lateral restraint. This nut could be removed, however, to allow the rod to move laterally and simulate the unrestrained testing condition. The connections allowed adequate spacing to install compressive or tensile load cells to measure the in-plane forces. A schematic of the connection can be found in Figure 3.4.3 and a picture of the assembled connection with a tensile load cell is seen in Figure 3.4.4.

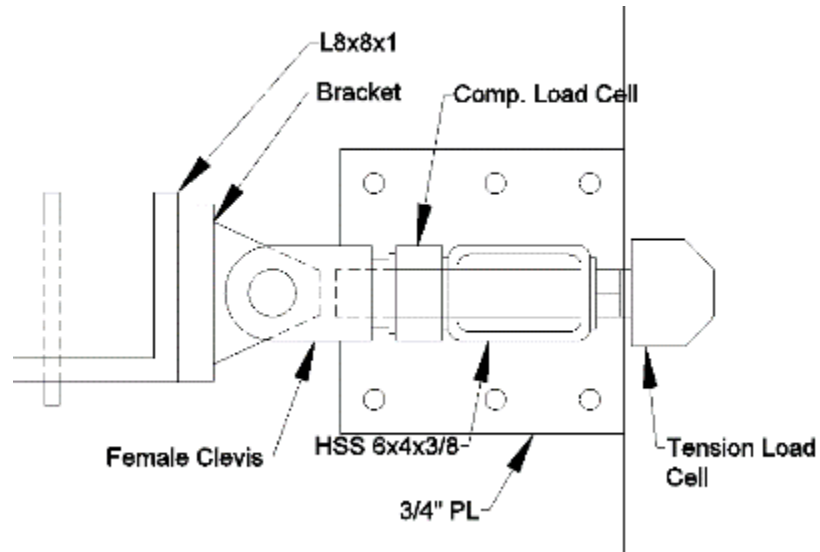


Figure 3.4.3 – Schematic of restrained connection



Figure 3.4.4 – Complete assembly of support connection to steel frame

It was important to keep in mind that these connections would need to be used to test each of the isolated slabs throughout this research project. The process of installing and removing these connections and the slab itself was carefully thought out to ensure

consistent testing and safety of those involved. Each new slab was initially supported by a fabricated wooden cart and rolled into the test setup. The 5/8 inch threaded anchors and vertical PVC holes cast into the slab were used to secure the base angle section to the slab. As seen in Figure 3.4.4, holes were drilled in both legs of the angle section. Before attaching the angle to the slab, the pinned clevis and rod assembly would be bolted to the vertical face of the angle. After attaching the angle to the slab, the pinned rod was free to rotate. The HSS section welded to the steel plate was then picked up and the threaded rod was slid through the hole in the HSS section. The plate welded to the HSS section was then bolted to the large vertical W14x132 support framework. After assembling each of the eight connections, it was important to check that the slab was level and properly centered beneath the hydraulic ram. Since not all slabs were cast in the same formwork, it was important to ensure the precast anchors and vertical holes would properly align with the pre-fabricated connections. Details of the anchorage setup can be seen in Figure 3.4.5 and a photo of the assembly just prior to casting the slab can be seen in Figure 3.4.6.

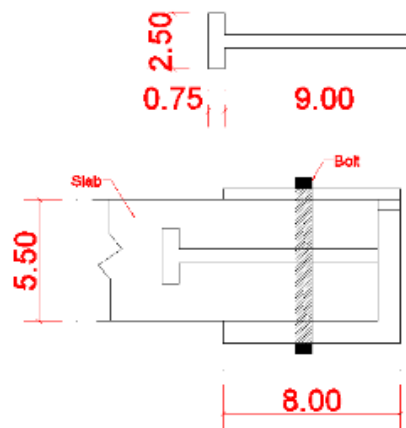


Figure 3.4.5 – Details of anchorage and connections to support angle



Figure 3.4.6 – Anchorage assembly and vertical PVC to be cast into slab

The goal of the test setup was to provide lateral restraint while vertically loading the slab. Although the large W sections seemed to provide the necessary lateral restraint, preliminary testing showed outward movement of the columns when testing specimens were loaded. To prevent movement of the columns, angles were welded to the lab floor at the base of the columns. Two bolts were threaded through the welded angle to rest against the base of the column and prevent the outward movement being observed. The angle and bolt setup can be seen in Figure 3.4.7.



Figure 3.4.7 – Angle stops welded at the base of each vertical column

Another modification was made to the vertical W-section columns. Physical testing and FE model analysis verified that the column flanges were twisting under the resulting lateral loads during the testing. The interior flanges were being spread apart while the exterior flanges were being pushed closer together. The flanges of the W section were modified by adding compression and tension bracing in the respective areas. The exterior flanges were braced to resist compression by welding a HSS section at the height of the applied lateral load. On the opposite side of the section, two high strength 7/8 inch threaded rods were used to resist the outward movement of the flanges. The rods ran through existing holes that were used to secure the support connections to the vertical columns. The HSS sections welded to provide compressive bracing can be seen in Figure 3.4.9.



Figure 3.4.8 – Compression brace welded to support columns

The final detail of the test setup was the hydraulic actuator used to load the specimen. The actuator was bolted to the horizontal cross bracing connecting the large vertical support sections. The first six slabs utilized a statically controlled ram, while the final

three tests required a different actuator capable of the necessary dynamic loading rates. In each test, a one inch thick steel plate was placed at the top of the column. With the same 11 inch by 11 inch area, the plate evenly distributed the loading force across the entire column cross-section. The dynamic actuator hung vertically from a pinned connection and was free to rotation. A picture of the actuator prior to testing can be seen in Figure 3.4.10. This dynamic actuator was powered by a separate accumulator, seen in Figure 3.4.11. This accumulator was used to achieve an increased flow rate through the dynamic system which was necessary to power the hydraulic ram. Once the hydraulic system was turned on, a valve was opened, allowing the accumulator to be filled with hydraulic oil at the pump pressure of 3000 psi. The test was initiated with a custom fabricated solenoid valve. A remote switch opened the solenoid valve and the oil in the accumulator moved into the actuator at a high flow rate. This higher flow rate enabled faster movement of the actuator and the ability to dynamically load the specimens. The actuator was rotated away from the column and chained in place to prevent any unintentional loading of the slab before testing.



Figure 3.4.9 – Test setup with dynamic actuator, full ram displacement



Figure 3.4.10 – Hydraulic tank used to power ram

3.5 Instrumentation

Various instruments were used to record data from the test specimens. The types of instruments included steel and concrete strain gages, load cells (tension and compression), string pots, and LVDT's (linearly varying displacement transducers). A high speed data acquisition system was developed to gather data from the dynamically tested isolated slabs. This section will discuss the manner in which each of these instruments was utilized.

Before the reinforcing bar was placed in the formwork and tied into the designed cage layout, strain gauges were attached. Critical areas of interest were chosen prior to slab

construction and layouts of strain gages locations were created. The strain gage layout was determined for the compression and tension reinforcement. In order to compare results from test to test, the strain gage layout remained the same for each isolated slab specimen. Minor differences did occur between slabs that were 1.0% reinforced and 0.64% reinforced, this is expected as the reinforcing bar layout is not identical for these two cases. The strain gage locations were chosen to observe the change in strain relative to the distance away from the interior column. The strain data is especially significant in comparing results of the static and dynamic isolated tests. It was important not to place too many gages nearby on the same reinforcing bar as this may interfere with the bar's bond to the concrete. The compressive and tensile strain gage layout for the 0.64% reinforcement ratio test specimens can be found in Figures 3.5.1 and 3.5.2, respectively.

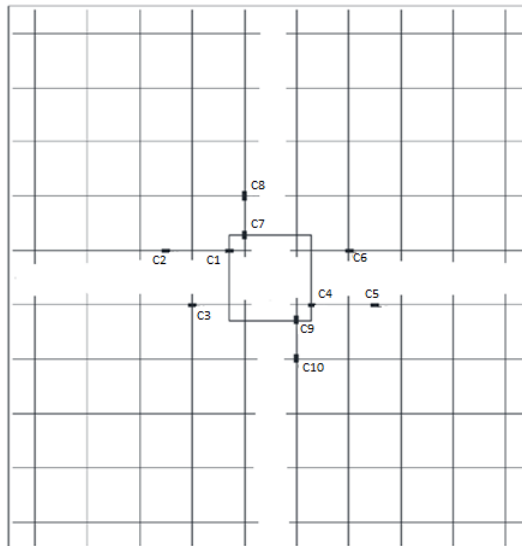


Figure 3.5.1 – Compression reinforcement strain gage layout for 0.64% reinforcement ratio

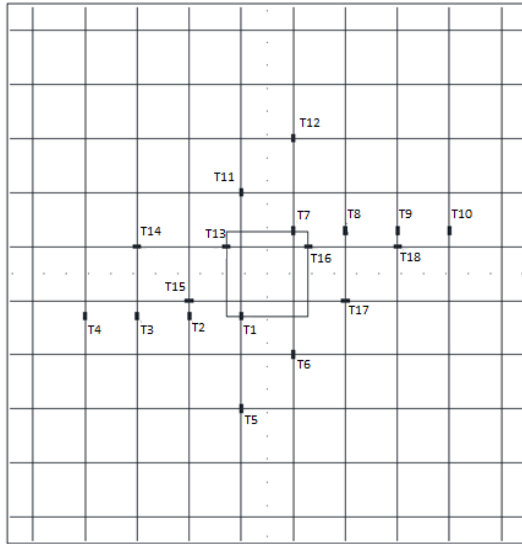


Figure 3.5.2 – Tension reinforcement strain gage layout for 0.64% reinforcement ratio

As previously mentioned, the layout for the 1.0% reinforcement ratio slabs had a slightly altered strain gage layout in comparison to the 0.64% reinforcement ratio slabs. The 1.0% reinforcement ratio slabs had 31 applied gages, 21 for the tension reinforcement and 10 applied to the compressive reinforcement. The gages were positioned to gather data from the same general locations, but a higher reinforcement ratio led to more reinforcing bar available for applying gages. The compressive and tensile strain gage layout for the 1.0% reinforcement ratio test specimens can be found in Figures 3.5.3 and 3.5.4, respectively.

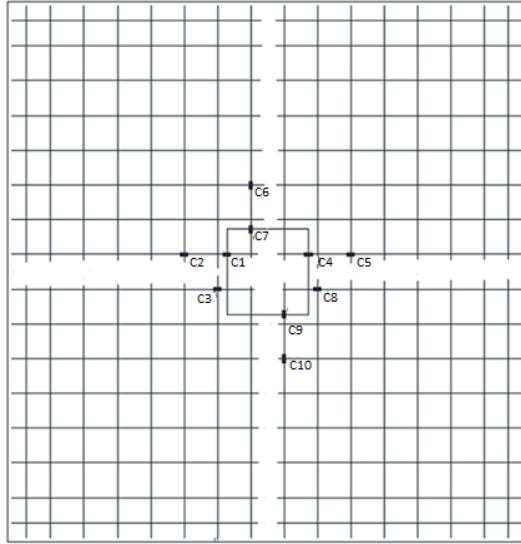


Figure 3.5.3 - Compression reinforcement strain gage layout for 1.0% reinforcement ratio

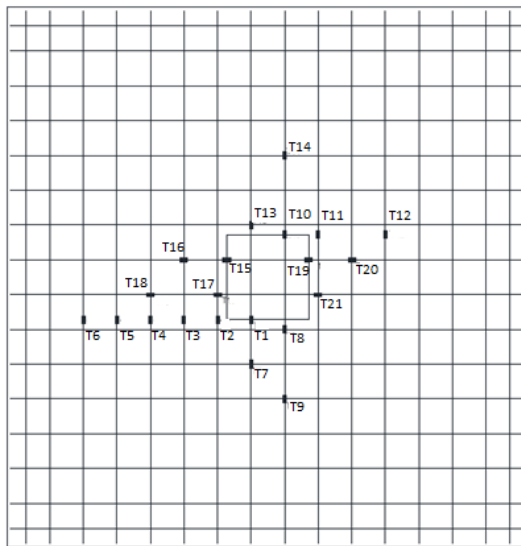


Figure 3.5.4 - Tension reinforcement strain gage layout for 1.0% reinforcement ratio

Any lateral movement or expansion of the slab during testing was recorded with LVDT's placed around the perimeter of the slab. Four LVDT's were used to measure the movement of the slab, one LVDT placed at the center of each outside facing edge of the slab. The outside faces of the slab were 70 inches long by 5.5 inches high; the midpoint

of the cross section was marked to be the point of contact for each LVDT. A picture of one of the four LVDTs placed against the slab exterior can be seen in Figure 3.5.5. It was important to measure all four directions to determine any possible translation, expanding, or contracting taking place as the specimen was loaded. These LVDT's were set up in the same fashion for each of the isolated slab tests. In addition to the four LVDTs used on the slab itself, additional LVDTs were placed at the end of the threaded rods and at the base of the clevis connection to obtain additional lateral movement data. A picture of a typical setup for these additional LVDTs can be seen in Figure 3.5.6.



Figure 3.5.5 – Picture from above slab showing LVDT against outer face of slab

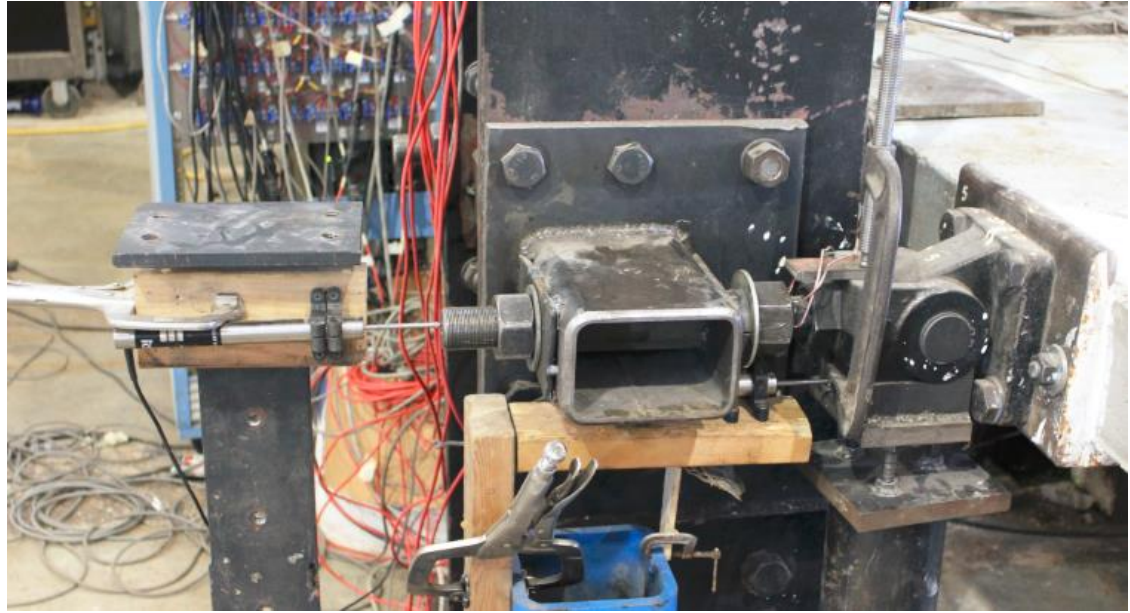


Figure 3.5.6 – lateral LVDTs placed against threaded rod and beneath pin connection

Vertical deflections were measured at various locations of the specimen itself and the test setup as well. The primary location of measuring vertical deflection was the column stub. The stub deflected downward as it was vertically loaded by the hydraulic ram. This deflection was measured in every test by a string pot placed beneath the slab. The string would be initially displaced and attached to the bottom of the column stub. As the test progressed, the string pot recorded the downward displacement of the column. For the dynamically loaded slabs, the hydraulic ram had an internal LVDT that would record the ram displacement as the slab was loaded. The final dynamic test also utilized an LVDT with a large enough displacement range to be used for the column deflection. The string pot located beneath the column for each test can be seen in Figure 3.5.7.



Figure 3.5.7 – String pot located directly beneath bottom column to measure deflection

Vertical displacements were measured at various other locations during the test. Two LVDT's were positioned at the slab surface to measure the downward deflection 10 inches outward from the column face. Vertical deflections were also made of the support movement. These vertical measurements were analyzed to calculate the rotation of the slab during the test as well as determining any resulting vertical translation from the applied loading. These LVDT's were placed at the same locations during each of the isolated slab tests to provide consistent data for comparison between each test.

Load cells were also placed in several different locations to record different resulting forces from the load applied to the center column. After securing the steel plate to the top column surface, a 200 kip compression load cell was placed between the hydraulic ram and the steel plate, a second custom plate was placed on top of the load cell as well. The casing of this specific load cell had three vertical alignment holes. Three identical holes

were drilled into the steel plates above and below the load cell and pins were inserted to keep the load cell and plates in place under the large compressive loading. This was necessary as the hydraulic ram was supported by a hinged connection and could possibly rotate outward during the test without these components fixed together. Figure 3.5.8 is a picture of a dynamic test specimen after testing is complete, the picture shows the ram, load cell with steel plates above and below, and also the remote switch used to operate the hydraulic ram.



Figure 3.5.8 – Dynamically loaded test specimen after failure has occurred

Two additional compression and two tension load cells were also used to measure the in-plane lateral forces for the restrained tests. The load cells were utilized by attaching them to the 1.5 inch threaded rods extending from clevis in the support assembly. The location of the compression and tension load cells in the test assembly can be seen in Figure 3.5.9.

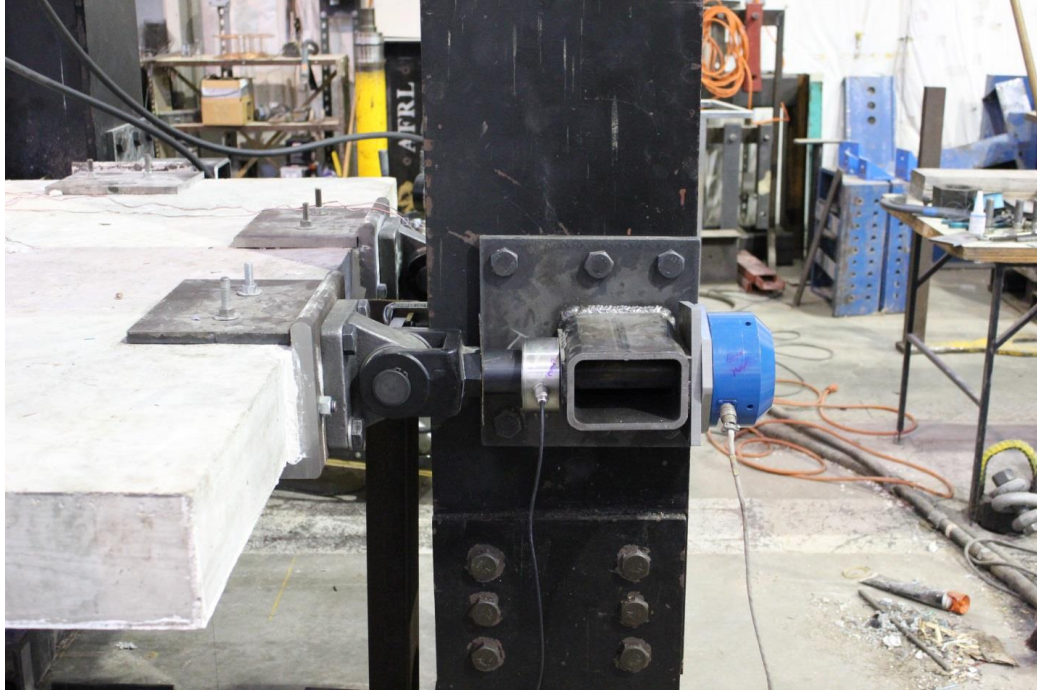


Figure 3.5.9 – Location of tension (blue) and compression (silver) load cells to measure lateral forces

Compression load cells were inserted on the rod before the threaded rod was slid through the supporting HSS section. The tension load cells were directly threaded to the 1.5 inch rods after being inserted through the HSS section. Since the tension rods were threaded, they could be used in place of an exterior nut to tighten the connection. Readings on the load cells were taken before testing to measure the applied loading prior to any force being applied to the column. The compression and tension cells were installed on adjacent columns such that the in plane forces were not being measured directly across from each other.

3.6 Material Properties

Material properties of concrete and steel for the specimens tested were determined according to American Society of Testing and Materials (ASTM) standards. The slab

specimens were designed using a target concrete strength of 4000 psi and steel reinforcement yield strength of 60,000 psi. To ensure accuracy of analysis and comparison between test results, material properties were measured for each of the slab specimen tests. Uniaxial compression tests were conducted on concrete cylinders molded from the same batch used to pour the slab specimens. Compression tests were performed in accordance with ASTM standards to determine the concrete strength at the time testing of the slab specimens took place. The concrete strengths of the three dynamic tests can be seen in Table 3.6.1.

Table 3.6.1 – Concrete compressive strengths for each dynamic test

Slab Specimen	Concrete Compressive Strength psi (Mpa)
Dynamic 1 - 0.64% Reinforced	5560 (38.3)
Dynamic 2 - 0.64% Reinforced	4295 (29.6)
Dynamic 3 - 1.0% Reinforced	4200 (29.0)

The steel reinforcement was tested to improve the analysis of test results as well. The reinforcement was tested in uniaxial tension according to ASTM standards to determine the yield stress, yield strain, and ultimate stress. Two different reinforcing bars were used in the concrete specimens; #3 reinforcing bar for compression mats and #4 reinforcing bar for tension mats. The #3 reinforcing bar had a yield stress of 60,000 psi, corresponding yield strain of 0.0022 in/in and an ultimate stress of 100,900 psi. The #4 reinforcing bar had a larger yield stress of 62,000 psi, corresponding yield strain of 0.0025 in/in and a lower ultimate stress of 98,900 psi.

4. Results

This section will present the results of the three dynamic isolated slab column test specimens. All three of the dynamically loaded specimens were tested under laterally restrained conditions. The first two slabs were constructed with a 0.64% reinforcement ratio while the third and final slab had a reinforcement ratio of 1.0%. The results of each individual test will be presented and discussed in the first portion of this chapter.

Following this will be a discussion and presentation of results between different tests; this will include data from each of the dynamic tests as well as data from previous static tests. Comparisons were made between tests with similar parameters, such as loading rate, reinforcement ratio, lateral restraint and measured concrete strength. A photo of a slab column specimen just prior to dynamic load testing can be seen in Figure 4.1.



Figure 4.1 – Overall view of test setup and slab specimen

4.1 Dynamic 1 Test - 0.64% Reinforced

The slab column test specimens were loaded dynamically with a hydraulic ram capable of a loading speed of 5 inches per second. The test was initiated with a remote switch connected to the hydraulic system, releasing the ram. Test data showed that the punching failure occurred around 0.12 seconds corresponding to a vertical load of 55.1 kips and center column displacement of 1.28 inches. Strain rates observed in the dynamically loaded specimens were observed to be approximately 0.1 strain/second for the steel reinforcement. It should also be noted that the strain rates reported in the results of the first multi-panel specimen tested in this research project reported strain rates ranging from 0.006 to 0.02 strain/sec. Therefore, the dynamic isolated tests achieved a strain rate that was approximately 10 times the strain rates seen in the multi-panel test.

One full second after the initial loading, the slab reached zero capacity at a center column deflection of 7.5 inches. The load response of the slab specimen vs. the time can be seen in Figure 4.1.1. After punching occurs in the slab column specimen, the load capacity of the connection steadily decreases with increased deflection.

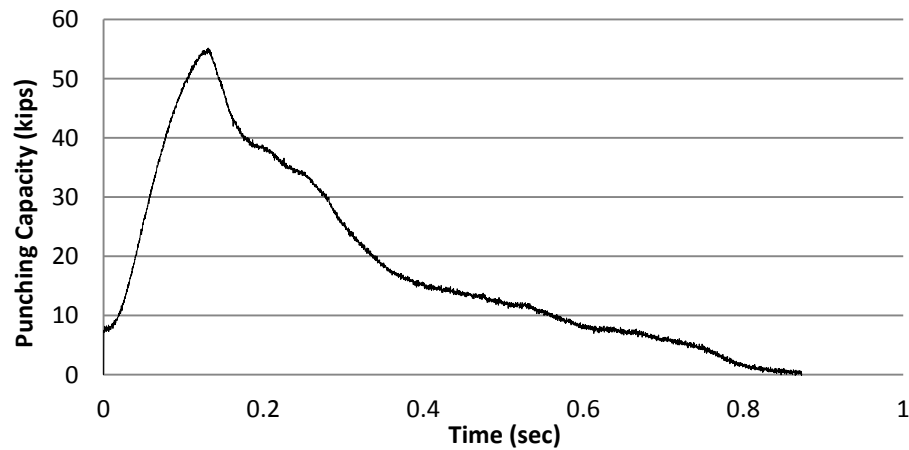


Figure 4.1.1 – Punching capacity vs. time for Dynamic 1 test

Unfortunately an error in the data acquisition system caused a delay in the reading of the load data. This delay was present on all tests. The delay caused a change in shape of the load deflection graph, but not a change in the peak load. Two additional tests will be conducted to determine the effect of the delay. Therefore, this thesis will focus on the only on the peak value of the load and the measured strain and displacement data.

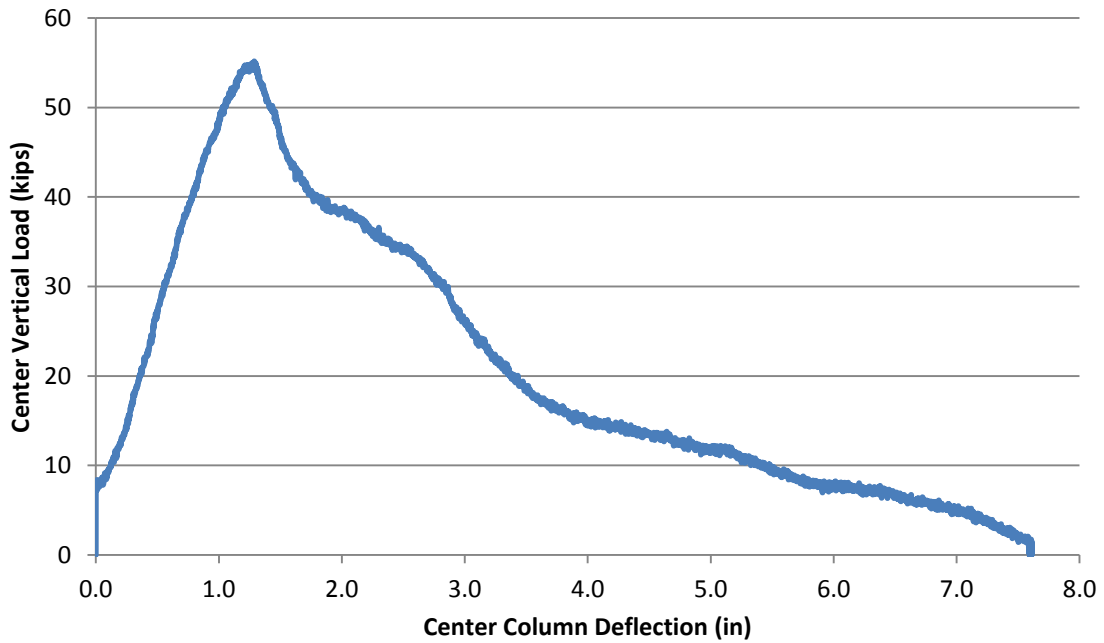


Figure 4.1.2 – Vertical load vs. center column displacement for Dynamic 1 test

The load vs. deflection response of the Dynamic 1 test can be seen in Figure 4.1.2. During each of the dynamic loading tests, as well as the six previous static tests, vertical deflections were measured at two points on the slab. The first location was the vertical deflection of the column; the second was the deflection of the top surface of the slab at a point 10 inches from the column face. Vertical displacements were also measured beneath the support connections that were bolted to the reaction frame. Downward movements recorded at these supports were used to find the true deflection of the slab

relative to its initial position. This was done by subtracting the vertical support movement from the column and 10” distance deflections measured at the slab surface. At punching capacity, the slab column had a deflection of 1.28 inches while the mid slab location deflection was 0.33 inches, 25% of the center column deflection.

The compression and tension reinforcement of the isolated slab specimens were instrumented with strain gages. The strain gages were applied at the same locations for each test specimen, there were minor variations between the 1.0% reinforced and 0.64% reinforced slabs due to differences in the reinforcement layout. A total of 18 strain gages were applied to the 0.64% reinforced dynamic specimens, 13 on the tension steel and 5 on the compression steel. The strain gage layout of the tension and compression reinforcement can be seen in Figures 3.5.2 and 3.5.1, respectively. The tension strain gages were applied to provide a strain distribution of the failure region extending outward from the column face. All but four tension strain gages were installed on reinforcing bars running perpendicular to the column face. The four tension gages applied to parallel bars formed a linear distribution extending outward from the interior of the column; these gages are denoted as T1-T4 in Figure 3.5.2. The response of all tension and compression gages vs. the center column deflection can be seen in Figures 4.1.3 and 4.1.4, respectively.

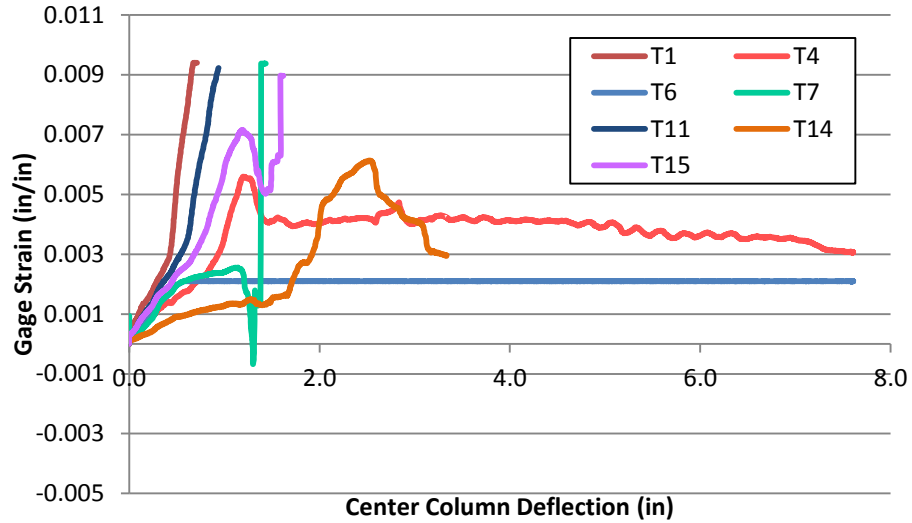


Figure 4.1.3 – Tension gage strain vs. center deflection for Dynamic 1 test

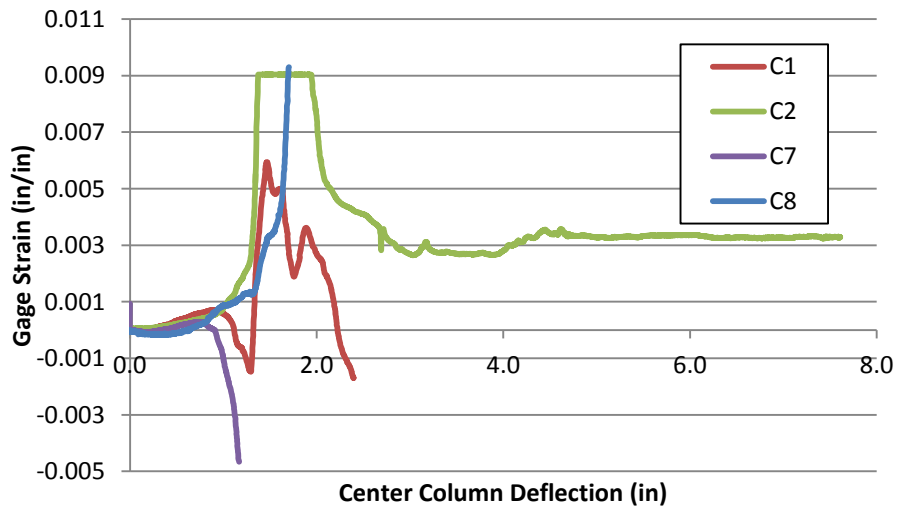


Figure 4.1.4 – Compression gage strain vs. center deflection for Dynamic 1 test

In order to better understand the strain data, the data has been processed by reducing the number of data points and averaging several of the gages together based on their distance from the column face. A plot of the applied vertical load and resulting average strain distribution in the Dynamic 1, 0.64% reinforcement ratio test can be seen in Figure 4.1.5.

The profile in the given plot focuses on the region prior to punching failure; this provides a more in-depth analysis of the strain gage behavior.

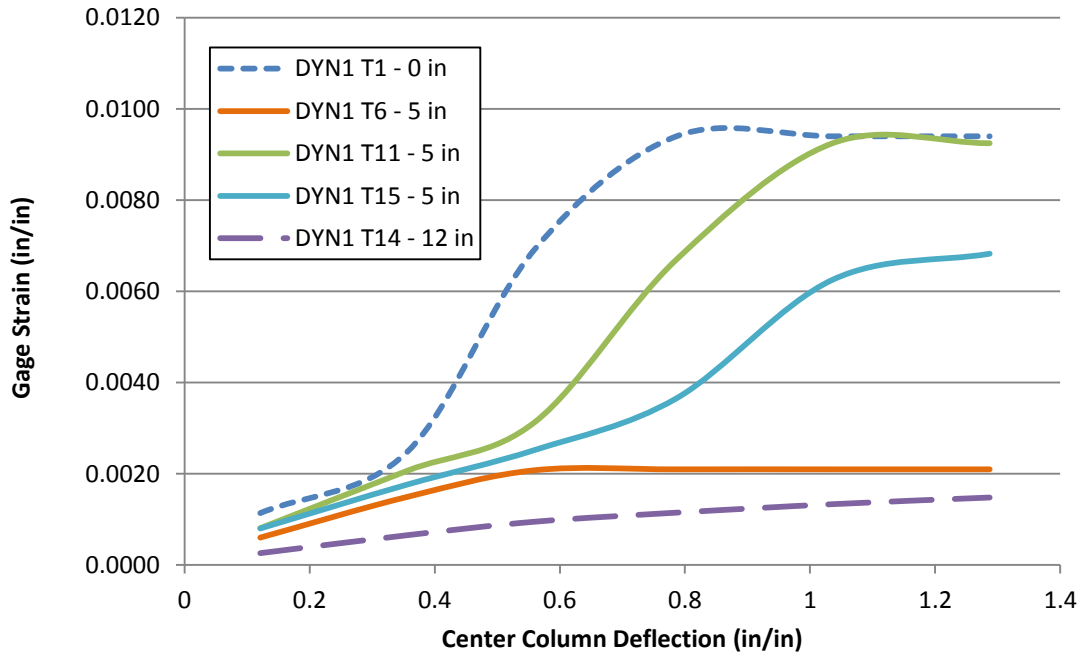


Figure 4.1.5 – 0.64% Dynamic 1 tension gages vs. column displacement pre-punching

The tension strain gages for the 0.64% reinforced test were applied at one of three locations; beneath the column face, 5 inches from the column face, or 12 inches from the column face. This distance is denoted in the legend of the plot following the actual gage label number. The resulting plot displays the approximate strain value at a certain distance from the column face as the applied load reached punching failure. It can be seen that the average strain values decrease with increasing distance from the column face. The strain reading of each tension gage was less than 0.002 in/in until approximately 0.3 inches of deflection. It is apparent in the strain data that cracking in the slab began just after reaching a center column deflection of 0.3 inches; at this point a sharp increase in the strain rate occurs in the gages at the slab column connection. The

gages at a distance of 5 inches increase at a higher rate when the deflection reached the 0.5 inch mark and continue this behavior, reaching a strain value just below 0.01 in/in at a deflection of 1 inch. The closer gages also show a reduction in the strain slope as the specimen nears punching failure at 1.28 inches. The strain readings 12 inches from the column face increased at a constant rate throughout the test, however, the strain readings were much lower and only reached a maximum strain value of 0.0013 in/in just prior to punching failure.

The Dynamic 1 test included five strain gages applied to the compressive reinforcement. The plot of center column displacement vs. compression gage strains can be seen in Figure 4.1.6. This plot also displays the behavior of each strain gage up until punching failure occurred.

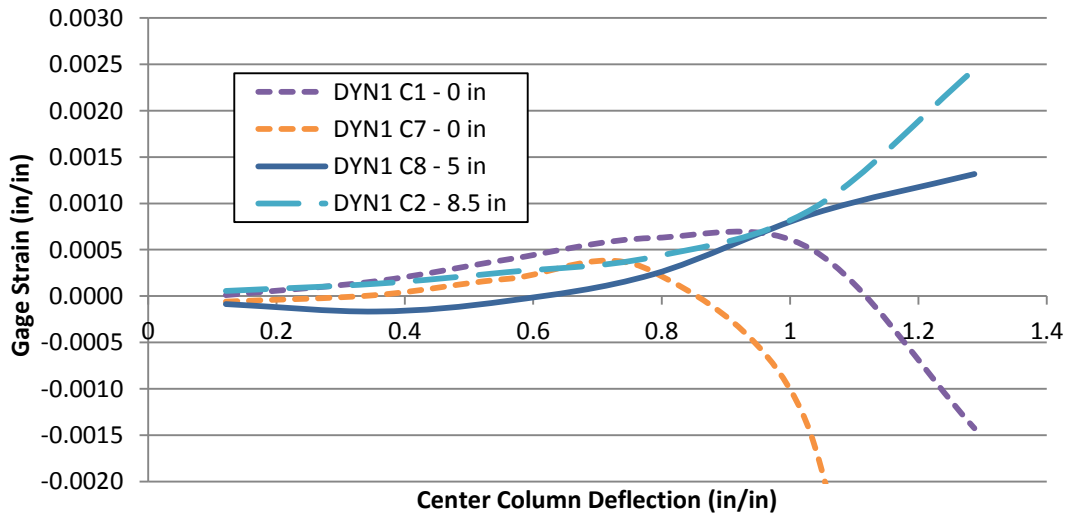


Figure 4.1.6 – 0.64% Dynamic 1 compression gages vs. column displacement pre-punching

Of the five compression zone gages, four gages produced usable data from the testing. The C8 compression gage was located 5 inches from the column face and was the only gage to display compressive behavior during the initial stages of the test. The other three compression gages display tensile strains throughout the entire pre-punching region. All gages develop tensile strains between 0.4 inches and 0.8 inches of deflection. At a center column deflection of 0.8 inches, the gages located at the column face begin to develop compressive strains. This behavior is seen by the rapid decrease in the drop of gage C7, with a more gradual drop displayed by gage C1. The change to compressive strains is likely due to the crushing of the concrete near punching failure leading to a transfer of compressive load to the reinforcement. None of the compression gages reached the yielding point of 0.002 in/in prior to the punching failure.

A photo of the failure region in the slab- column connection can be seen in Figure 4.1.7. In this photo it can be seen that the tension reinforcement has ripped from applied column loading, causing the connection to lose all load carrying capacity. The compression zone reinforcement that was non-continuous through the column can also be seen ripped out from the interior column face as well.



Figure 4.1.7 – Dynamic test 1 after failure of the connection

The parallel and perpendicular concrete strains were measured at the top surface of the concrete next to the column face. A plot of the average measured parallel and perpendicular concrete strains can be seen in Figure 4.1.8. This plot shows the relationship between the concrete strain and the time of the test to give an idea of the concrete strain rate at the column-slab interface. The concrete strain rate can be related to a proposed DIF, as presented in the literature review on material strength increase factors (UFC 340). The maximum time value of 0.12 seconds corresponds to the time at which punching failure occurred. The maximum strain rate perpendicular to the column face was calculated and the result was approximately 0.0018 strain/second.

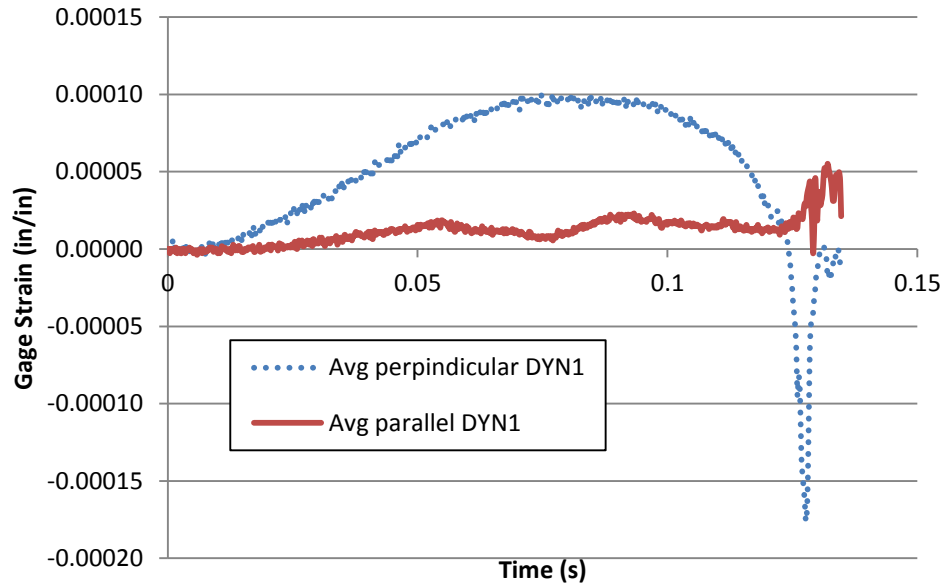


Figure 4.1.8 - Concrete strain parallel and perpendicular vs. time

According to the strain rates observed in the Dynamic 1 test, a DIF of only 1.2 would be applied to increase concrete strength (UFC 340). While this would indicate a higher punching capacity than the static test, the strain rates were not constantly this large throughout the test and the increase in material strength is not significant. The UFC code and previous dynamic tests were conducted to simulate blast and seismic loadings where the DIF and corresponding material strength increase is much larger than what is displayed in this test.

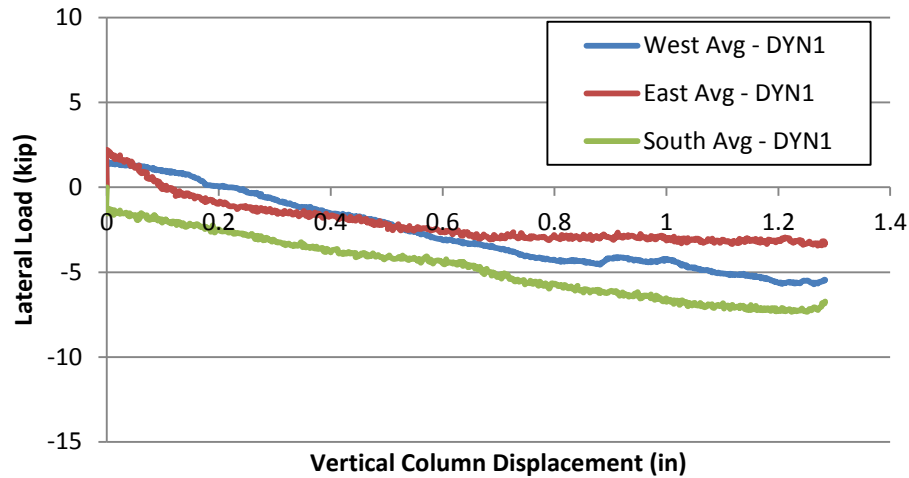


Figure 4.1.9 – Lateral load measured from threaded rod restraints

Due to errors in the data acquisition system, the lateral displacements of the Dynamic 1 tests could not be accurately determined. In Figure 4.1.9, the resulting lateral loads on the restrained setup were recorded by measuring the strain in the threaded rod connections and converting it to a compressive (or tensile) load. The tightening of the rod before the test caused an initial compressive load reading. Once the test began, there was a constant compressive force being applied to the lateral restraints due to outward expansion of the slab. The average compressive force in the East-West direction was around five kips prior to the punching failure. There was no usable data for the North connections, but a compressive loading near 7.5 kips was measured in the south threaded rod just before punching failure. Each of the threaded rods recorded an increasing compressive strain until a deflection of approximately 0.7 inches was reached, at this point the compressive loading remained relatively constant until failure occurred.

4.2 Dynamic 2 Test – 0.64% Reinforced

The second dynamic test was conducted for an additional 0.64% reinforced slab specimen under laterally restrained conditions. In terms of the test setup and specimen construction, it was designed to be identical to the Dynamic 1 test. While the tests were designed to be the same, it is important to note that the concrete compressive strength of Dynamic test 2 (4300 psi) was much lower than that of dynamic test 1 (5500 psi). The punching failure of the Dynamic 2 specimen occurred at a rise time of 0.19 seconds at a vertical load of 50.2 kips and corresponding deflection of 1.7 inches. As with the first dynamic test, the connection reached zero capacity approximately 1 second after the test began, the column deflection at this point was 7.6 inches. The load deflection response of the second 0.64% reinforced dynamic test can be seen in Figure 4.2.1. The post punching behavior of the specimen was similar to the first 0.64% dynamic test, displaying a relatively consistent decrease in load capacity with increasing deflection. There was, however, a second peak in the loading near the end of the Dynamic 2 test seen below. This peak is attributed to the column rotating and binding in the punching cone hole, therefore the second peak in capacity is not related to the capacity of the connection.

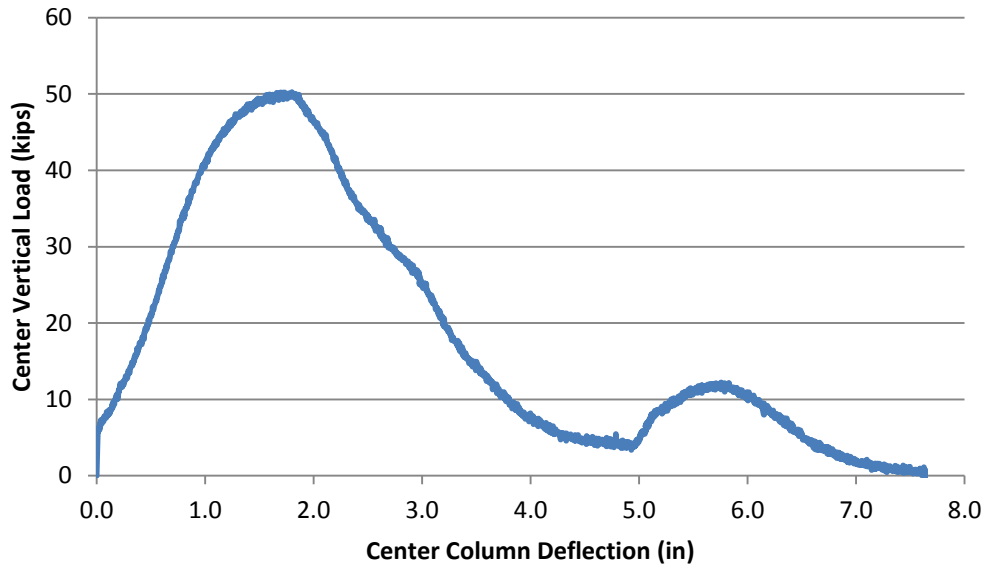


Figure 4.2.1 – Vertical load vs center column displacement for Dynamic 2 test

A plot of the vertical deflection and resulting tension mat gage readings throughout the entire Dynamic 2 0.64% reinforced test can be seen in Figure 4.2.2.

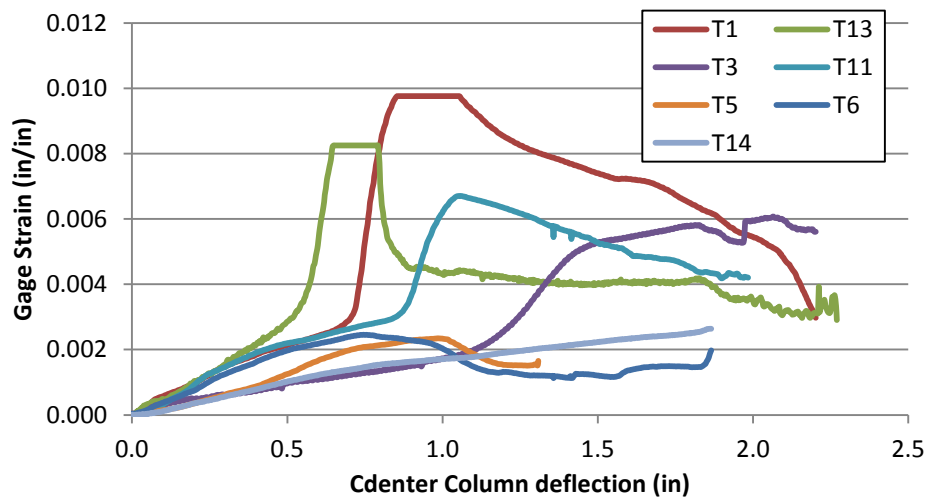


Figure 4.2.2 - Tension gage strain vs. center deflection for Dynamic 2 test

The tension strain gages for the 0.64% reinforced test were applied in the same locations as the Dynamic 1 test; beneath the column face, 5 inches from the column face, and 12

inches from the column face. The strain behavior is further analyzed by observing behavior from the initial column deflection until punching failure occurred at a deflection of 1.7 inches. This detailed plot of the strain profile can be seen in Figure 4.2.3.

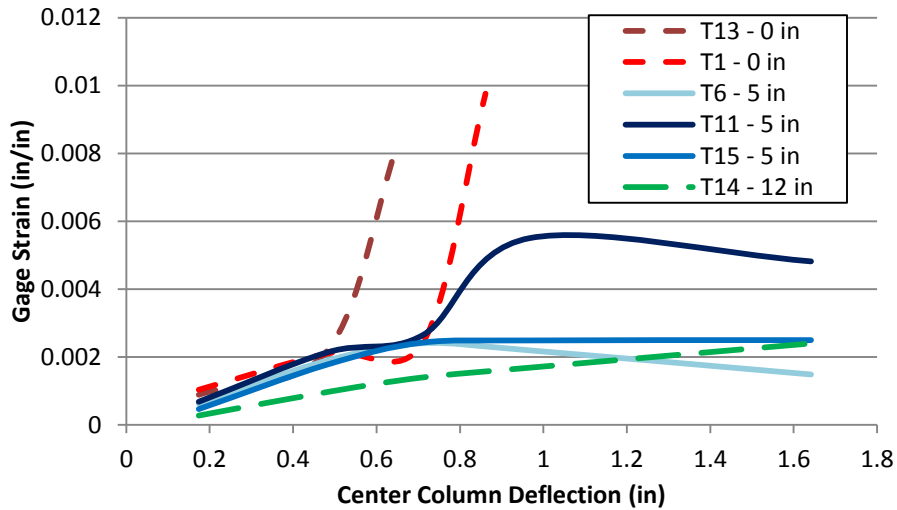


Figure 4.2.3 - 0.64% Dynamic 2 tension gages vs. column displacement pre-punching

The strain readings of gages closer to the column are larger than gages further away throughout the loading of the specimen; as seen in the Dynamic 1 test. All gages 5 inches from the column and closer reached yielding strain of 0.002 in/in at approximately 0.5 inches of center column deflection. The two gages installed at the column face, T1 and T13, displayed a rapid strain increase at deflections of 0.7 inches and 0.5 inches, respectively. Both gages increased from 0.002 in/in strain to the maximum gage value near 0.009 in/in after only a 0.1 inch increase in the column deflection. Different behavior of gages at identical distances from the column face can likely be attributed to uneven loading of the slab, causing a different strain response outward from each of the four column faces. Furthermore, although care was taken to place the gages accurately, if the gage is placed just inside or outside of the column face a substantial difference in

the gage readings may be possible. For the rest of the gages small changes in their placement location will not have such a large effect.

The Dynamic 2 test included five strain gages applied to the compressive reinforcement, although one gage was damaged and did not produce useable data. The plot of center column displacement vs. compression gage strains can be seen in Figure 4.2.4.

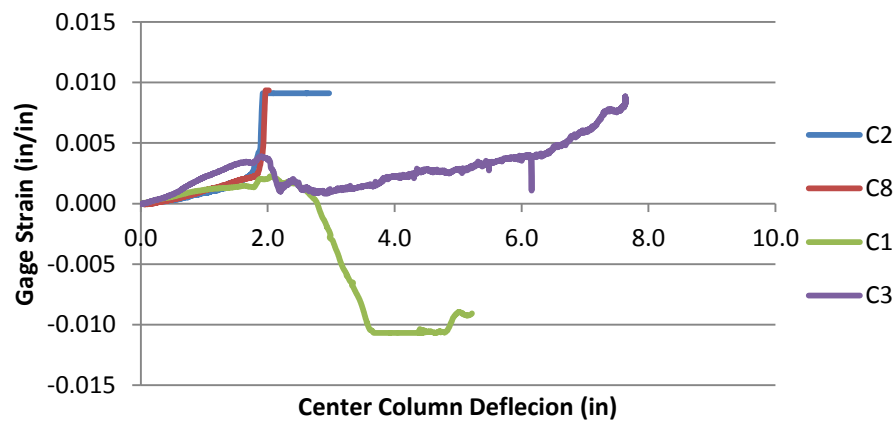


Figure 4.2.4 - Compression gage strain vs center deflection for Dynamic 2 test

This plot in Figure 4.2.5 displays the behavior of each individual strain gage up until punching failure occurred. Although these gages were applied to the reinforcement mat located in the compression region, the gages displayed increasing tensile strains from initial loading until punching failure occurred. Overall the gages located closer to the column recorded higher strains throughout the test. One exception to this would be the C1 gage located at the column face. The strain readings of gages at the column face could vary due to the sensitivity of their installation location. As with the previous dynamic test, the gages all increased at a relatively constant rate until the column

displacement reached 0.5 inches, the gage readings at this point ranged from 0.00025 to 0.00075 in/in. After reaching this displacement, the gages increased at a higher rate until punching failure occurred at a displacement of approximately 1.6 inches. However a change to compressive strains near punching was not seen in the 0 in. gage as seen in the Dynamic 1 test.

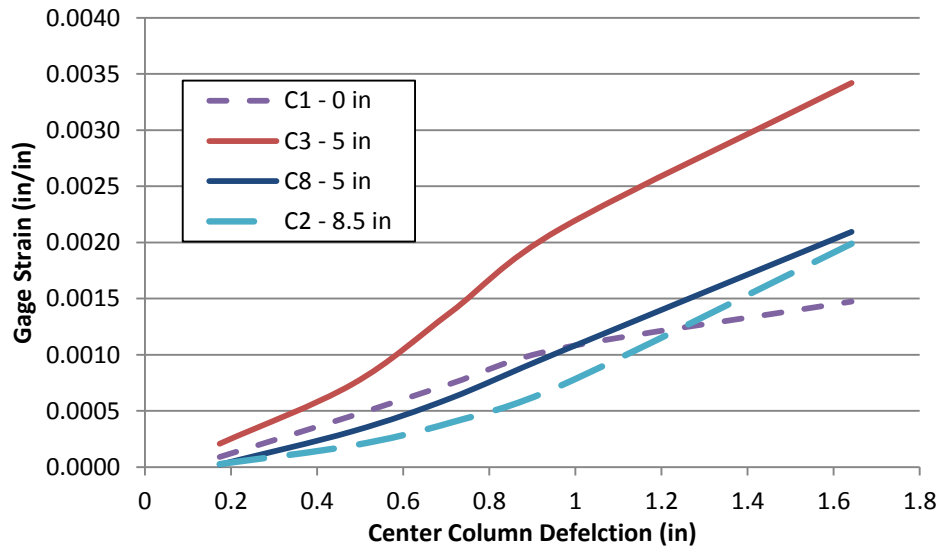


Figure 4.2.5 - 0.64% Dynamic 2 compression gages vs. column displacement pre-punching

A picture of the failure region after the test completed can be seen in Figure 4.2.6.

Similar to the Dynamic 1 test, it can be seen that the reinforcement bars ripped out of the concrete rather than remaining embedded and fracturing under the applied loading. Both pictures display the compressive reinforcement that was cast a few inches into the column completely pulled out from the interior face. If the compression reinforcement were continuous through the column, providing additional integrity reinforcement, the reinforcement would need to fracture rather than simply pulling out, providing much larger capacity after initial failure.



Figure 4.2.6 – Failed Dynamic 2 specimen

The average parallel and perpendicular concrete strains measured at the slab surface near the column face can be seen in Figure 4.2.7. It can be seen that the parallel and perpendicular concrete strains had a similar increase over the initial deflection of the slab. Once the perpendicular strain reached a maximum near 0.0005 in/in, it began to decrease and nearly reached 0 strain at the time of punching failure. The parallel strain reached a peak near 0.0005 in/in as well, but remained at this strain value until punching failure occurred. The concrete strains are plotted as a function of the time during the test to observe the strain rate of the concrete materials.

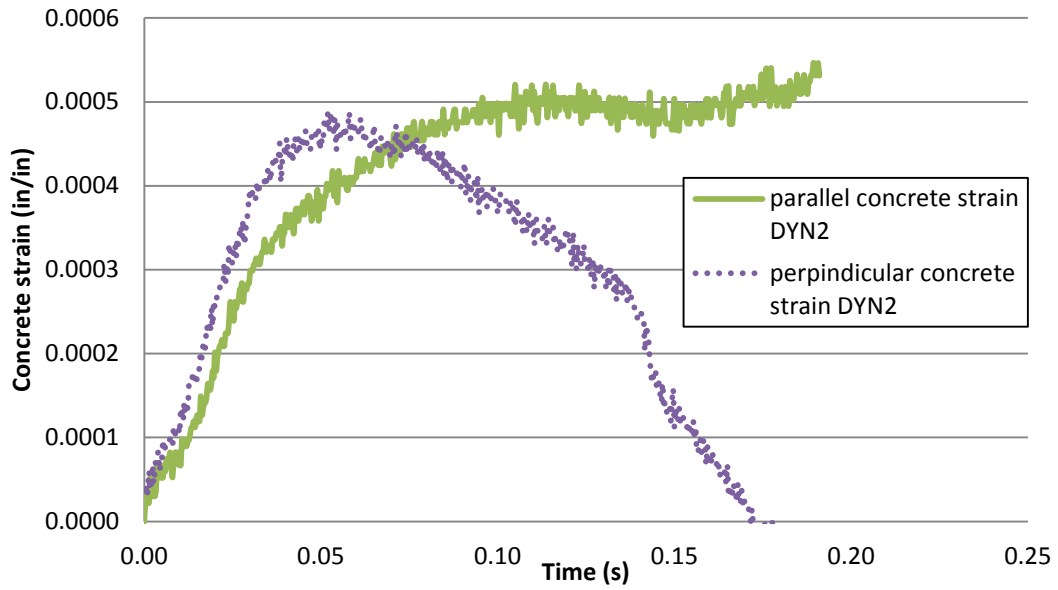


Figure 4.2.7 – Concrete parallel and perpendicular vs. time for Dynamic 2 test

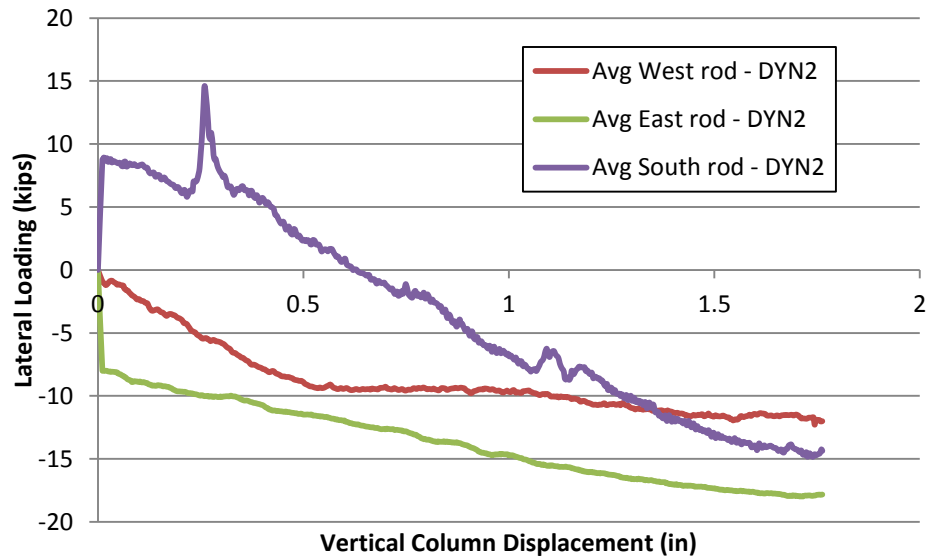


Figure 4.2.8 – Lateral load measured from threaded rod restraints

In Figure 4.1.8, the resulting lateral loads on the restrained setup are plotted against the vertical column deflection. Once the test began, there was a constant compressive force being applied to the lateral restraints, as seen in the Dynamic 1 test. The average

compressive force in the East-West direction was around 15 kips. Both the East and West compressive loads moved about 10 kips in the compressive direction from their initial applied loads. There was no usable data for the North connections once again, but a compressive loading near 15 kips was measured in the south threaded rod just before punching failure. This south connection also began at a tensile load of about 7 kips, therefore it moved a total of 22 kips in the compressive direction.

4.3 Dynamic 3 Test – 1.0% Reinforced

The third dynamic test was conducted for a second 1.0% reinforced slab specimen under laterally restrained conditions. All parameters of the slab and test setup were identical to previous dynamic tests, aside from the increased reinforcement ratio. The punching failure of the Dynamic 3 specimen occurred at a rise time of 0.065 seconds at a vertical load of 58.6 kips and corresponding deflection of 1.1 inches. As expected, this slab with higher reinforcement experienced a higher stiffness and punching strength while sacrificing ductility. The maximum deflection at zero load capacity did reach a displacement of 7.8 inches, which was similar to the lower reinforced specimens. The load deflection response of the 1.0% reinforced Dynamic 3 test can be seen in Figure 4.2.1. The overall post punching behavior of the specimen was similar in comparison to the two 0.64% reinforced dynamic tests, displaying no residual peak in capacity after initial failure.

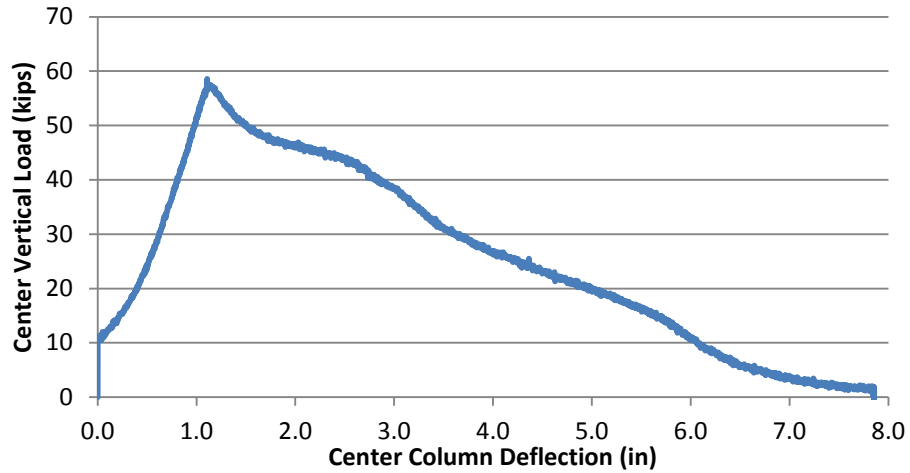


Figure 4.3.1 – Vertical load vs. center column displacement for Dynamic 3 test

Seven strain gages applied to the tension reinforcement were used to determine the response of the 1.0% reinforced dynamic test. All strain data for the tensile reinforcement can be seen in Figure 4.3.2.

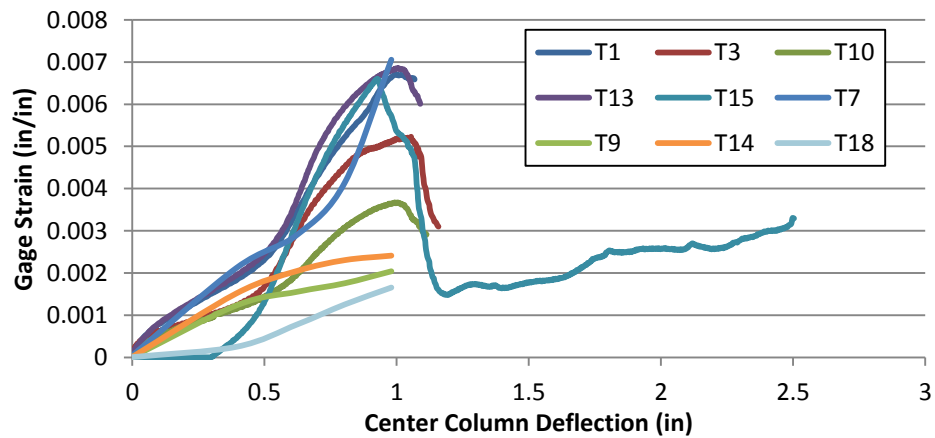


Figure 4.3.2 – Tension gage response for Dynamic 3 test

The tension gages were placed at four different locations with respect to the column face, the distances from the face are as follows; column face (0 inches), 1.25 inches, 5.75

inches, and 10.25 inches. The plot of tensile reinforcement strain vs. the center column vertical deflection in the region before punching failure can be seen in Figure 4.3.3.

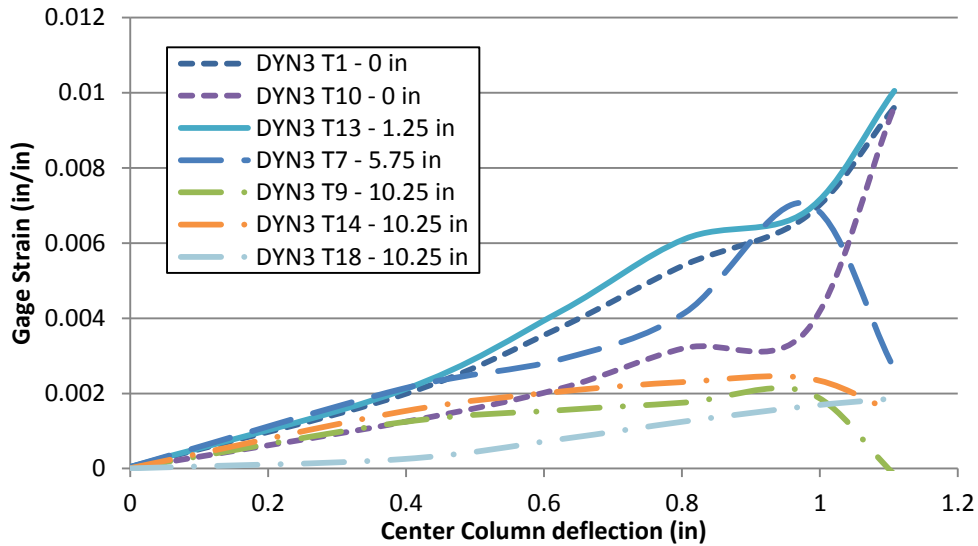


Figure 4.3.3 – 1.0% Dynamic 3 tension gages vs center column deflection pre-punching

The strain data response was quite consistent for each group of strain gages. Multiple strain gages recorded data for two different locations; at the column face and 10.25 inches away. As seen in the previous test specimens, the strain gages closer to the column face recorded larger strain values than gages further away throughout the pre-punch loading phase. Gage T13 was applied 1.25 inches from the column face and displayed the largest strain values, with the overall response being very similar to the gages at the column face. All gages had a constant increase in strain from initial loading through a deflection of approximately 0.4 inches. At this point, the gages at 0, 1.25, and 5 inches reached yielding strain of 0.002 in/in. The further gages were at slightly lower strain values, near 0.0015 in/in, when the slab reached a deflection of 0.4 inches. When comparing gage values it is important to reference the reinforcement layout and consider

the location of each gage. For example, gage T18 displays a similar, but delayed, response in relation to the other two gages (T9, T14) 10.15 inches from the column. This difference is likely attributed to the T18 gage being installed to a reinforcement bar running perpendicular to the reinforcement bar containing T9 and T14.

The compression gages for the 1.0% reinforced dynamic test were applied to three different locations; at the column face, 1.25 inches from the column face, and 5.75 inches from the column face. A total of four gages provided the compression zone data for the 1.0% reinforced specimen. The compression gage strain vs. center column deflection throughout the whole test can be seen in Figure 4.3.4.

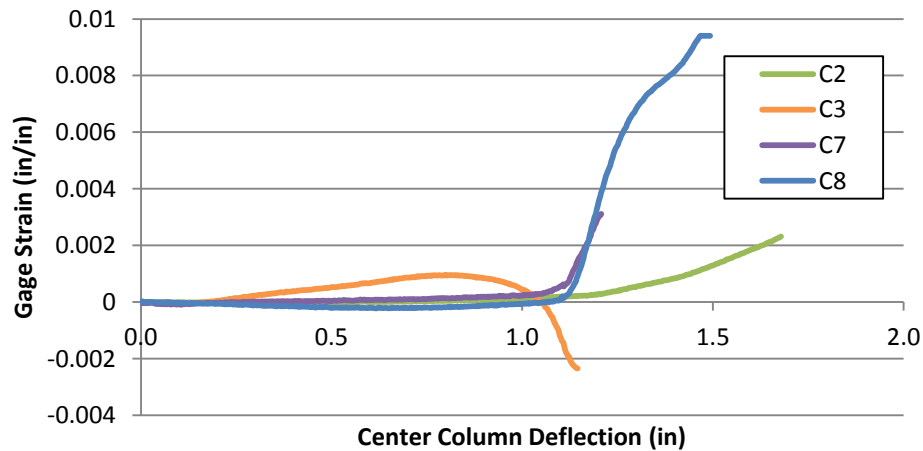


Figure 4.3.4 – Compression gages throughout Dynamic 3 test

The behavior of the compression gages in the Dynamic 3 test closely resembles that of the Dynamic 1 test, although they had different reinforcement ratios. As seen in the Dynamic 1 test, the gages further from the column, 5.75 inches in this case, develop small magnitude compressive strains until a column deflection of approximately 0.7

inches. The strain gage values up until punching failure occurred can be seen in Figure 4.3.5.

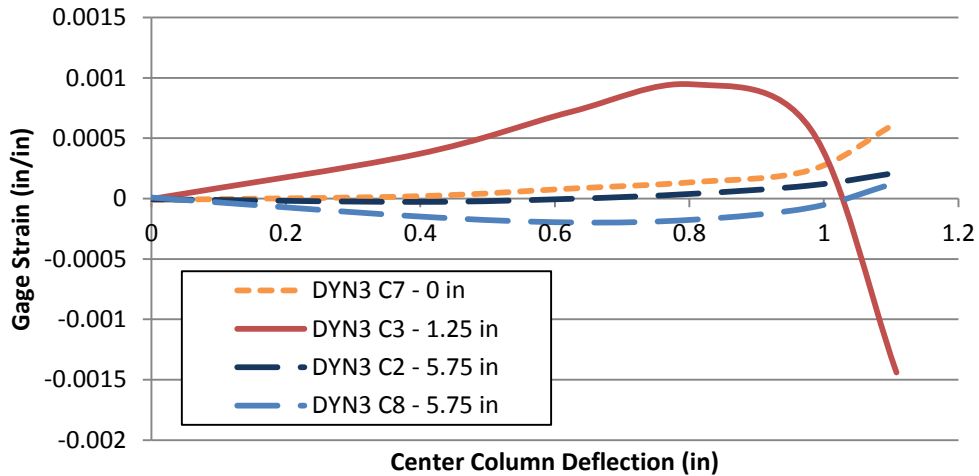


Figure 4.3.5 – 1.0% Dynamic 3 compression gages vs. column displacement pre-punching

The strain values are less than 0.00025 in/in at the maximum, with the C2 gage barely developing any compressive strain. The gage at the column face, C7, displays a very small tensile strain throughout the test with a small jump between deflections of 1.0 inches and 1.1 inches. The C7 gage reaches a maximum tensile strain of 0.0006 in/in just prior to punching failure. The C3 gage was located 1.25 inches from the column face and displayed an immediate increase in tensile strain as the specimen was loaded. The strain rate was relatively constant until the column reached a deflection of 0.8 inches. At this point the gage experienced a slight delay before dropping into the negative region, indicating compressive strain on the reinforcement. This behavior was also seen by the gages placed beneath the column face in dynamic test 1. The high rate compressive strain continued on gage C3 until punching failure occurred in the specimen at a deflection of 1.1 inches.

A plot of the parallel and perpendicular concrete strains measured near the column can be seen in Figure 4.3.6. The maximum time value of approximately 0.065 seconds corresponds to the punching failure of the Dynamic 3 specimen. As seen in the previous tests and according to Broms theory, the average concrete strain perpendicular to the column face is decreasing as the connection approaches punching failure. The Dynamic 3 test experienced a maximum strain rate of roughly 0.014 strain/second from the initial loading until reaching the peak tensile strength. This was a similar strain rate to the Dynamic 2 test, both of which were larger than the strain rate observed in dynamic test 1.

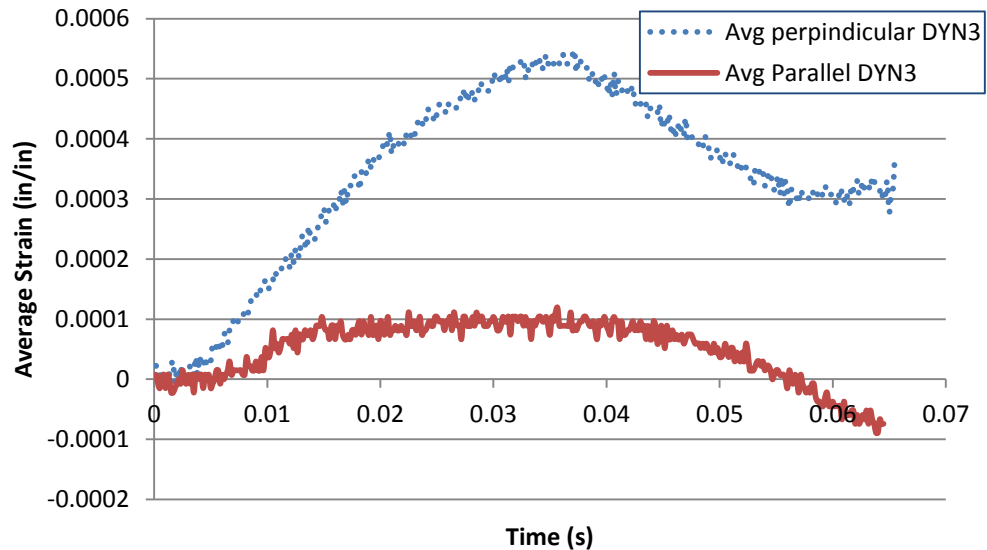


Figure 4.3.6 – Concrete parallel and perpendicular vs. time

Data on the lateral displacements and resulting lateral loads in the restrained test setup are seen in Figure 4.3.7 and Figure 4.3.8.

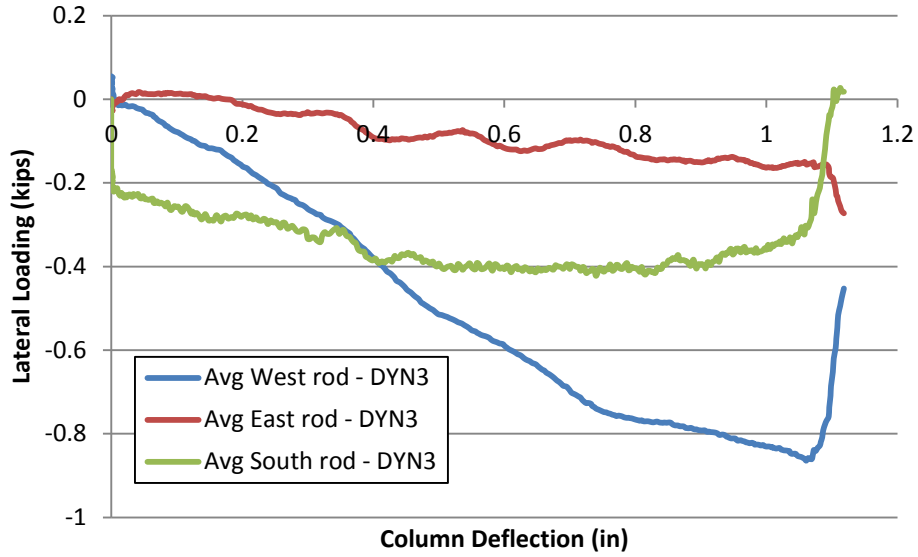


Figure 4.3.7 – Lateral loads calculated from threaded rods in support connection

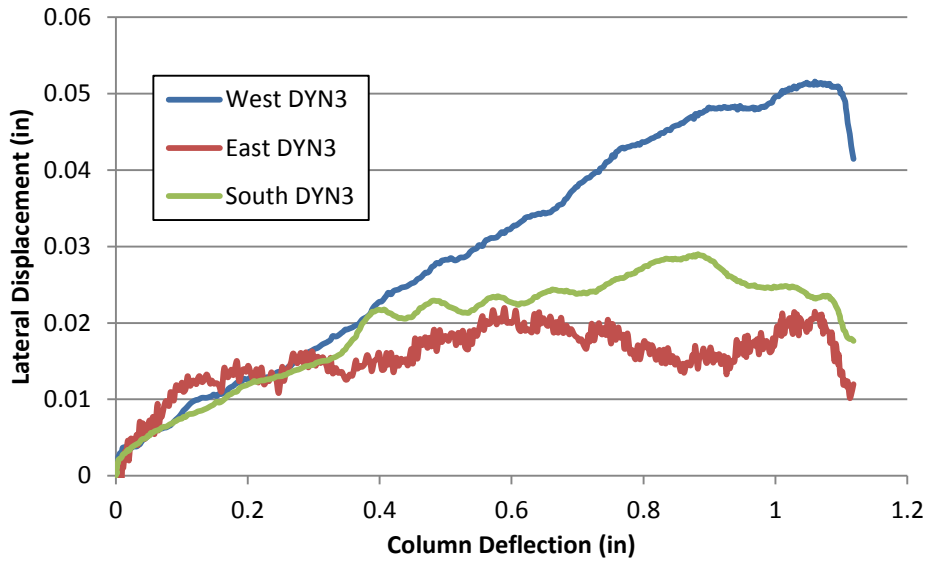


Figure 4.3.8 – Lateral displacements recorded from exterior LVDTs

In both the load and displacement data seen above, a drop in each reading can be seen as punching shear failure occurs at approximately 1.1 inch. The compressive and tensile forces recorded in the dynamic three tests were less than 1 kip. The forces in the previous dynamic tests reached values of at least 5 and up to 20 kips. This shows that the

lateral loading data applied to the restrained connections was of very low magnitude. The maximum lateral displacement of the slab was seen on the North face of the specimen. Before punching failure occurred, the lateral deflection reached 0.05 inches. Positive deflections seen on the three faces of the specimen in Figure 4.3.8 suggest a consistent outward movement of the slab until punching failure occurred.

4.4 Comparison of Static and Dynamic Test Results

The following sections will highlight the notable comparisons between the dynamic and static isolated slab-column connection tests. The first two dynamic tests, with 0.64% reinforcement ratio, will be compared to a corresponding static test with the same reinforcement ratio and lateral restraint. This corresponding static test can be seen in Table 1.2.1 as specimen #6 in the test matrix and denoted as 0.64STA in the following plots. The Dynamic 3 test will be compared with the results obtained in the corresponding static test with lateral restraint and a 1.0% reinforcement ratio. This static test is #3 in the test matrix and denoted as 1.0STA in the following results.

4.4.1 Comparison of 0.64% Reinforced Tests

The comparison made in this section will be between the Dynamic 1, Dynamic 2 and 0.64% reinforced static test, seen as specimens #7, #8 and #6 in the test matrix Table 1.2.1. Photographs taken of the 0.64% static and dynamic tests can be seen in Figures 4.4.1.1 through 4.4.1.4. It can be seen that the punching cone of the static and dynamic tests were of similar dimensions at the initiation of punching failure. The failure region in the static test is over a much larger portion of the bottom of the slab, both at punching shear failure and at the completion of the test. Both figures displaying the bottom of the

slab after failure occurred for the dynamic tests display much more localized damage, while also occurring at 2 inches more of total deflection at the end of the test.



Figure 4.4.1.1 – Underside of 0.64% static test at punching failure of testing



Figure 4.4.1.2 – Underside of the Dynamic 1 test at punching failure



Figure 4.4.1.3 – Underside of the static 0.64% test at conclusion of testing



Figure 4.4.1.4 – Underside of the Dynamic 1 test at the conclusion of testing

A comparison between the load-deflection response of the 0.64% static and dynamic tests can be seen in Figure 4.4.1.5.

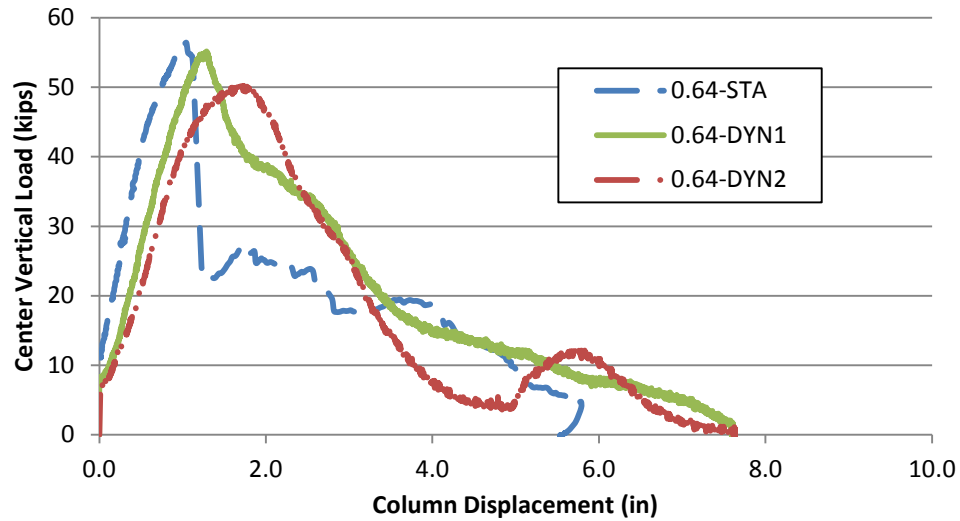


Figure 4.4.1.5 – Comparison of Static and Dynamic 0.64% Load-Displacement Curves

The first observation is that the peak punching capacity of dynamic test 1 and the corresponding static test were both near 55 kips while the Dynamic 2 test was only 50 kips. Although the stiffness obtained for the dynamic tests is unverified due to a delay in the data acquisition device recording the loading data, the peak loading value obtained is correct. The concrete strength of each slab was measured at the time of each test; the static specimen had a compressive strength of 5300 psi, Dynamic 1 was 5500 psi, and Dynamic 2 was much lower at 4290 psi. The difference in concrete strength alone could explain the peak punching capacity for Dynamic 2 being 5 kips less than the static test. The statically loaded test specimen does display a significant post-punching capacity near 25 kips following the initial punching failure while the dynamic tests display a constant

drop in load carrying capacity following the punching failure. The dynamic tests do however display approximately 2 more inches of center column deflection before the load carrying capacity of the connection reaches zero. This additional ductility displayed by dynamically loaded connections can be seen in the results of research by Criswell and Ghali reviewed in sections 2.5.2 and 2.5.1, respectively.

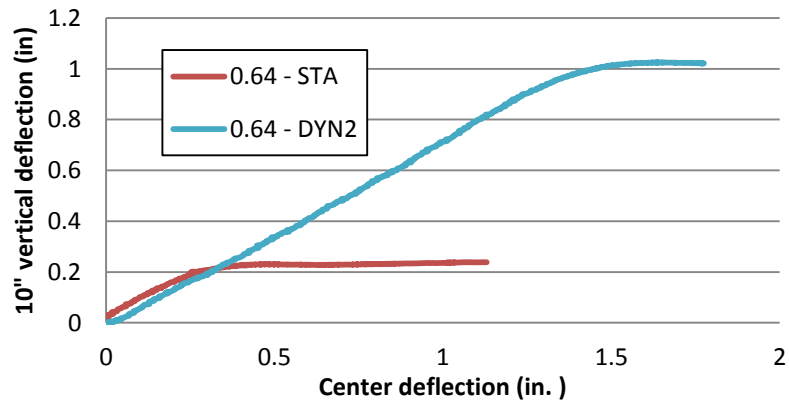


Figure 4.4.1.6 – Center and mid-span deflections prior to punching failure

The column deflection and vertical deflection 10 inches from the column face can be seen in Figure 4.4.1.6. This plot displays a comparison of the two displacement values plotted against each other until punching failure occurred. It can be seen that the static and dynamic tests initially followed the same slope in the figure above. Once a center deflection of approximately 0.25 inches was reached, cracking began to occur and deflections were localized near the column, with no increase in deflection 10 inches from the column face. This response was seen in the dynamic specimen as well, but the column-only deflection began at a larger displacement. A study by Kinnunen and Nylander (1960) suggest that the angle of rotation displayed by the slab can be an indication of the punching shear capacity, with results depending on the reinforcement

ratio of the slab. From the given column and mid-span vertical displacements, the slab rotations could be estimated. The rotation in dynamic test was estimated to be 0.075 radians at punching failure, and 0.092 radians in the static test. These slab rotations, however, are very large and do not correspond to values on the Kinnunen and Nylander plot. Both the static and dynamic tests display ductile behavior upon reaching a peak deflection where the center column continues to deflect with no additional deflection at the 10” distance until failure occurs.

A comparison of the tension strain gage readings until punching failure display the ductility and response of strain gages at different locations through the test and can be seen in Figure 4.4.1.7. The strain distribution was created by averaging the strain results of gages located the same distance away from the column face; this was done for each of the three tests being compared. The resulting plot displays the approximate strain value at a certain distance from the column face as the center column deflection reached its maximum value, at which punching failure occurred in the specimen.

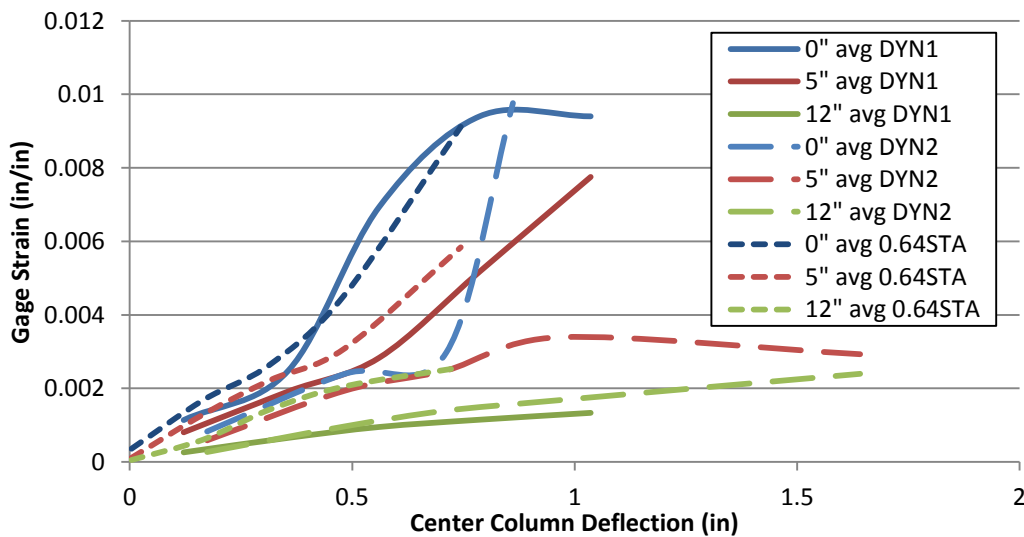


Figure 4.4.1.7 – Average Gage Strain vs. Center Deflection for 0.64% Tests

The plot of average gage strains seen in Figure 4.4.1.7 display the strain profile of each dynamic test completed and the corresponding static test with 0.64% reinforcement ratio (denoted in this plot as 0.64STA). The deflection data for this plot corresponds to an applied loading of 10 kips through 50 kips. The punching failure of the Dynamic 1, Dynamic 2, and the static test occurred at approximate column deflections of 1.2 inches, 1.7 inches, and 1.0 inches, respectively. The strain average at distances of 5 inches and 12 inches from the column face were larger for the static test than both of the dynamic tests. This indicates that the strains in the dynamic tests were localized around the column in each of the dynamic tests. The rate at which the strain increased was similar among the three different distances for the static test, while the dynamic test displayed much larger strain increase rates at the column face than those seen at the 5 inch and 12 inch interval. The dynamic tests did experience larger deflections in comparison to the static test, as a result the, maximum strains obtained at the gages closer to the column were larger just before punching failure occurred.

4.4.2 Comparison of 1.0% Reinforced Tests

The comparison made in this section will be between the Dynamic 3 and 1.0% reinforced static test, seen as specimens #9 and #3 in the test matrix Table 1.2.1. Photographs taken of the 1.0% static and dynamic tests can be seen in Figures 4.4.2.1 and 4.4.2.2, respectively. As with the punching cone comparison between the 0.64% tests, the 1.0% tests display a similar size punching cone when comparing the static and dynamic test pictures as well.



Figure 4.4.2.1 – Dynamic 3 test just after punching failure



Figure 4.4.2.2 – Static 1.0% test just after punching failure



Figure 4.4.2.3 – Underside of 1.0% static test at the conclusion of testing



Figure 4.4.2.4 – Underside of the Dynamic 3 test at the conclusion of testing

The center load vs. column displacement curve for each of the two specimens with 1.0% reinforcement ratio can be seen in Figure 4.4.2.5. As with the previous comparison made between the corresponding 0.64% reinforced specimens, it is important to consider the concrete strength of the test specimens being compared. The two slab-column specimens being compared in this section had a large difference in concrete compressive strength; the dynamic strength being 4300 psi, and the static concrete strength tested to 5500 psi. The plot in Figure 4.4.2.5 shows the load capacity vs. deflection response for each specimen, with the load capacity being displayed on a normalized scale that accounts for the difference in concrete strength, the equation used to obtain the normalized value is seen as equation 7..

$$V_{norm} = \frac{V}{b_o d \sqrt{f'_c}} \quad \text{Equation 7}$$

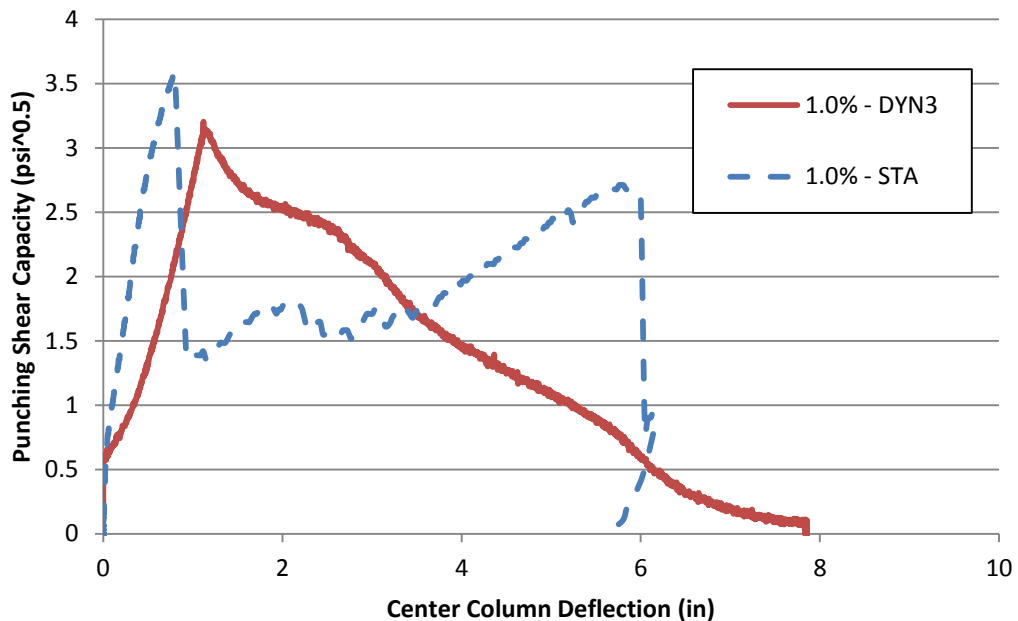


Figure 4.4.2.5 – Normalized capacity vs. Deflection for 1.0% test specimens

As seen in the comparison between the 0.64% reinforced slabs, the statically tested slab develops significant post-punching capacity after initial punching failure occurs while the dynamic test loses capacity at a relatively constant rate. The Dynamic 3 test did display approximately 2 additional inches of column displacement before reaching zero load carrying capacity in the connection. It is typical to see this additional ductility in dynamically loaded slab-column specimens.

It can be seen that the overall capacity of the dynamic specimen is still less than that of the static test after normalizing the load capacity to account for differences in concrete compressive strength. Without accounting for the concrete strength difference, the dynamic capacity was 25% lower than the static capacity. After normalizing the curve, the dynamic capacity was only 10% lower than the static capacity. The column deflection and vertical deflection 10 inches from the column face can be seen in Figure 4.4.2.6.

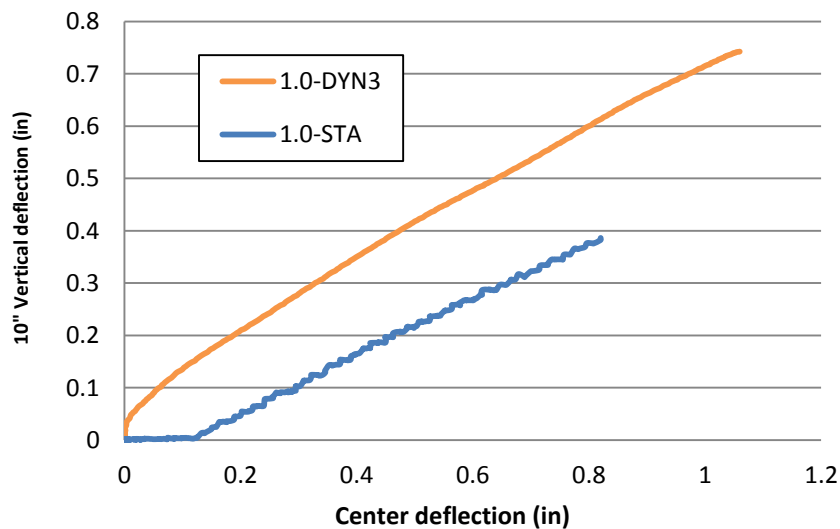


Figure 4.4.2.6 – Center and mid-span deflections prior to punching failure

This plot displays a comparison of the two displacement values plotted against each other until punching failure occurred. As seen in the comparison of the 0.64% tests, the initial slopes of the deflections are the same. The static test did display a delay in the 10 inch deflection initially, this delay was caused by an error in the data acquisition process. For the larger reinforcement ratio of 1.0%, it can be seen that the deflections of both the column and 10 inch distance increased with a constant rate until punching failure occurred. This is a different response prior to failure than the 0.64% test where only center column deflections occurred prior to the punching failure. The calculated rotation for the Dynamic 3 test is 0.035 radians, and the rotation for the corresponding static test had a calculated rotation angle of 0.041 radians. The smaller rotation angle calculated in the dynamic test is likely attributed to calculation of the rotation angle using only two points, at the column face and a distance of 10 inches outward. The rotation angle of the dynamic specimen would likely be larger if additional displacement measurements closer to the column were known.

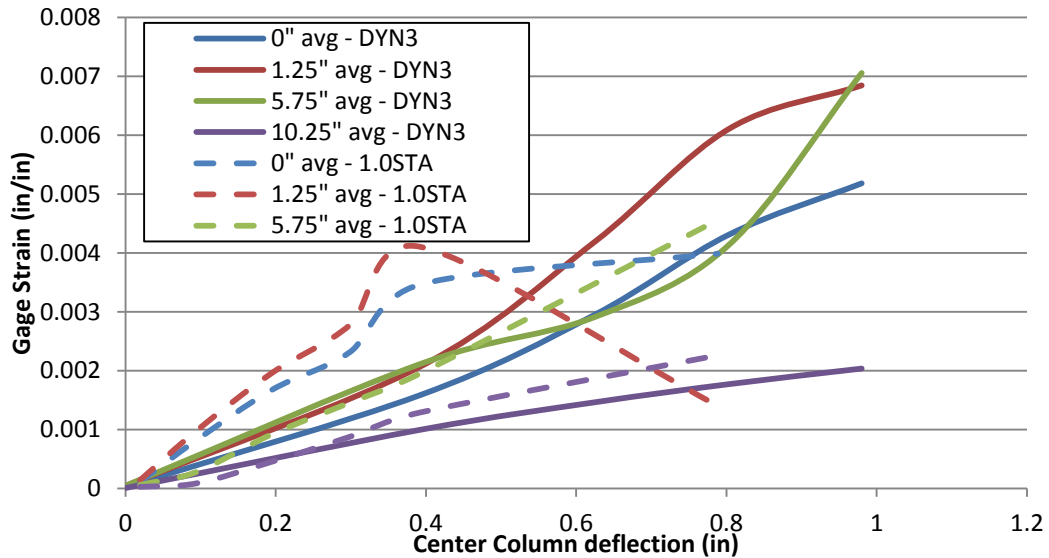


Figure 4.4.2.7 – Average tension strains for 1.0% reinforced specimens

The strain profile of the Dynamic 3 test and corresponding static 1.0% reinforced test can be seen in Figure 4.4.2.7. As with the previous comparison between the 0.64% reinforced specimens, the strains in the static tests were higher than those in the dynamic at early stages of deflection. There is a change in the static strain behavior, in which they begin moving downward indicating compressive strains, when the deflection reaches 0.4 inches. This behavior is attributed to the large shear forces localized around the center column. It can also be seen that the static test reached the punching capacity at a lower column deflection than the dynamic test. With the additional deflection capacity displayed by the dynamic test, the strain gages near the column-slab interface reached higher strain values just prior to the punching failure. Just before the punching failure in the dynamic test the average strain value at this distance was 0.007 in/in while the static test average was approximately 0.0045. This relationship would show that the peak strains in the tensile region at this distance from the column face were over 50% larger in the dynamic test. This is seen in the gage data obtained for a distance 1.25 inches from the column face as well, with the maximum dynamic strain reading nearly 60% of the maximum static value obtained. This indicates that as in the 0.64 reinforcement ratio tests that the strain was concentrated near the column in the dynamic tests.

5. Summary and Conclusions

The goal of this research project was to evaluate the response of isolated slab-column connections under a dynamically applied axial loading. Consideration of the connection type under this dynamic loading further replicates the loading scenario experienced by a slab-column connection in a flat plate structure immediately following the loss of a supporting column. There has been little research to date on the resistance of flat-plate structures to progressive collapse, and even less in regard to dynamic loading of these test specimens. Results of three dynamically tested isolated connections were presented in this research paper and compared to corresponding static tests to further understand the dynamic loading effects and response of the slab-column connection.

A total of three specimens were tested using a hydraulic actuator capable of loading the specimen at 5 in/second. The results of the dynamic tests and the corresponding static tests to which their behavior was compared can be found in Table 5.1. While the load-displacement interaction was skewed due to issues with the data acquisition, the overall peak capacity values are still accurate, along with the displacement data throughout the test. Conclusions from the dynamic testing of the slab-column specimens can be found following Table 5.1.

Table 5.1 – Punching capacity data for dynamically tested slabs

Slab Specimen		Punching capacity (kips)	Deflection at Punching (in)	Time (s)
0.64% RE	Dynamic 1	55.0	1.28	0.13
	Dynamic 2	50.2	1.76	0.19
	Static 0.64	56.4	1.04	576
1.0% RE	Dynamic 3	58.6	1.12	0.65
	Static 1.0	74.0	0.78	539

The following conclusions could be drawn from the dynamically tested slabs:

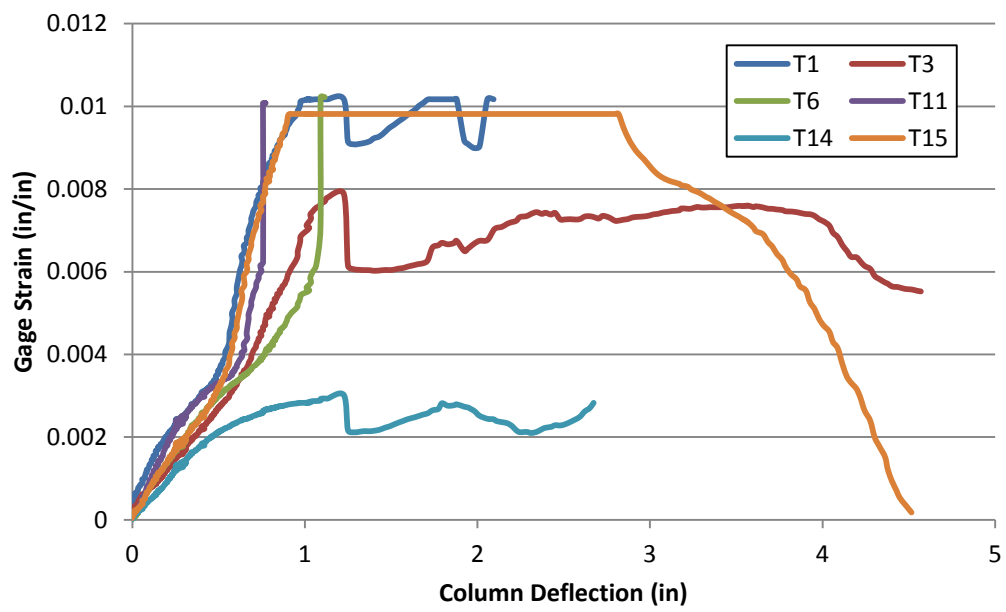
1. The dynamically loaded slabs did not display significantly greater punching shear capacity than the statically loaded tests. For the 0.64% reinforcement tests; the Dynamic 1 test showed 98% of the punching capacity of the 0.64STA test and the Dynamic 2 test showed 90% of the 0.64STA test. The Dynamic 3 test, with 1% reinforcement displayed 75% of the punching strength displayed by the corresponding static test.
2. The dynamic tests did display more ductility than the static tests for both punching and deflection at zero load capacity. The deflection of the 0.64STA test at punching capacity was only 56% of the Dynamic 2 and 78% of the Dynamic 1 deflections at that point. At punching, the 1.0STA test was at 70% of the Dynamic 3 deflection.
3. The strain profile of dynamic tests displayed a much higher concentration near the slab-column interface in comparison to the static tests. Static tests displayed much larger strain values further from the column face in comparison to dynamic strain values at the same distance from the column face.
4. The loading rate of these dynamic slabs was not sufficient to develop any significantly large strain rates in the concrete or reinforcement materials. As a result the DIF values were not large enough to expect a significant increase in punching capacity.

Upon further investigation of the loading data, it was deemed necessary to perform additional isolated dynamic tests to further improve the results obtained in this research. The data from each of these isolated slab-column tests will be along with tests on two multi-panel specimens, concluding this research project.

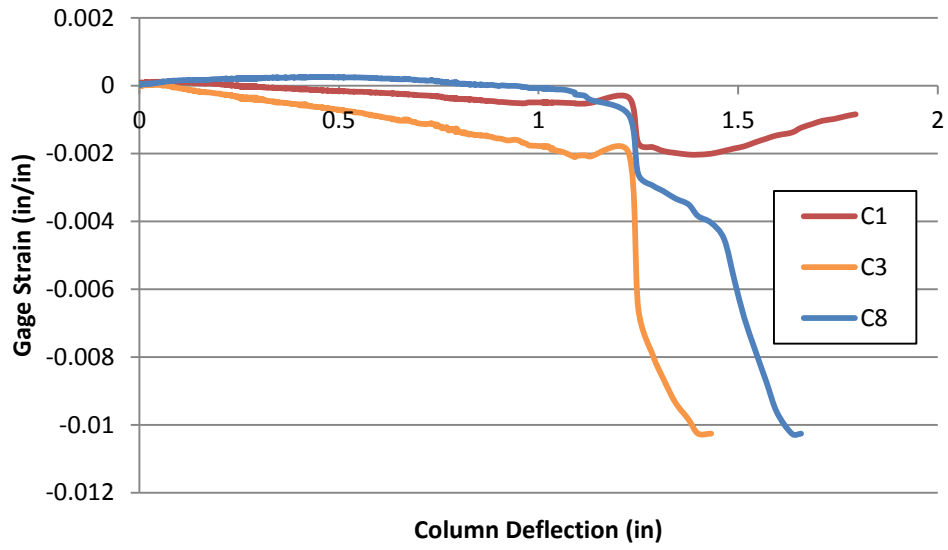
References

- American Concrete Institute. (1971). "Building Code Requirements for Reinforced Concrete (318-71)." Detroit, MI.
- American Concrete Institute. (2008). "Building Code Requirements for Structural Concrete (318-08)." Farmington Hills, MI.
- Broms, Carl E. (1990). "Punching of Flat Plates – A Question of Concrete Properties in Biaxial Compression and Size Effect." *ACI Structural Journal*, No. 87-S30, June 1990.
- Criswell. "Static and Dynamic Response of Reinforced Concrete Slab-Column Connections."
- Elstner, Richard C. and Hognestad, Eivind. (1956). "Shearing Strength of Reinforced Concrete Slabs." *ACI Journal*, July 1956.
- Ghali, Elsmari and Dilger (1976). "Punching of Flat Plates Under Static and Dynamic Horizontal Forces." *ACI Structural Journal*, No. 73-47, October 1976.
- Habibi, F. Cook W.D. and Mitchell D. (2012). "Assessment of CSA A23.3 Structural Integrity Requirements for 2-Way Slabs." *Can. J. Civ. Eng.* Vol. 39, 2012
- Harris, Devin K. (2004). "Characterization of Punching Shear Capacity of Thin UHPC Plates" Masters Thesis, 2004.
- Jacobs and De Roeck. "Dynamic Testing of a Pre-Stressed Concrete Beam" Kasteelpark Arenberg, Heverlee
- Kulkarni S. and Shah S. (1998). "Response of Reinforced Concrete Beams at High Strain Rates." *ACI Structural Journal*, No. 95-S64, December 1998.
- Park (2012). "Inspection of Collapse of Sampoong Department Store." *Forensic Science International* 217, No. 119-126, 2012.
- Unified Facilities Criteria. (2009). "Design of Buildings to Resist Progressive Collapse (UFC 4-023-03)."
- Vecchio, F.J. and Tang, K. (1989). "Membrane action in reinforced concrete slabs." Toronto, Ont., Canada. 1989.
- Zinzeddin M. and Krauthammer T. (2007) "Dynamic Response and Behavior of Reinforced Concrete Slabs Under Impact Loading". *International Journal of Impact Engineering*, 2007.

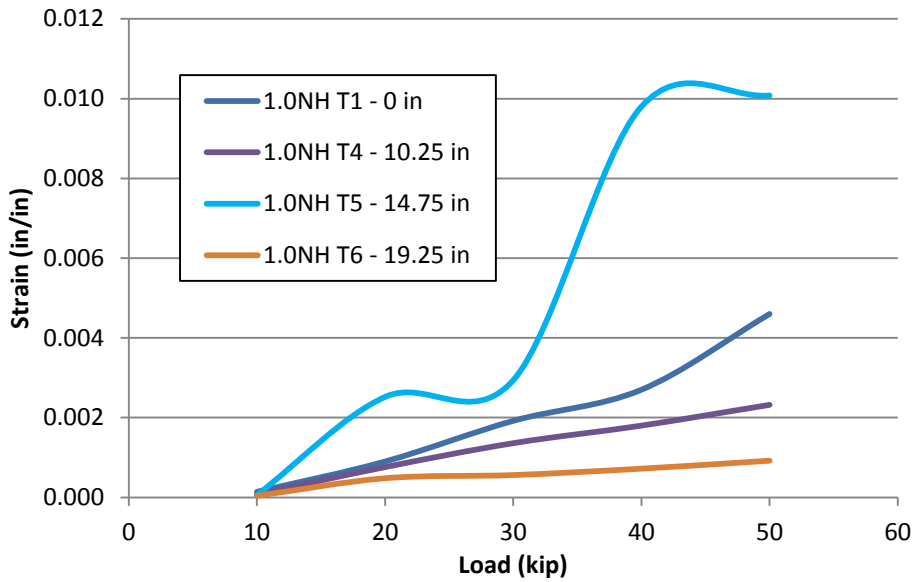
Appendix



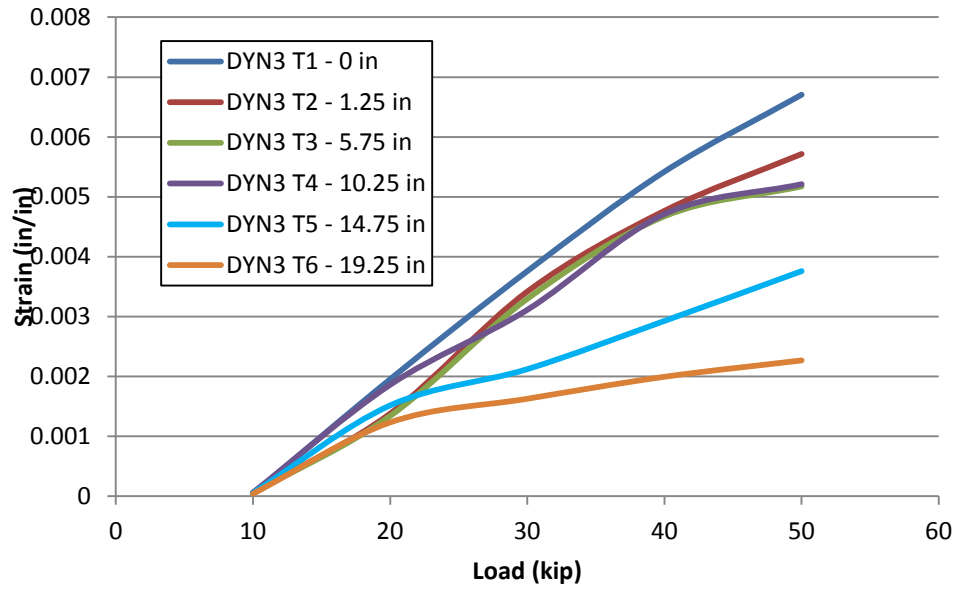
Tension strain gages for static 0.64% RE test



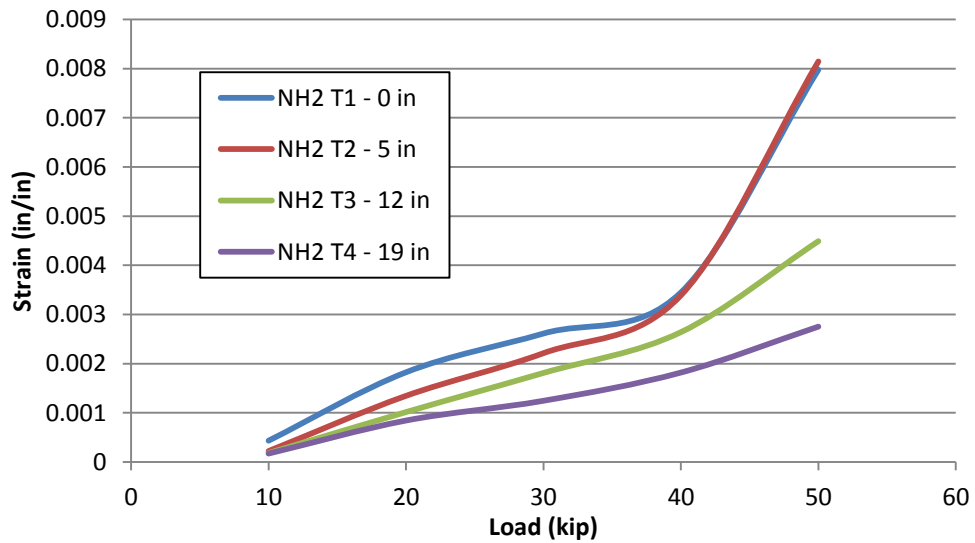
Compression strain gages for static 0.64%RE test



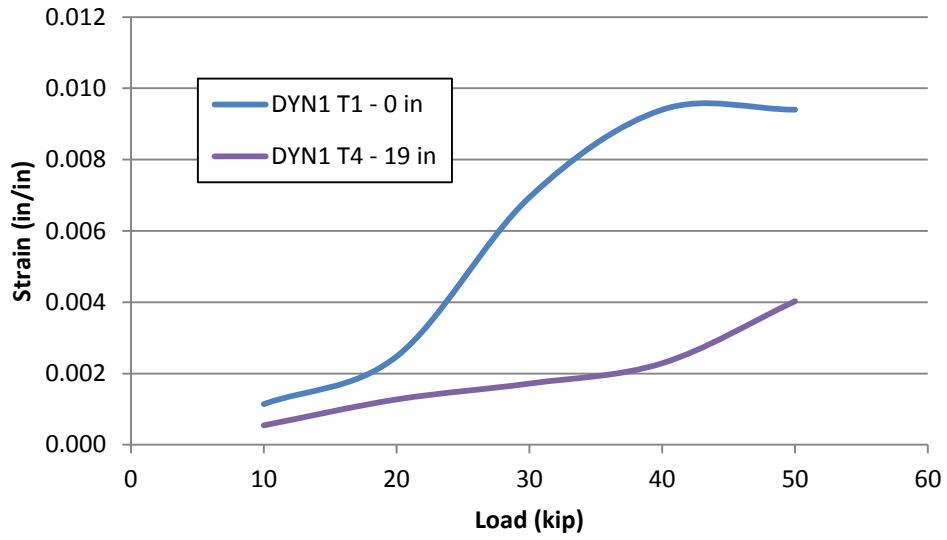
Strain gage profile on parallel reinforcement 1.0STA



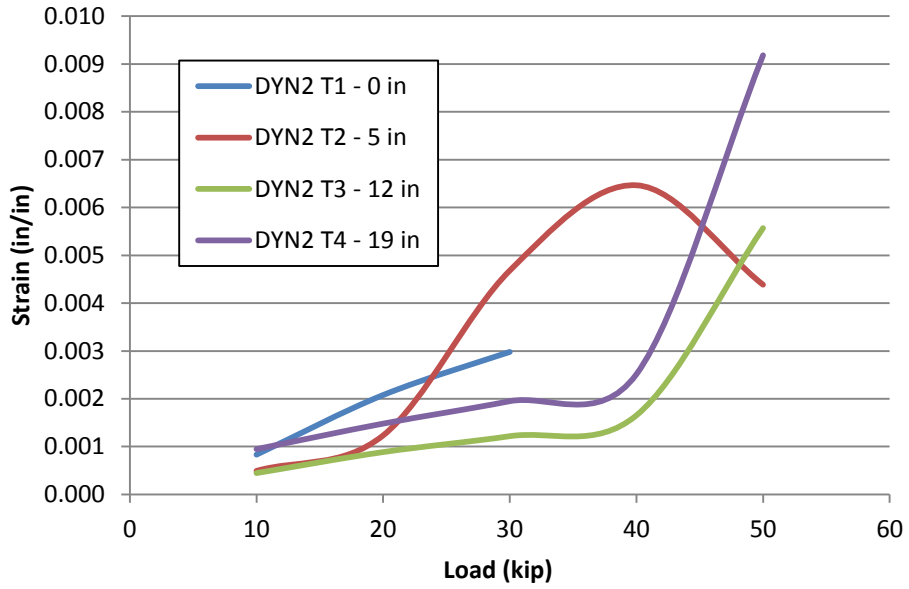
Strain gage profile on parallel reinforcement DYN3



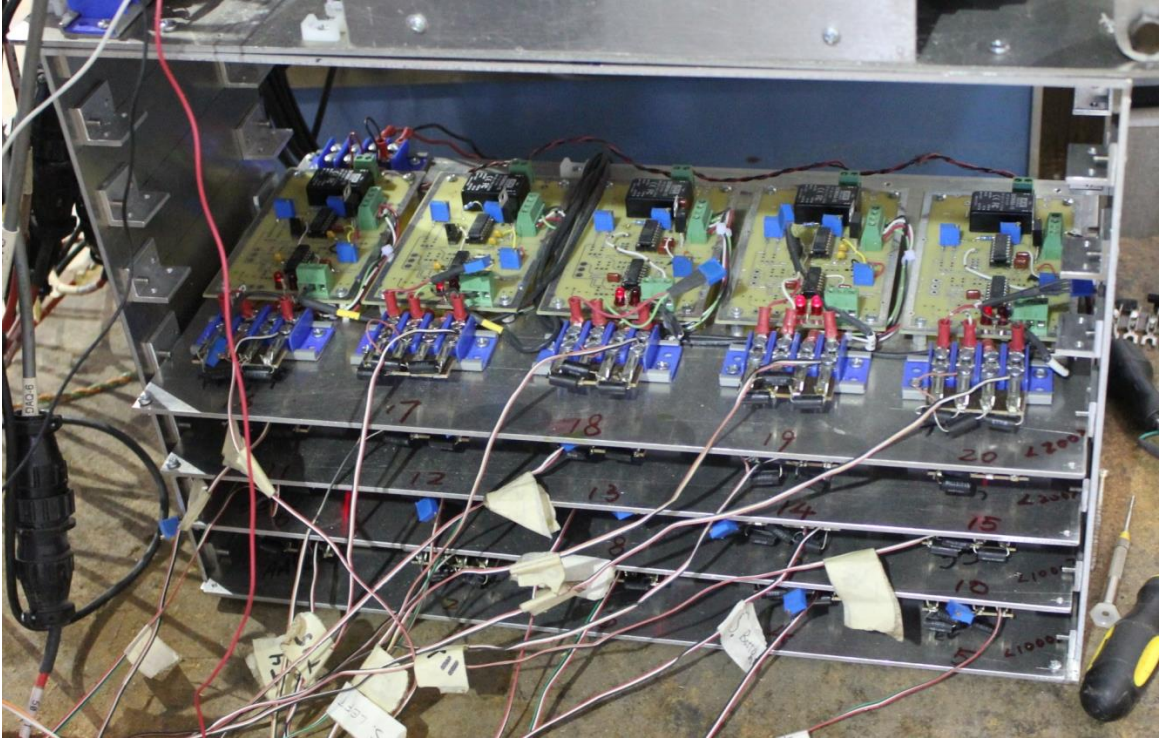
Strain gage profile on parallel reinforcement 0.64STA



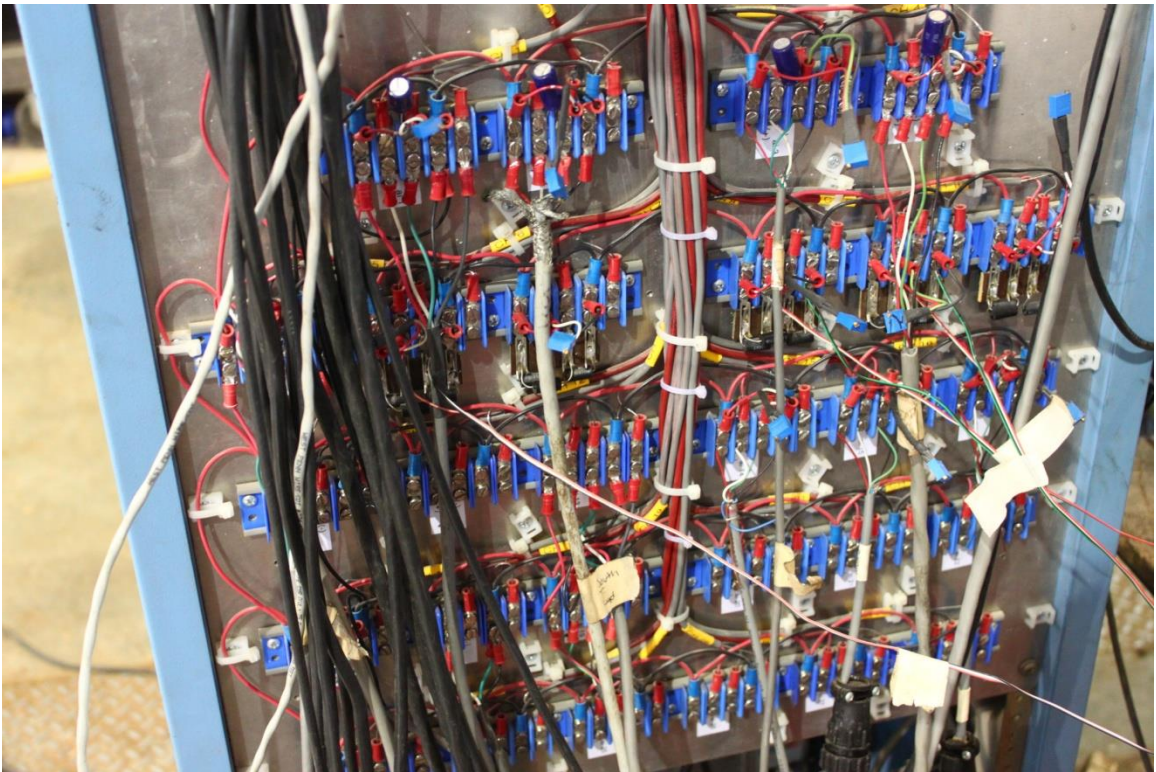
Strain gage profile on parallel reinforcement DYN1



Strain gage profile on parallel reinforcement DYN2



Fast data acquisition system (DAQ)



Original DAQ system used in static and dynamic tests



Overall view of dynamic test setup